Universidade do Minho
Escola de Engenharia

Maria Santos Crispiniano Vieira

Electrochemical immunosensor for improved diabetic retinopathy diagnosis in minimally invasive biological fluids

February 2021

Electrochemical immunosensor for improved diabetic retinopathy diagnosis in minimally invasive biological fluids

Maria Crispiniano Vieira

UMinho | 2021

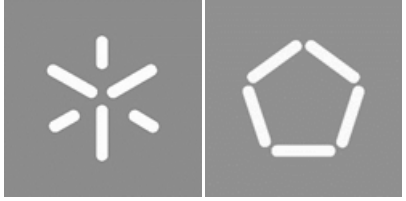

Universidade do Minho
Escola de Engenharia

Maria Santos Crispiniano Vieira

Electrochemical immunosensor for improved diabetic retinopathy diagnosis in minimally invasive biological fluids

Master's Dissertation
Integrated Master's in Biomedical Engineering
Medical Electronics

Dissertation oriented by:
Dr. Vanessa Fernandes Cardoso, University of Minho
Dr. Inês Mendes Pinto, International Iberian Nanotechnology Laboratory

February 2021

Acknowledgements

First of all, I would like to acknowledge the collaboration between the University of Minho (UMinho) and the International Iberian Nanotechnology Laboratory (INL) led by Dr. Vanessa Fernandes Cardoso from the UMinho's Center for Microelectromechanical Systems (CMEMS) and Dr. Inês Mendes Pinto from the INL's Cell Mechanics Laboratory, allowing the realization of this master project.

In particular, I would like to thank Dr. Inês Mendes Pinto for guiding and supervising my work, and for all the encouragement in embracing different research fields. I am very grateful for all the support given by Inês and the entire research group, including Dr. Diana Pinho, Dr. Catarina Abreu, Dr. Sofia Domingues, Francisca Fonseca and Rita Cacho. A special thank you to Dr. Andrea Cruz, for her remarkable guidance in the lab, and for sharing her knowledge that was crucial for this work to progress.

I would also like to thank Dr. Vanessa Cardoso for all her support throughout the entire year, and for believing in my work. Her kind words will remain in my memory for many years.

Also, I would like to thank Prof. Dr. Rosa Fernandes and Prof. Dr. Francisco Ambrósio from the University of Coimbra for providing the know-how in diabetic retinopathy and clinical basis of this work.

To my dear friends whose presence I miss so much, for always making me smile even when times were hard.

To my boyfriend for all his love and for always being there for me.

Finally, I would like to thank my family for all the emotional support provided. Words cannot explain how lucky I am for having you.

STATEMENT OF INTEGRITY

I hereby declare having conducted this academic work with integrity. I confirm that I have not used plagiarism or any form of undue use of information or falsification of results along the process leading to its elaboration.

I further declare that I have fully acknowledged the Code of Ethical Conduct of the University of Minho.

Resumo

Imunossensor eletroquímico para melhor diagnóstico da retinopatia diabética através de fluidos biológicos minimamente invasivos

A retinopatia diabética (RD) é uma das complicações mais comuns da diabetes, que afeta a retina e pode levar à cegueira. Em 2017, estimou-se que cerca de 150 milhões de pessoas sofriam desta doença, sendo expectável um crescimento na ordem dos 30 % até 2030. Os tratamentos existentes para a RD são ineficazes a travar a sua progressão numa percentagem significativa de pessoas. O diagnóstico convencional da RD depende de métodos de imagiologia qualitativos, dispendiosos e complexos. Tecnologias que permitam uma análise *in situ* quantitativa do impacto da RD são, até ao momento, inexistentes no mercado, revelando assim o potencial e a motivação para a presente investigação.

O uso de fluidos biológicos minimamente invasivos (como lágrimas e saliva) para o estudo de potenciais biomarcadores da RD é preferível aos fluidos oculares altamente invasivos analisados atualmente em investigação clínica. No entanto, é necessário o desenvolvimento de métodos com alta sensibilidade e seletividade em volumes de amostra diminutos. As concentrações de IL-6 e MMP2, dois biomarcadores associados à RD, foram determinadas em lágrimas de controlos e pacientes com RD, utilizando o método de quantificação de proteínas Luminex, verificando-se um aumento estatisticamente significativo em caso de doença. Estes resultados provieram de uma colaboração estreita com a Universidade de Coimbra. Foram desenvolvidos imunossensores para a deteção de cada biomarcador, em concentrações relevantes para o diagnóstico da RD em lágrima, recorrendo primeiramente a soluções padrão. Foram utilizados anticorpos como elementos de bio-reconhecimento específico, e voltametria cíclica e espectroscopia de impedância eletroquímica para deteção e quantificação dos mesmos. Os biossensores apresentados revelaram ainda ser a única tecnologia adequada a todos os métodos de colheita de lágrimas, quantificando ambos os biomarcadores em concentrações críticas para a RD, usando apenas 1 µL de amostra. Como estudo complementar, o sensor IL-6 foi testado em amostras de saliva, e o seu perfil analítico comparado com o método de quantificação de proteínas *Enzyme-linked immunosorbent assay* (ELISA). O biossensor apresentou resultados semelhantes em concentrações detetáveis por ELISA, e capacidade de quantificar concentrações inferiores ao limite de deteção deste método. Deste modo, este trabalho apresenta uma tecnologia inovadora, que poderá ser integrada em dispositivos analíticos *point-of-care* para o diagnóstico e monitorização da RD *in situ*, construindo assim uma base para trabalhos futuros, com elevado potencial para transferência de tecnologia.

Palavras chave: biomarcadores, biossensor, *point-of-care*, retinopatia diabética

Abstract

Electrochemical immunosensor for improved diabetic retinopathy diagnosis in minimally invasive biological fluids

Diabetic retinopathy (DR) is one of the most common diabetes mellitus (DM) complications, that affects the retina and can lead to blindness. In 2017, it was estimated that approximately 150 million people suffered from this disease, and a rising tendency of around 30 % is expected until 2030. Available DR treatments are inefficient on halting disease progression in a significantly high percentage of people. Conventional DR diagnostics relies on qualitative, expensive and complex imaging methods. Technologies that enable an *in situ* quantitative analysis of DR's impact do not exist, until this moment, in the market, thus revealing the potential and motivation for the present investigation.

The use of minimally invasive biological fluids (like tears and saliva) for studying DR's potential biomarkers is preferred to the highly invasive ocular fluids currently analyzed on clinical research. However, it is necessary to develop methods with high sensitivity and selectivity in minute sample volumes. The concentrations of IL-6 and MMP2, two biomarkers associated with DR, were assessed on the tears of controls and DR patients, using the Luminex protein quantification method, and statistically significant increased levels were found in case of disease. These results were provided by a close collaborative work with the University of Coimbra. Immunosensors for the detection of each biomarker were developed, in concentrations considered relevant for the diagnosis of DR in tears, primarily using standard solutions. Antibodies were used as specific biorecognition elements, and cyclic voltammetry and electrochemical impedance spectroscopy were used for their detection and quantification. The presented biosensors further revealed to be the only technology adequate for all tear sampling methods, quantifying both biomarkers in DR critical concentrations, using only 1 µL of sample. As a complementary study, the IL-6 sensor was tested in saliva samples, and its analytical profile was compared with the Enzyme-linked immunosorbent assay (ELISA) protein quantification method. The biosensor achieved similar results in ELISA-detectable concentrations, and an ability to quantify concentrations lower than this method's limit of detection. Therefore, this work presents a novel technology, that may be integrated in point-of-care analytical devices for an *in situ* diagnosing and monitoring of DR, thus building a foundation for future work, with great potential for technology transfer.

Key words: biomarkers, biosensor, diabetic retinopathy, point-of-care

Contents

Abbreviations and symbols

Abbreviation	Definition
2D	Two-dimensional
3D	Three-dimensional
8-OHdG	8-Hydroxy-2'-Deoxyguanosine
AC	Alternating current
AGE	Advanced glycation end-products
AH	Aqueous humor
B2M	β2-microglobulin
BRB	Blood-retinal barrier
BSA	Bovine serum albumin
CE	Counting electrode
CMEMS	Center for Microelectromechanical Systems
CSF	Cerebrospinal fluid
CV	Cyclic voltammetry
DM	Diabetes mellitus
DME	Diabetic macular edema
DR	Diabetic retinopathy
DRS	Diabetic retinopathy study
EIS	Electrochemical impedance spectroscopy
ELISA	Enzyme-linked immuno-assay
ETDRS	The early treatment diabetic retinopathy study
FA	Fluorescein angiography
HbA1c	Glycated hemoglobin
HPLC	High-performance liquid chromatography
IHP	Inner Helmholtz plane
IL-1ra	Interleukin-1 receptor antagonist
IL-6	Interleukin 6
INL	International Iberian nanotechnology laboratory
IP-10	Interferon-induced protein-10

IPA	Isopropanol
LCF	Lactoferrin
LCN1	Lipocalin 1
LOD	Limit of detection
LR	Linear range
MCP-1	Monocyte chemoattractant protein 1
MMP2	Matrix metalloproteinase 2
NaCl	Sodium chloride
NGF	Nerve growth factor
NPDR	Non-proliferative diabetic retinopathy
OCT	Optical coherence tomography
OCTA	Optical coherence tomography angiography
OHP	Outer Helmholtz plane
PB	Phosphate buffer
PBS	Phosphate buffer saline
PCB	Printed circuit board
PDR	Proliferative diabetic retinopathy
PKC	Protein kinase C
PKK	Plasma Kallikrein-Kinin
POC	Point-of-care
RE	Reference electrode
REP	Rapid electro-kinetic patterning
ROS	Reactive oxygen species
RSC	Royal Society of Chemistry
RT	Room temperature
SAM	Self-assembled monolayer
SD-OCT	Spectral-domain optical coherence tomography
SEM	Standard error of the mean
Sulfo-LC-SPDP	6-(3'-(2-pyridyldithio)propionamido)hexanoate
TNF-α	Tumor necrosis factor alpha
UMinho	University of Minho

UWF	Ultra-widefield
VEGF	Vascular endothelial growth factor
VH	Vitreous humor
WE	Working electrode
WESDR	Wisconsin epidemiologic study of diabetic retinopathy
$[Fe(CN)_6]^{3/4-}$	Ferricyanide couple

Symbol	Units	Definition
$\boldsymbol{A}$	cm^2	Area
$\Delta \boldsymbol{E_p}$	Volts, V	Wave peak-to-peak potential
C_{dl}	F	Double-layer capacitance
E	Volts, V	Potential
$\boldsymbol{E^0}$	Volts, V	Standard potential
$\boldsymbol{E_0}$	Volts, V	Initial amplitude of the potential
$\boldsymbol{E_{p,a}}$	Volts, V	Anodic peak potential
$\boldsymbol{E_{p,c}}$	Volts, V	Cathodic peak potential
$\boldsymbol{F}$	$C\ mol^{-1}$	Faraday constant
$\boldsymbol{f}$	Hz	Frequency
$\boldsymbol{I}$	Amperes, A	Current
$\boldsymbol{I_0}$	Amperes, A	Initial amplitude of the current
$\boldsymbol{i_c}$	Amperes, A	Double-layer charging current
$\boldsymbol{i_f}$	Amperes, A	Faradaic current
$\boldsymbol{i_{p,a}}$	Amperes, A	Anodic peak current
$\boldsymbol{i_{p,c}}$	Amperes, A	Cathodic peak current
$\boldsymbol{j}$	-	Imaginary number
$\boldsymbol{k_a}$	$cm\ s^{-1}$	Oxidation reaction rate constant
$\boldsymbol{k_c}$	$cm\ s^{-1}$	Reduction reaction rate constant
$\boldsymbol{n}$	mol	Number of mols

$[O'_{ads}]$	mol cm^{-1}	Concentration of the oxidized species adsorbed on the electrode's surface
[Oxidized form]	mol L^{-1}	Concentration of the oxidized species
R	J K^{-1} mol^{-1}	Gas constant
R	Ohms, Ω	Resistance
R^2	-	Coefficient of determination
$[R'_{ads}]$	mol cm^{-1}	Concentration of the reduced species adsorbed on the electrode's surface
R_{ct}	Ohms, Ω	Resistance to charge transfer
[Reduced form]	mol L^{-1}	Concentration of the reduced species
R_s	Ohms, Ω	Solution resistance
T	Kelvin, K	Absolute temperature
t	s	Time
v	mol cm^{-2} s^{-1}	Electron transfer rate
v_a	mol cm s^{-1}	Oxidation reaction rate
v_c	mol cm s^{-1}	Reduction reaction rate
Z	Ohms, Ω	Impedance
Z_0	Ohms, Ω	Initial amplitude of the impedance
Z'	Ohms, Ω	Impedance real value
Z''	Ohms, Ω	Impedance imaginary value
Z_f	Ohms, Ω	Faradaic impedance
Z_w	Ohms, Ω	Warburg impedance
θ	°	Phase angle
ω	rad	Angular frequency

List of figures

List of tables

1. Introduction

In the present section, a contextualization on diabetic retinopathy (DR) is given, highlighting the downfalls of current diagnosing and monitoring strategies. DR's biomarkers and biomarker source fluids are introduced, as well as the advantages of developing a point-of-care (POC) diagnosing technology. Thereafter, the motivation and proposed objectives for the work performed on the present dissertation are stated. Finally, this dissertation's structure is presented.

1.1. Contextualization

Diabetes mellitus (DM) is a chronic condition that affects millions of people worldwide, and predictions for its rising tendency in a near future are extremely concerning [1].

One of DM's most dreaded and common complications is DR. This eye-threatening disease was estimated to affect more than 149 million people in 2017 [2], and projected to reach about 191 million people by 2030. It is considered the leading cause of acquired vision loss in working-aged adults [3], with 1 % of the total blind population worldwide being supposedly caused by this disease. It has been estimated that at least one third of the diabetic population will develop some form of DR in their lifetime, and diabetes increases the probability of their patients to become blind by 25 times [4]. The costs associated with diagnosing and monitoring, allied with vision impairment-related expenses cause DR patients to be an economic burden to the society where they are inserted [5].

The complex pathophysiology of DR is still to be fully understood. Nevertheless, some factors have been strongly linked to the onset and development of this disease, including hyperglycemia, mitochondrial dysfunction, oxidative stress and inflammation. More recently, neurodegeneration has also been proved to play a significant role in DR's onset and development [6].

A variety of treatment options is now available for DR management. However, none of them are truly capable of hampering disease progression, and therapies fail for a large number of patients. Despite that, early diagnosis is of utmost importance to enable tight risk factor control, which has a massive impact on the initiation and progression of the disease [7].

A decades-old method based on seven-field 30 ° stereoscopic color fundus photographs is still considered the gold standard for DR grading [8]. Despite that, it is a complex, laborious method, that requires and

relies on the qualitative judgment of trained professionals. Only a small area of the retina is examined, and functional and non-imageable alterations are ignored with this conventional imaging method [9].

In a recent past, studies identifying DR biomarkers in multiple fluids have emerged in the literature, and it is now obvious that, in the future, structural and functional assessment of the retina will be complemented by a molecular approach for improved DR diagnosis [10]. Furthermore, biomarker analysis will contribute to the development of new therapeutic approaches, clarifying the entire spectrum of diabetic retinal disease. Moreover, the quantification of multiple biomarkers as opposed to single biomarker analysis increases disease specificity [11].

Tears and saliva are two biological fluids collected through minimally invasive techniques, as opposed to the ocular fluids typically used for DR biomarker research. Sampling for these ocular fluids is extremely invasive and can only be performed when the subject is undergoing eye surgery, making it difficult to obtain a significant number of disease samples, and comparison with healthy controls is disabled [12]. Recent studies have revealed that pathological changes can be detected in patients' tears and saliva samples, including DR [13,14]. Therefore, these forms of minimally invasive biomarker profiling are very promising for DR pre-screening, diagnosis, staging and monitoring. However, scantiness of fluid and low biomarker concentrations make this process very demanding in terms of sample volume requirements and limit of detection (LOD) [15].

Interleukin-6 (IL-6) and metalloproteinase-2 (MMP2) are two proteins that have been identified as potential biomarkers for DR diagnosing, monitoring and stratification [16,17]. However, very few studies have used minimally invasive biological fluids as biomarker source for IL-6 and MMP2 quantification, making this information very important and timely for the DR research field.

Biosensing has been explored widely in the past, not only for medical diagnosis purposes, but also for very different fields like agriculture, industry and military. Electrochemical biosensors bring high sensitivity, fast and simple detection at reduced costs [18]. The use of antibodies as biorecognition elements is often applied, due to their high specificity, stability and versatility for biomarker detection [19]. Biosensors have revolutionized the quantification of different molecules for very distinct applications, and device technology is constantly improving and miniaturizing, making this field very attractive for disease diagnosis at the POC, and potentially for DR diagnosing through biomarker analysis. This knowledge area is still in its infancy, given the very few publications found in literature and exposed in Section 2.4.4. There is an unmet need for technologies such as the one presented in this dissertation, that appears timely and with great potential for the DR research community.

1.2. Motivation and objectives

As exposed in the previous section, DR is a dreadful disease that causes a significantly high percentage of worldwide blindness [4]. Treatment options are inefficient on halting disease progression and are mostly applied on advanced stages of the disease [7]. Diagnosing methodologies do not comprise multiple factors that are crucial for disease onset and progression, adding to the fact that they are of subjective nature, extremely complex and highly expensive [9].

The present dissertation introduces a novel technology approach for improved DR diagnosis through biomarker profiling of minimally invasive biological fluids. It brings together the use of antibody-antigen interactions, known for their high specificity, sensitivity and versatility [19], and electrochemical detection techniques that carry high sensitivity themselves, as well as low complexity, fast evaluation and enabled integration on mobile devices [20].

The use of non to minimally invasive fluids (like tears and saliva) as biomarker source fluid is obviously advantageous, as mentioned in the previous section, but comes with demanding challenges. This project aims to contour the downfalls of tear analysis by achieving very sensitive results in minute sample volumes. In addition, the biomarkers selected have been linked with DR, but are almost unexplored in minimally invasive biological fluids, which brings valuable knowledge to the field. A simple technology capable of making the distinction between DR patients and controls in a fast, simple, cheap and accurate way, using a very low amount of a minimally-invasively obtained biological fluid could revolutionize DR diagnosing methodologies, and add quantitative factors to this subjective method.

The proposed objectives for the present dissertation are:

- Analysis of the concentrations of IL-6 and MMP2 in the tears of healthy control subjects and DR patients achieved with the Luminex technique, and determination of disease-critique values;
- Biofunctionalization of two different antibody-based immunosensors, using electrochemical detection techniques for IL-6 and MMP2 quantification;
- Immunosensors' validation for the quantification of IL-6 and MMP2, using standard solutions prepared according to tears' concentration ranges obtained in the previous Luminex analysis;
- Comparative analysis between the proposed immunosensors and two conventional biomolecule quantification techniques, namely Luminex and ELISA, for the quantification of IL-6 and MMP2 in tears for DR diagnosing;
- Complementary study based on the quantification of IL-6 in saliva samples using the developed immunosensor, and comparison with ELISA.

1.3. Dissertation structure

Considering the objectives proposed, the present document is organized in 5 sections that are now to be summarized.

1st Section - Introduction

The current section presents the introduction and motivation for the selected theme, and corresponding objectives. Lastly, the dissertation structure is stated.

2nd Section – Theoretical framework

In the second section, DR is introduced as the clinical focus on the present dissertation. Current information about its prevalence, risk factors, costs associated, known pathophysiology, clinical signs, disease staging and finally treatments available is provided. A brief introduction to conventional methods for DR diagnosis is then made, highlighting the need for new quantitative technologies. Next, IL-6 and MMP2 are presented as two potential biomarkers that have been linked with DR, but not yet fully explored in minimally invasive biological fluids. Afterwards, the biomarkers found to be linked with DR, both in invasive and non-invasive biological fluids, are presented. The advantages of using minimally invasive biological fluids are then highlighted. Conventional and novel technologies for biomarker quantification for DR diagnosing purposes are compared afterwards. The final subsection consists on an introduction to electrochemical biosensors, which are used in the present dissertation. Antibodies are highlighted as biorecognition elements, the Randles equivalent circuit is proposed as a simplification to complex biosensing systems, and detection techniques used for electrochemical measurements are stated.

3rd Section – Materials and experimental procedures

In this section, the materials and reagents required for the experimental procedures are enunciated, and methodologies applied are presented and explained. The first experimental procedure results from a collaboration between INL and the University of Coimbra and consists on the quantification of IL-6 and MMP2 in the tears of healthy controls and DR patients, using the Luminex method. Afterwards, the protocols used to functionalize and test the performance of two immunosensors for the quantification of IL-6 and MMP2 are explained, considering the previously obtained results. Then, a comparative study

analyzing the developed immunosensors and two conventional biomolecule quantification methods (namely Luminex and ELISA) is explained. Finally, the last experiment consisted on the assessment of the IL-6 concentrations from 15 saliva samples, using the developed IL-6 immunosensor and the conventional ELISA method.

4th Section – Results and discussion

The resultant experimental data, as well as its analysis and discussion are addressed in this section. First, the IL-6 and MMP2 concentrations found on the tears of healthy subjects and DR patients are presented, and a critical analysis on the potential of using these biomarkers for diagnosing DR is made. The results from the development and optimization of the immunosensors are then analyzed, followed by their performance. Afterwards, the results from the comparative study between conventional biomarker quantification tools (Luminex and ELISA) and the developed immunosensors for IL-6 and MMP2 quantification in tear samples are presented and discussed. Finally, the resultant salivary IL-6 concentrations from the complementary study are analyzed, and the IL-6 immunosensor's performance is compared with ELISA's.

5th Section – Concluding remarks and future work

In this dissertation's final section, conclusions drawn from this work are exhibited, and closing remarks are made. Lastly, suggestions for future work that would improve this dissertation's value are presented.

2. Theoretical framework

In this section, topics that are key for understanding the importance of the present work are presented. First, DM is introduced as a world concern, with high prevalence and frightful future prospects. DR, one of the most dreaded consequences of DM, is presented next. Its prevalence, risk factors and disease-related costs are exhibited, followed by the explanation of how the disease develops and affects the eye. The clinical signs that characterize each disease stage, and how it is stratified are the followingly introduced topics. Afterwards, treatments applied to DR patients nowadays are stated, focusing on the fact that these treatments are mostly applied to late stages, and highlighting the importance of early diagnosis. The following section introduces the conventionally used methods for DR diagnosing, which the present dissertation means to improve. Potential molecular biomarkers for DR, the biological fluids where they can be detected and quantified are the subsequent matters clarified. The potentially POC technologies described in the literature for improved minimally invasive DR diagnosis are then highlighted. The last section of the theoretical framework explains how an electrochemical sensor works, and how it can be used for biomarker quantification.

2.1. Diabetes

DM is a chronic condition where either a lack of insulin or an inability of the cells to respond to it (also known as “insulin resistance”) occurs, leading to high blood sugar levels (hyperglycemia). More than 463 million people live with DM nowadays, and the predictions for 2030 and 2045 are extremely upsetting, as can be seen in Figure 1. Approximately 4.2 million people between the ages of 20 and 79 years old died from diabetes-related causes in 2019, which is equivalent to one death every 8 seconds. 11.3 % of global deaths from all causes are attributed to diabetes, in this age group [1].

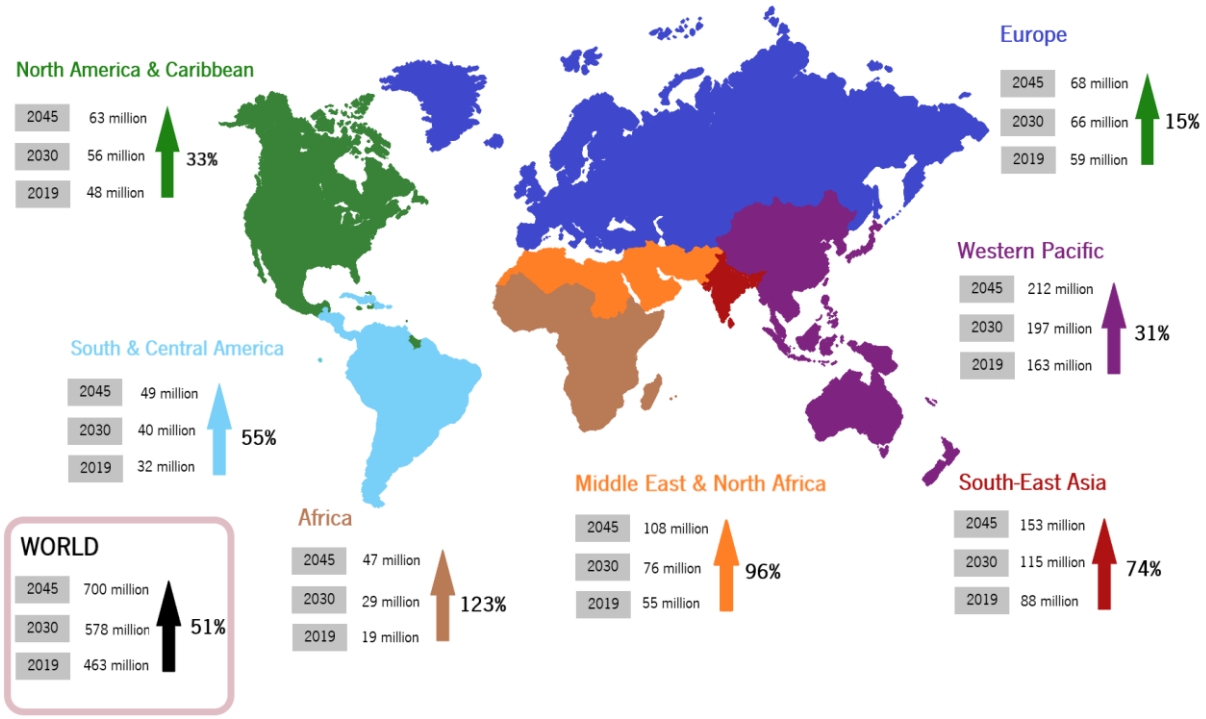

Figure 1. Number of people between 20 and 79 years old with diabetes worldwide, and per international diabetes federation region in 2019, and predictions for 2030 and 2045.

Type 1 DM is characterized by damaged insulin-producing beta cells of the pancreas, caused by an autoimmune reaction that leads to limited or no insulin production. Children and young people are the most affected groups [1].

On the other hand, type 2 DM is initially caused by insulin resistance. During this stage, the hormone's ineffectiveness leads to a rise in its production. With time, failure of the pancreatic beta cells to keep up with demand may occur, causing inadequate insulin production. Type 2 DM is most commonly seen in older adults, but is increasingly seen in children and younger adults. Comparing with type 1 DM, its symptoms are usually much milder, and a lack of them is also very common, leading to long pre-diagnostic periods. The prevalence of type 2 diabetes is high and rising across the globe, following population aging, economic development and increasing urbanization that lead to more sedentary lifestyles and greater consumption of unhealthy foods linked with obesity [1].

It is also important to highlight the alarmingly high number of undiagnosed cases (overwhelmingly type 2 DM), with more than 50 % of the type 2 DM population living unaware of their condition. Prolonged

undiagnosed diabetes increases the risk for diabetes-related complications, healthcare use and related costs [21].

2.2. Diabetic retinopathy

DR, the most common microvascular complication arising as a consequence of diabetes, is considered the leading cause of acquired vision loss across the world, in working-aged adults [3], with 1 % of blindness worldwide being linked to this disease [22]. This disease develops in the eyes of diabetic patients, affecting their vision acuity and ultimately leading to blindness.

2.2.1. Prevalence, risk factors and costs

In 2017, more than 149 million people were estimated to be suffering from DR [2]. This number is expected to follow the DM's rising tendency, and reach about 191 million people by 2030, with 56.3 million people being vision-threatening forms of the disease. About one third of the diabetic population is expected to acquire some form of DR in their lifetime, and people with diabetes are 25 times more likely to become blind than people without diabetes [4].

Some of the main risk factors for DR include diabetes type (with type 1 DM being the most affected), duration of diabetes, glycated hemoglobin (HbA1c) values, blood pressure, and cholesterol [23]. More recently, inflammation, metabolic hormones, oxidative stress, vitamin D deficiency, as well as genetic predisposition have also been linked with the development of DR. Estimates are similar for men and women, highest in African Americans, and lowest in Asians. During the first 20 years of disease, nearly all patients with type 1 DM and more than 60 % of patients with type 2 DM develop DR [24].

A patient with DM brings high expenses to his society, and the presence of diabetes-related complications greatly increases these costs. In fact, visual impairment has wide-ranging implications in terms of the burden of dependence, the potential loss of earning capacity and the need for greater social support due to impaired quality of life, and reduced physical, emotional and social well-being. Health and social care systems are at risk of being overwhelmed due to personal and social costs of severe visual impairment. Besides, a great percentage of adults with diabetes live in low and middle-income countries, where healthcare resources are already severely challenged. Nevertheless, it has been proved that both direct and indirect economic weight would be significantly reduced if diabetic patients underwent regular DR screening and received treatment according to the severity of their condition [5,25,26].

Understanding how DR develops and affects the eye, leading ultimately to blindness is yet to be fully understood. The following subsection elucidates the reader on what is known so far about this disease's pathophysiology.

2.2.2. Pathophysiology

An introduction to how a disease-free eye works is needed, to better understand the alterations caused by DR. The human retina is composed of three nerve cell body layers interspaced by two plexiform layers where synapses occur. Rod and cone photoreceptors form the outer nuclear layer. The inner nuclear layer is composed of bipolar, horizontal and amacrine cells. Finally, ganglion cell bodies and displaced amacrine cells form the ganglion cell layer. The last form a nerve fiber layer that takes the visual sign to the visual cortex in the brain, through the optic nerve (Figure 2). This complex neuronal component is a big contributor to the exceptionally high metabolic demands of the retina, with availability of oxygen and nutrients being crucial to the process [27], and make it particularly vulnerable to vascular disease in DR.

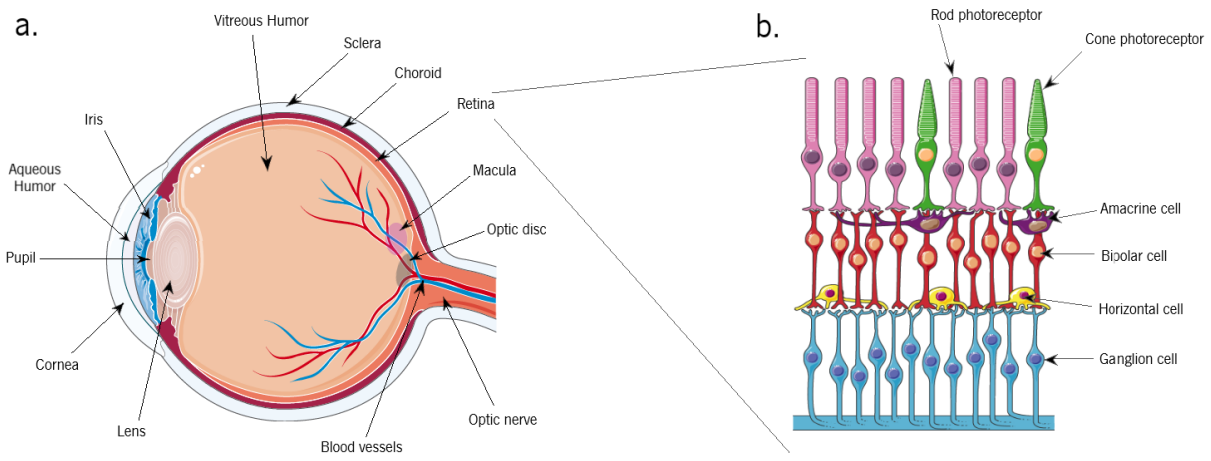

Figure 2. a. Eye's anatomy and b. retinal nervous components.

The vascular component of the retina has two plexuses: the choroid (which supplies 90 % of the total blood volume to the retina) and the intraretinal vasculature (that supplies the inner layer of the retina, sparing the macula) [28].

The blood-retinal barrier (BRB) is a fundamental element to keep the eye as a privileged site in the body, regulating the contents of its inner fluids and protecting the internal ocular tissues from variations that occur constantly in the whole circulation. It is a particularly tight and restrictive barrier that regulates ion, protein, and water flux into and out of the retina. It also regulates fluids and molecular movement between the ocular vascular beds and retinal tissues, and prevents leakage into the retina of macromolecules and other potentially harmful agents [29].

Retinal blood vessels are complex multicellular units with structural and functional comparability to vessels in the brain. This often called neurovascular unit regulates oxygenation and nutrition of the neuropil through blood flow regulation and integrity of the BRB, dynamically responding to circulatory and neuronal cues [30]. The pericytes wrapped around retinal capillaries not only provide structural support, but also modulate endothelial cell function [28].

The neuronal component of the retinal vessels is composed of the retinal glia, which includes Müller cells and astrocytes. They provide metabolic support to neurons and play a critical role in maintaining the inner BRB [31]. Glial processes are responsible for maintaining normal retinal homeostasis, with Müller cells regulating glucose flux between the circulation and retinal neurons.

Microglia are the resident innate immune cells of the retina. Their function evolves through time: in the developing retina, they are involved in the pruning of neuronal and vascular networks through the phagocytic removal of apoptotic cell debris [32]; in the adult retina, they exist in two stages: resting and activated microglia. Resting microglia are continuous monitors of their environment, supporting neuronal survival. However, when activated due to infection or ischemia, these cells become mobile and macrophagic, and produce of a wide range of pro-inflammatory cytokines [33]. Microglial activation in disease evokes profound changes to the normal function of the retina.

While diabetes may also cause conditions such as cataract, glaucoma, loss of focusing ability and double vision, DR needs to be spotlighted given the rapidly rising incidence of this largely avoidable form of vision loss. The diabetic milieu and hyperglycemic episodes arising from suboptimal glycemic control in patients with either type 1 or 2 DM have drastic consequences over time. Hyperglycemia causes metabolic dysfunction, and retinal blood vessels dilate and experience blood flow changes, as a metabolic autoregulation mechanism to increase retinal metabolism in diabetic patients [34]. Multiple metabolic pathways have been implicated in hyperglycemia-induced vascular damage: there is an increase in glucose flux through the polyol and hexosamine pathways, an activation of protein kinase C (PKC) pathway, overactivation of the plasma Kallikrein-Kinin (PKK) pathway and accumulation of advanced

glycation end-products (AGE) [35,36]. Mitochondrial dysfunction increases vascular and neuronal apoptosis [37], but most important, the consequence of reactive oxygen species (ROS) overproduction causes oxidative stress in retinal tissues, which some consider to be the stressor linking all of the pathways above mentioned [38].

Reduced insulin activation in retinal neurons and vascular cells leads to neurodegeneration. Also, hyperglycemia and consequent increase in glycolytic metabolites activate chronic low-grade inflammatory signaling, which has been detected in both diabetic animal models and patients [39].

The earliest detectable histologic microvascular change in DR is pericyte loss [40]. Also, apoptosis of endothelial cells occurs, with evidence shown in both *in vitro* and *in vivo* models [41]. Endothelial cells and pericyte loss lead both to the thickening of the capillary basement membrane and to the impairment of the BRB [30,35]. Furthermore, pronounced loss of pericytes and endothelial cells results in vascular obstruction and tissue ischemia, which itself leads to the upregulation of vascular endothelial growth factor (VEGF) and neuronal death [42].

Inflammation plays an essential role in the pathogenesis of DR, with pro-inflammatory cytokines being present in the first stages of the disease [43,44]. Inflammation causes vascular permeabilization, BRB dysfunction, leukostasis, leukocyte-endothelium adhesion, and glial cell dysfunction [45]. Retinal glial cell dysfunction is also presumed to be involved in the initiation and amplification of the retinal inflammation in DR [46]. Under hyperglycemic stress, once dormant glial cells get activated and amplify inflammation responses by producing angiogenic and pro-inflammatory factors [47].

Even though it is classically regarded as a microvascular disorder, advances in understanding early cellular changes in the diabetic retina combined with improved retinal imaging techniques have proved that there is a strong neurodegeneration component in the pathogenesis of DR, and it should in fact be considered a disease of the retinal neurovascular unit [48].

2.2.3. Clinical signs

DR is characterized by leaky retinal vasculature, retinal ischemia, angiogenesis, retinal inflammation and neurodegeneration. These result in recognizable clinical features such as microaneurysms, retinal hemorrhages, hard exudates, cotton wool spots, venous dilation and beading, intraretinal microvascular abnormalities and neovascularization [27,49]. These alterations can be observed in Figure 3.

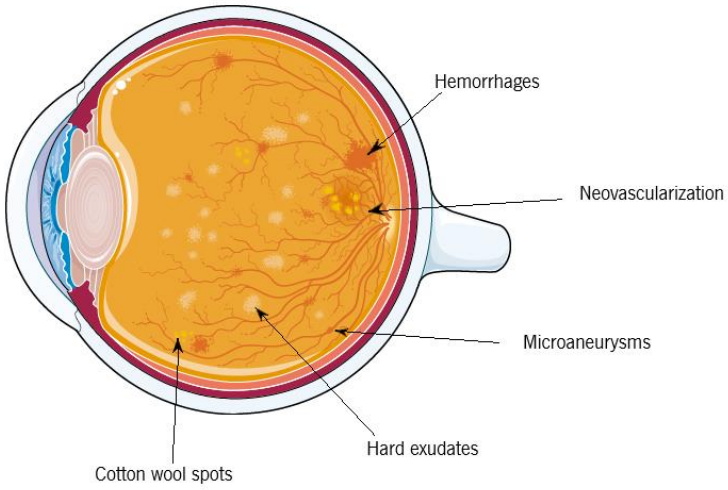

Figure 3. Schematic of the finger-print signs of DR.

- Microaneurysms are a result of ischemia due to capillary occlusion and nonperfusion, and are often the first clinically recognizable features of DR. They present as "balloon-like" protrusions of the capillary wall, and recruit inflammatory cells which further damage the endothelial lining. Late-stage microaneurysms are sometimes sclerotic and frequently exist in the absence of an endothelial lining, and are associated with regions of extensive capillary degeneration;
- Retinal hemorrhages result from loss of vessel integrity and present as small spots of blood that leak into the retina;
- Hard exudates are associated with increased risk of visual loss. They are lipid deposits that appear after the reabsorption of localized edemas following hemorrhages or leakage of fluid from microaneurysms into the retina;
- Cotton wool spots are localized neuronal infarctions caused by disturbed axoplasmic flow;
- Intraretinal microvascular abnormalities appear as abnormal branching or dilation of existing blood vessels, and may represent attempted vascular remodeling in areas of ischemia;
- Neovascularization is the final sign of DR. Retinal ischemia causes upregulation of pro-angiogenic cytokines, resulting in over proliferation of capillary endothelial cells and ultimately neovascularization. It occurs in the interface between perfused and non-perfused retina and is associated with poor prognosis for visual outcome. These new vessels often grow on the surface of the retina and penetrate the inner limiting membrane into the vitreous. They are typically fenestrated, brittle and leaky, which can result in vitreous hemorrhage. Repeated vitreous

hemorrhaging is associated with gliosis and fibrovascular scar formation. Contraction of fibrous tissues can result in tractional retinal detachment and sudden loss of vision.

The presence, amount and severity of these abovementioned clinical signs are the factors that dictate the stage of the disease. The patient's two eyes may be classified into two different stages.

2.2.4. Disease stages

The rate at which DR progresses is different from person to person. It advances from preclinical to non-proliferative DR (NPDR) and proliferative DR (PDR) [50,51].

Within weeks to months of the onset of DM, multiple adaptive responses start to take place in the human eye. These include reduced electrical activity, reduced biosynthetic activity such as protein and lipid synthesis, autophagy and apoptosis [52,53]. In this first stage, the adaptive responses compensate for the metabolic insults, making vision intact, and the retina free of clinical alarming signs. Thereafter, it is considered that there is no DR, until adaptive responses start to decompensate and clinical signs appear [54].

NPDR represents the most common form of DR [55], wherein vascular permeability and capillary occlusion are two main observations in the retinal vasculature. Adaptive changes begin to decompensate, and the hallmark microvascular features of NPDR appear, which include microaneurysms, intraretinal hemorrhages, hard exudates and cotton wool spots [56]. NPDR is further subdivided into mild, moderate and severe, depending on the presence of microaneurysms in the retina and severity of intraretinal hemorrhages [10]. Mild NPDR is characterized by visible damage to small retinal blood vessels, wherein microaneurysms may occur. In moderate NPDR, there is evidence of blood vessel blockage, causing a decrease in the supply of nutrients and oxygen to certain areas of the retina. Finally, severe NPDR is characterized by a significant number of small blood vessels becoming blocked, causing ischemia. In the areas where this occurs, there is a release of signals to stimulate the growth of new blood vessels in order to reestablish the supply of oxygen [57]. Although usually asymptomatic, some patients with NPDR experience impaired visual field, color discrimination and vision acuity, and a lack of contrast sensitivity [54,58].

The most advanced stage of DR appears after additional time and suboptimal diabetes control. In patients with type I DM, PDR it is the most prevalent vision-threatening condition [59]. PDR is driven by hypoxia and characterized by neovascularization. In attempt to supply blood to the deprived areas, aberrant,

fragile ad highly permeable new vessels form across the retina's surface and in more severe cases into the vitreous [10,60]. Severe and sometimes irreversible vision impairment, or even total loss, may happen in this stage. When the new abnormal vessels rupture, blood can get to the vitreous, a condition known as vitreous hemorrhage. As it progresses, scar tissue may develop, which may pull and distort the retina, causing retinal detachment [49,55].

Diabetic macular edema (DME) can occur at any stage of DR and is caused by an excess of fluid that accumulates in the macula. This leads to vision-threatening swelling or thickening of the macula, and consequent distortion of visual images and decrease in visual acuity. DME is the number one cause of visual impairment between diabetic patients, and the presence and severity of DME is usually assessed separately from the DR stage, on clinical practice [56,61,62].

As stated in Section 2.2.1, diabetes duration is a very important factor for DR onset and progression. The prevalence of DR's different stages and their evolution through time was assessed in the Wisconsin Epidemiologic Study of Diabetic Retinopathy (WESDR). After 3 years of DM diagnosis, 8 % of patients had some form of DR. This percentage increased with diabetes duration: 25 % of patients had some form of DR after 5 years of diagnosis, 60 % after 10 years and 80 % after only 15 years [24]. Even though no patient was diagnosed with PDR after 3 years of diagnosis, 25 % of patients developed this advanced form of DR after 15 years of diagnosis [63]. Managing DR has been a topic widely studied worldwide for a long time. The next subsection presents the treatments available nowadays.

2.2.5. Treatments for diabetic retinopathy management

Due to DR's asymptomatic nature, sometimes even in advanced stages, early and periodic ophthalmic examinations should occur for diagnosing, staging and treatment guiding purposes. This tight control could significantly limit visual loss from DR. The complexity of DR reflects on the variety of treatment options now available. Laser surgery, anti-VEGF therapy and steroids are some of them [9,64].

Surgical procedures include laser and pan-retinal photocoagulation. By sealing or destroying specific and dysfunctional retinal vessels, these surgical methods can induce the regression of abnormal new vessels, decrease oxygen tension and reverse angiogenesis in the retina, therefore preventing further progression of DME and PDR [65].

Vitrectomy is often applied when initial treatment options fail. It is another form of surgical treatment where the VH is removed, and can improve or restore the patient's vision, preventing progressive vision loss [66].

In a more recent past, pharmacotherapy agents have been investigated, and some have revealed to be very promising for DR management. Anti-VEGF agents are the most widely applied, and improve the vision acuity of patients with center-involved DME [64,67]. On the other hand, steroids can be applied when other therapies fail. They are administrated by intravitreal injection and, in some cases, may inhibit VEGF expression, leading to a decrease in the severity of DME [68,69]. In spite of their effectiveness, pharmacotherapies are invasive, expensive, and associated with many side-effects. Moreover, there are patients that do not respond to this treatment [70].

As exposed, most of the treatments are applied when vision is already compromised, on late disease stages. It is also important to note that none of the treatment options available are fully capable of halting progression or reversing retinal damage, and a large subset of patients do not respond to therapies available. Moreover, frequent administration and high occurrence of side-effects lower patient compliance. With that being said, the onset and progression of DR can be largely delayed by a tight control of DR's risk factors (like the control of glycemic levels, blood pressure and lipidemia) [7,71]. As so, early diagnosis of DR would greatly improve patients' disease progression, representing an urgent and unmet need. The techniques used for DR diagnosing and monitoring are introduced in the next subsection.

2.3. Conventional methods for diabetic retinopathy diagnosing and monitoring

DR may progress silently, causing clinically invisible and asymptomatic retinal and microvascular changes for many years. The unawareness of these changes speeds disease progression and leads to vision-threatening events [72]. Consequently, the correct identification of disease stages and associated treatments has vital importance. Intense investigation over the past decades has led to the use of novel technologies to study the natural course of DR [73].

The Early Treatment Diabetic Retinopathy Study (ETDRS) is considered a landmark study that constituted the basis for our knowledge on DR's natural course [8]. From this study resulted the standardized guidelines that, despite being a decades-old method, are still considered the gold standard for DR diagnosis and stratification. This method can be used with or without pupillary dilation, and uses seven-field 30 ° stereoscopic color fundus photographs, searching the eye's posterior pole for structural and

vascular alterations, namely microaneurysms, hard exudates, hemorrhages, cotton wool spots, intraretinal microvascular changes and neovascularization. Dimension and quantification of these abnormal events are also assessed by this method. The downfalls of the ETDRS diagnosing technique are its complexity, and the need for trained professionals not only to perform the analysis, but also for interpretation. Moreover, it does not take into consideration retinal functional changes like delayed implicit times and visual field defects [9], and unimageable alterations (namely inner retinal layer disruption or peripheral changes) for the diagnosis and grading of DR [8,74–77]. These result in an incomplete assessment of DR-caused alterations. Recent advances have brought forward a new generation of ultra-widefield (UWF) cameras that can detect peripheral lesions by covering a wider field when compared to conventional fundus cameras [78]. Many other imaging methodologies are now available for DR screening [9,79].

Optical coherence tomography (OCT) is often used due to its non-invasive nature, giving cross-sectional views of tissue structures *in vivo*. High resolution is achieved by the use of interferometry of low-coherence infrared light, surpassing fundus photography in imaging the vitreoretinal interface, neurosensory retina and the subretinal space. Retinal thickness can be assessed using OCT, retinal layers can be evaluated separately, and DME is easily identified [80]. However, OCT is not accurate for DR severity assessment, and is a very expensive technique. OCT angiography (OCTA) has enormous potential for improving DR diagnosing and stratification, because it reveals common vascular lesions and regions of capillary nonperfusion in the retinal plexuses and choroid, without the need of a contrast dye [81]. This technique brings, however, many projection artifacts, cannot detect leaks, and no guidelines are available for structure segmentation [80,82,83].

Fluorescein angiography (FA) is another imaging technique effective in identifying DME and PDR. The need for a fluorescent dye injection, however, makes it an invasive technique that, moreover, is linked with abundant serious complications [84,85].

Another non-invasive technique specially used for PDR assessment is B-scan ultrasonography. This method enables the assessment of vitreous hemorrhage dimension and density, the existence of vitreoretinal detachment and fibrovascular membranes [86].

The search for potential DR biomarkers has been growing in a recent past. As exposed, even though imaging techniques have been greatly evolving, recent studies have suggested that the combination of not only structural but also molecular alterations caused by DR could greatly improve not only diagnostic, but also grading and prognostic performances, by reflecting a much larger spectrum of DR-caused

alterations [9]. The next section exposes molecular biomarkers that have been found altered in DR patients.

2.4. Molecular biomarkers for diabetic retinopathy diagnosis and monitoring

As exposed in the previous section, DR diagnosing relies on imaging assessment of retinal lesions. The use of biomarkers has enormous potential for improving accuracy, and also for a worldwide DR screening at reduced costs. Furthermore, including biomarker quantification in the diagnosing process could aid in the development of a more reproducible system based on a quantitative approach, with greater staging and prognostic value.

In the context of DR, a vast number of studies have identified molecular biomarkers that reflect DR's hallmark events like the patient's glycemic levels (e.g. serum HbA1c), angiogenesis (e.g. VEGF), AGE formation, inflammation (e.g. tumor necrosis factor-alpha - TNF-α, IL-6, MMP2, lipocalin 1 - LCN1), among others, which have been linked with disease onset and progression [87–89]. In the present dissertation, IL-6 and MMP2 were chosen as representative biomarkers with potential for DR diagnosing and grading. Accordingly, these two biomarkers are now introduced in more detail.

IL-6 is a pleiotropic cytokine responsible for multiple processes, from the control of the immune response (both acute and chronic) to the maintenance of pathological states [90]. Altered concentrations of this cytokine have been linked with multiple diseases, including inflammatory bowel disease and arthritis [91,92]. In DR, it acts as a pro-inflammatory cytokine, and Table 1 reviews the published papers where IL-6 has been linked with DR.

Table 1. Published articles that quantify IL-6 in different biological fluids from DR patients.

Fluid	Population	Key findings	Technique	Reference
VH	73 patients with PDR	Six months after vitrectomy, IL-6 levels were significantly higher in eyes from progression group than in eyes with PDR regression	ELISA	[93]
	38 patients with PDR and 16 controls	Concentration was significantly higher in PDR than in controls.	Multiplex assay	[94]
	26 diabetic subjects with active PDR and 27 controls	Concentration was significantly higher in PDR than in controls.	Chemiluminescence assay mimicking ELISA	[95]
	22 patients with PDR and 16 controls	Concentration was significantly higher in PDR patients than in controls	ELISA	[96]
AH	51 non-diabetic patients (controls), 50 diabetics without DR, 101 DR patients	Concentration was significantly higher in diabetic patients than in non-diabetics, and increased with disease severity.	Multiplex bead immunoassay	[97]

Table 1. Published articles that quantify IL-6 in different biological fluids from DR patients (cont.).

Fluid	Population	Key findings	Technique	Reference
Serum	85 controls, 39 children with type 1 DM without DR, and 163 type 1 DM children with DR	Concentration significantly increased from controls to diabetic children with no DR, and from diabetic children to children with DR	ELISA	[16]
	13 controls, 12 NPDR patients, and 12 PDR patients	Concentration increased from controls to NPDR patients and again to PDR patients	Cytometric bead multiplex array	[98]
Tears	15 diabetic patients without DR, 15 DR patients, and 15 controls	No significant difference was found between any of the groups	Multiplex bead immunoassay	[13]

MMP2 is one of the most pervasive members of the matrix metalloproteinase family, responsible for the cleavage of collagen of the extracellular matrix, thus maintaining equilibrium between matrix synthesis and degradation. The balance of this protein is critical for cell integrity and survival [99,100]. In diabetic patients, a link with increased expression of MMP2 has been described in the past [101]. More recently, it has also been connected with DM and DR development and progression. Table 2 reflects the studies where MMP2 levels have been quantified in DR and diabetic patients.

Table 2. Published articles that quantify MMP2 in different biological fluids from DR and DM patients.

Fluid	Population	Key findings	Technique	Reference
VH	24 PDR patients and 13 controls	Concentration was significantly higher in PDR patients than in controls	Enzyme immunoassay (EIA)	[17]
Plasma	93 type 1 diabetic patients and 50 healthy controls	Concentration was significantly higher in diabetics than in controls	Luminex	[102]
	306 type 1 DM patients with vascular complications (including DR) and 187 without vascular complications	Severity of retinopathy was significantly associated with higher levels of MMP-2	ELISA	[103]
Tears	27 type 1 DM children and 17 healthy controls	Significantly higher levels in disease group	ELISA	[104]

As noted in Tables 1 and 2, there are few studies that quantify IL-6 and MMP2 in DR patients, and the present dissertation brings more knowledge to the field. To study molecular biomarkers in DR, the most widely used fluids are the vitreous humor (VH) and aqueous humor (AH) collected by invasive means. Recently, less invasive methods using tears, saliva, urine and blood samples have come into play.

2.4.1. Invasive sampling for molecular biomarker profiling

DR's biomarker research was initially focused on the ocular fluids obtained during surgery, which include the VH and the AH.

The VH is a transparent gelatinous mater found in the eye's posterior segment (as exposed in Figure 2.a, in-between the lens and the retina). It gives the eye its spherical shape, comprising about 80 % of the eyeball's volume. The VH provides the lens and cornea with nutrients, coordinates eye growth, aids in light transmission and supports the retina [105]. The VH is avascular in nature, which means that much of the its protein content is derived from the retina itself, making retinal pathologies reflect in the VH's composition. Therefore, this fluid can be used to monitor retinal diseases, DR included [12,106–108]. VH samples can be obtained during a vitrectomy (Figure 4.a), through a needle biopsy or *post mortem* [12]. All of the previously mentioned methods are highly invasive, which means that VH can only be obtained from individuals undergoing treatment for DR management, and recurrent sampling is disabled. As a matter of fact, no true healthy controls can be used as comparison, so controls are usually patients with other ophthalmic diseases undergoing vitrectomy.

The AH is stored in the anterior chamber of the eye (Figure 2.a), after being produced by the ciliary body. Its main functions are nutrient and oxygen supply, removal of metabolism derived excretory products, ocular immunity, shape and refraction [109]. The AH has a much lower protein content when compared to the VH, hampering biomarker analysis. However, protein concentration increases in disease [109]. Despite not being in direct contact with the retina, retinal-derived proteins are present in the AH because of BRB disruption, through cilio-retinal circulation, or diffused by the VH through the VH-AH barrier [110]. Consequently, it is also used as biomarker source fluid. Like the VH, the sampling procedure is highly invasive and performed during surgery (Figure 4.b). Tables 1 and 2 features some studies where both the VH and AH were used for DR biomarker analysis.

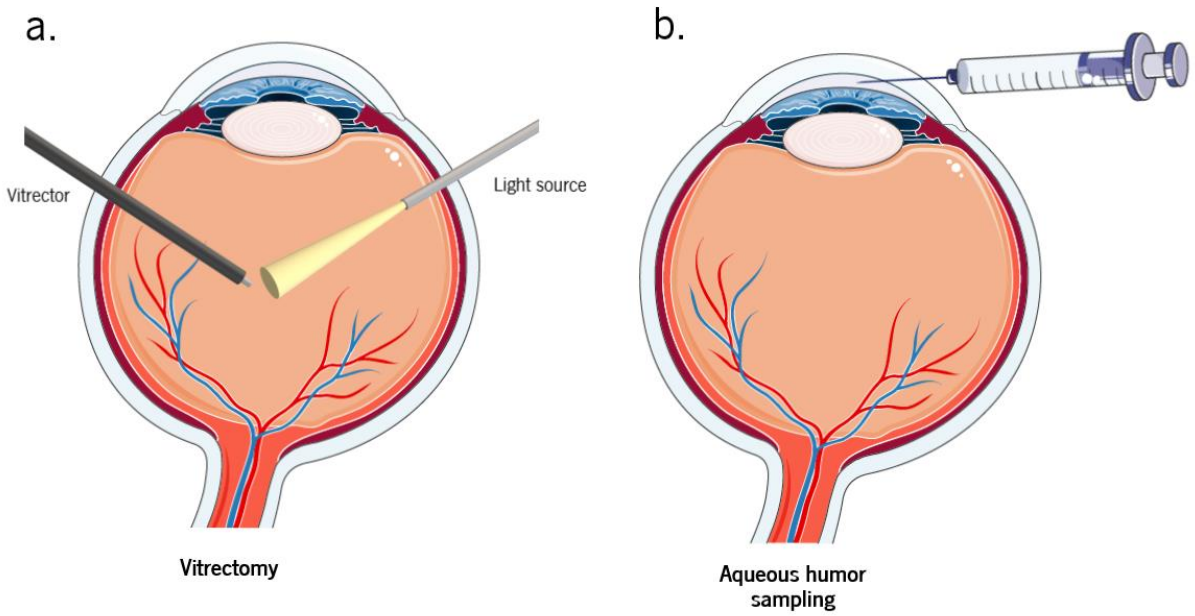

Figure 4. Invasive ocular fluids sampling. a. Schematic representation of a vitrectomy and b. the procedure for AH sampling.

Biomarker-based diagnosis can only be achieved if a large number of samples from patients and true controls is possible. Therefore, the search for minimally invasive biological fluids is notoriously advantageous and has been highly researched recently, as explained in the next section.

2.4.2. Minimally invasive sampling for biomarker profiling

Because DM is a systemic disease, biomarkers are found in the patients' circulation, and can be used for detecting and monitoring disease progression. Blood serum and plasma can be used as source fluid for detecting altered proteomic levels in DR, given its notorious microvascular component. Even though blood sampling is an invasive procedure, it is commonly performed for multiple purposes, allowing for continuous collection of samples, and also the comparison between control populations and DR patients in multiple clinical stages [87].

Tear fluid contains proteins, lipids, salts, mucins and other organic molecules, making it a complex aqueous solution produced by the lacrimal gland at a 1 – 2 µl min^{-1} production rate. They act as a lubricant agent, protect and maintain the underlying tissues' health [111]. In a recent past, studies have found the potential of using tears for diagnosing and monitoring mainly ophthalmic diseases, including DR. The main reason for the potential of using tears as biomarker source fluid is the fact that they are collected

by minimally invasive means, contrary to other ocular fluids abovementioned. Because of this, pre-screening, diagnosing and staging is enabled by the use of tears [13]. Figure 5 is a schematic representation of the methods used for tear sampling.

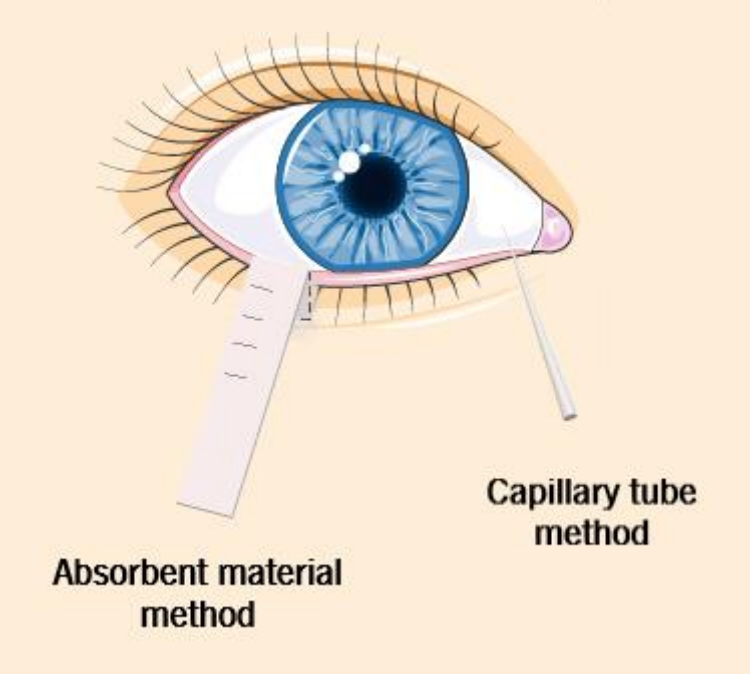

Figure 5. Schematic representation of tear collection methods.

In the first method, an absorbent material (namely blotting paper, filter paper, cellulose or cotton) is placed in the lower conjunctival sac where it is soaked with tears, and posteriorly eluted. A low-grade inflammatory response takes place, resulting in a variable amount of the mucous layer and the contents of disrupted epithelial cells being collected. The sample volume acquired with the absorbent material method varies with the material used, but is usually between 10 and 60 µL. On the other hand, when small glass capillaries are used, capillary suction delivers pure basal tear fluid, and no inflammation disturbs the eye. However, this method usually results in sample volumes between 2 and 10 µL [112]. As exposed, tear samples have the disadvantage of delivering very low volumes, which can be further hampered by evaporation, alterations in the patient's secretion rate and mixing. Moreover, it is important to highlight that DM progression is associated with dry eye disease, and PDR patients commonly suffer from it [15].

Saliva is another non-invasive biological fluid used as a biomarker source, particularly for oral diseases, but also in systemic disorders. Studies have proved the potential of salivary proteome analysis for DR diagnosing and monitoring [14,113].

Urine has also been used as a non-invasive biological fluid. In fact, urinary albumin to creatinine ratio has been proposed as an estimate of microalbuminuria, which is a risk factor for cardiovascular complications in individuals with DM [114]. Furthermore, urine is often used as a biomarker source fluid for diabetic nephropathy assessment, since the kidneys are the organ most affected by this condition [115]. When it comes to DR, a study has used urine for biomarker assessment. However, the biomarker selected is related to oxidative stress, which is a concern for all diabetic patients. The authors also mention the correlation of the selected biomarker with diabetic nephropathy, and assume their technique to be a screening tool, rather than a diagnosing one [116]. This study will be addressed with more detail in section 2.4.4. The complexity of urine and anatomic distance to the eye make retinal alterations hard to assess in urine.

When comparing all abovementioned fluids, the VH and blood have the advantage of being in direct contact with the retina. However, the collection of AH and VH is performed in highly invasive procedures, during different surgeries for DR managing. Acquiring these samples is only possible when necessary for the patient's health, disabling the obtainment of adequate amounts of samples from patients and, more important, healthy individuals. As so, AH and VH are not adequate biomarker source fluids for diagnosing and monitoring. On the other hand, blood, urine, saliva and tears can be collected with minimal discomfort. Even though tears do not directly contact with the retina, they can be used as a window for pathological events occurring there [117]. Tears' anatomical position in the eye brings them an advantage over blood, urine and saliva samples, since local variations can be measured only on the proximity of the eye. From all of the biological fluids mentioned, saliva sampling is one of the least invasive and uncomfortable methods. Even though the use of this fluid for DR diagnosing and monitoring has not been widely explored, it would greatly facilitate the process of sample acquisition and thus can be an alternative or complement option to tear fluid.

After covering the most used fluids for DR biomarker analysis, an introduction to the conventionally used techniques to quantify biomarkers is in order.

2.4.3. Conventionally used technologies for molecular profiling

Using minimally invasive biological fluids such as tears and saliva as biomarker source for diagnosing and staging DR is notoriously preferable to the other commonly used ocular fluids because of the minimally invasive nature of the sampling process. Altered biomarker levels could potentially complement other DR diagnosing techniques, and enable an early and personalized diagnosis. However, there is a need for technologies that can achieve great sensitivity and selectivity in minute sample volumes.

Conventional techniques such as electrophoresis, high-performance liquid chromatography (HPLC), ELISA, mass spectrometry, and microarrays approaches have been successfully applied in many DR biomarker studies (as will be exposed next). In the present dissertation, ELISA and Luminex technologies were used as conventional methods for comparison purposes.

ELISA is a quantitative analytical technique that relies on antibody-antigen interactions. The use of a labeled enzyme results in a color change that is proportional to the concentration of analyte in solution. This color change is measured optically and a single analyte is quantified [118].

Luminex is another biomolecular detection technology that brings the advantage of multi-biomolecule detection in a single sample. It has high throughput, high sensitivity, requires lower sample volumes (50 µL) when compared with ELISA (typically 100 µL), and also lower costs. The technique used to quantify molecules in Luminex is flow cytometry. Multiple beads labeled with different dyes bind to different target analytes. Subsequently, a reporter molecule binds to the conjugated beads, enabling the detection of that analyte in solution [119]. Table 3 lists the studies where conventional methods have been applied for different DR biomarkers, in different fluids.

Table 3. The use of conventional technologies for molecular biomarker detection and quantification in DR patients.

Biomarker	Fluid	Technique	Volume	Sensitivity (LOD)	Reference
Interleukin-1 receptor antagonist (IL-1ra)	Tears	Multiplex bead immunoassay	50 µL	5.5 pg mL^{-1}	[13]

Table 3. The use of conventional technologies for molecular biomarker detection and quantification in DR patients (cont.).

Biomarker	Fluid	Technique	Volume	Sensitivity (LOD)	Reference
IL-6	VH	ELISA	100 µL	0.70 pg mL^{-1}	[93]
	AH	Multiplex bead immunoassay	25 µL	0.4 pg mL^{-1}	[97]
	Serum	ELISA	100 µL	0.03 pg mL^{-1}	[16]
	Serum	Cytometric bead multiplex array	50 µL	2.4 pg mL^{-1}	[98]
	Tears	Multiplex bead immunoassay	50 µL	2.6 pg mL^{-1}	[13]
Interferon-induced protein-10 (IP-10)	VH	Bio-Plex assays	50 µL	6.1 pg mL^{-1}	[44]
	AH	Multiplex bead immunoassay	25 µL	0.3 pg mL^{-1}	[97]
	Tear	Multiplex bead immunoassay	50 µL	6.1 pg mL^{-1}	[13]
Monocyte chemoattractant protein-1 (MCP-1)	VH	Bio-Plex assays	50 µL	1.1 pg mL^{-1}	[44]
MMP2	VH	EIA	100 µL	2.4 pg mL^{-1}	[17]
	Plasma	Luminex	50 µL	25.4 pg mL^{-1}	[102]
	Plasma	ELISA	25 µL	120 pg mL^{-1}	[103]
Nerve growth factor (NGF)	VH	ELISA	100 µL	14 pg mL^{-1}	[120]
	Serum	ELISA	100 µL	14 pg mL^{-1}	[121]
	Tears	ELISA	100 µL	14 pg mL^{-1}	[121]

Table 3. The use of conventional technologies for molecular biomarker detection and quantification in DR patients (cont.).

Biomarker	Fluid	Technique	Volume	Sensitivity (LOD)	Reference
TNF-α	VH	ELISA	100 µL	39.1 pg mL^{-1}	[120]
	Serum	ELISA	200 µL	39.1 pg mL^{-1}	[122]
	Serum	ELISA	0,1 mL	39.1 pg mL^{-1}	[123]
	Tears	ELISA	100 µL	39.1 pg mL^{-1}	[124]
VEGF	VH	Bio-Plex assays	50 µL	3.1 pg mL^{-1}	[125]
	VH	Bio-Plex assays	50 µL	3.1 pg mL^{-1}	[44]
	AH	Multiplex bead immunoassay	25 µL	1.73 pg mL^{-1}	[97]
	Serum	ELISA	50 µL	15.6 pg mL^{-1}	[126]
	Serum	ELISA	0,1 mL	15.6 pg mL^{-1}	[123]

As can be seen in Table 3, sample volume requirements for some of these techniques make them incompatible with direct tear analysis. Furthermore, these methods are expensive and demand tedious preparations. In the next section, POC technologies meant to improve DR diagnosis using minimally invasive fluids are presented.

2.4.4. Point-of-care molecular-based technologies for improved diabetic retinopathy diagnosis through minimally invasive fluids

Recently, some studies have emerged with novel technologies for DR diagnosing. They present better sensitivity and lower sample volume requirements, using non or minimally invasive methods [127]. However, this research field is still in its infancy and only a few innovative studies have been reported in the literature (Table 4).

Table 4. Analysis of the published POC technologies for biomarker detection and DR diagnosis in minimally invasive fluids.

Biomarker	Fluid	Technique	Volume	Linear range (LR)	LOD	Reference
8-Hydroxy-2'-Deoxyguanosine (8-OHdG)	Urine	Colorimetric immunosensor	80 µL	0 - 70 ng mL^{-1}	5 ng mL^{-1}	[116]
Lactoferrin (LCF) + β2-microglobulin (B2M)	Tear	Impedimetric immunosensor	2 µL	0.001 - 1 ng $mL^{-1}$and 0.1 - 10 mg mL^{-1}	0.001 ng mL^{-1} and 0.1 mg mL^{-1}	[128]
LCN1 + VEGF	Tear	Optoelectrokinetic bead-based immunosensor	1.5 µL	100 pg mL^{-1} - 10 µg mL^{-1}	100 pg mL^{-1}	[129]
TNF-α	Tear	Diffusometric immunosensor	10 µL	1 pg mL^{-1} - 10 µg mL^{-1}	10 pg mL^{-1}	[130]
	Tear	Impedimetric immunosensor	1 µL	1 - 25 pg mL^{-1}	0.085 pg mL^{-1}	[131]

For instance, it has already been pointed out that DR development and progression, and glycemic control are strongly correlated. HbA1c is a reflector of glycemic levels and is the only validated marker of DR, routinely measured in clinical practice. However, POC HbA1c assays (which use finger-prick technology to collect a single drop of blood and are, therefore, minimally invasive) have not been used for DR diagnostic purposes, due to their lack of accuracy [88]. To the author's knowledge, no POC technologies are available to diagnose or assess the stage of DR through blood.

In 2020, a gold nanoparticle-based colorimetric lateral flow immunoassay incorporated in a paper strip was presented, for the quantification of urine 8-OHdG and subsequent differentiation between low risk (no or mild DR) and high risk (moderate or severe DR) patients [116]. 8-OHdG, a biomarker associated with oxidative stress, produced color changes in the paper strip upon contact with the sample (Figure 6.a.), and a smartphone was used for distinguishing different colors, and thus quantifying 8-OHdG. This

technology achieved a sensitivity and specificity of 91 % and 81 %, respectively. The average concentration of 8-OHdG in the low risk group was 22 ± 10 ng mg^{-1} of creatinine and 55 ± 11 ng mg^{-1} of creatinine, in the high risk group (Figure 6.b.). However, PDR patients were excluded from the study population, and 8-OHdG is also present in diabetic nephropathy that often coexists with DR [11], making this biomarker not DR-exclusive. This technology shows great potential for self-monitoring and may be used as a screening tool, but not a diagnostic one.

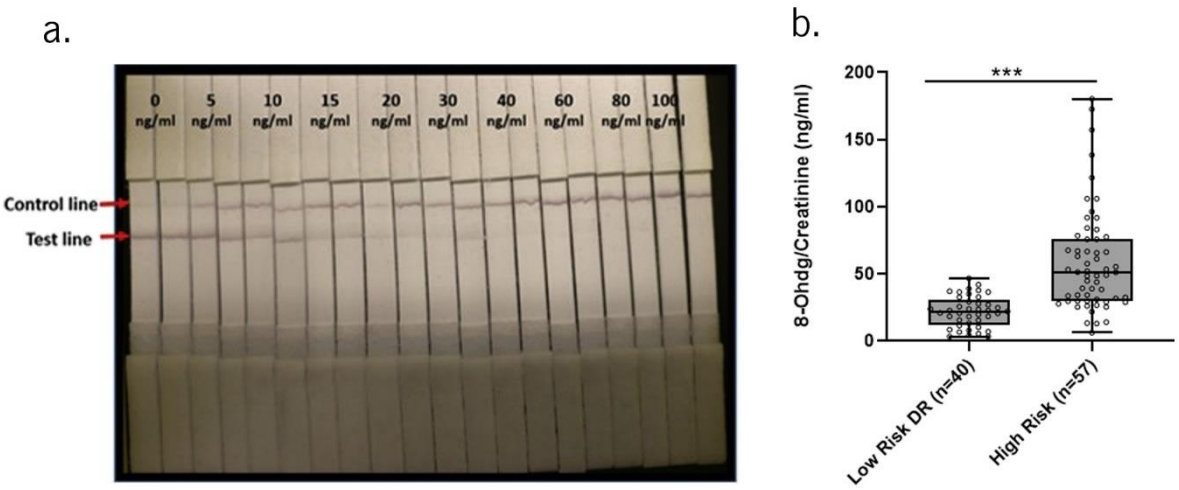

Figure 6. Lateral flow immunoassay paper strip for 8-OHdG detection in urine. a. Photograph of the paper strip and b. distribution of urine 8-OHdG/creatinine values of patients with low and high risk DR. Reproduced with the permission of Elsevier [116].

A bead-based sandwich immunoassay combined with rapid electrokinetic patterning (REP) was recently described for the detection of LCN1 in tear fluid [132]. To achieve high sensitivity of low-biomarker concentrations, the fluorescent signal was enhanced by using immunocomplex conjugated particles with amine-modified particles functionalized with anti-LCN1 antibody, secondary antibodies conjugated with dyes or quantum dots, and REP-induced particles. With 1.5 µL of tear sample, the LOD achieved by this technology was 110 pg mL^{-1}.The authors suggest that it can be used for DR diagnosing purposes because the concentration of LCN1 in tears of DR patients is 2 to 3 times higher than in healthy controls [133,134]. The authors also point out the possibility of using multiple biomarker detection.

A similar method was applied for the simultaneous measurement of LCN1 and VEGF in tear fluid [129]. The presence of these two biomarkers was primarily enhanced by the formation of sandwiched

immunocomplexes on the microbeads, leading to dose dependent fluorescent intensities, and secondary signal enhancement was achieved by REP. This way, a LOD of 100 pg mL^{-1} was achieved. Analyzing a study population of PDR and non-PDR patients (the latter including healthy subjects and NPDR patients), they determined values of 250 µg mL^{-1} and 10 ng mL^{-1} as threshold for LCN1 and VEGF, respectively, for the detection of PDR, with 92.9 % sensitivity, 90.9 % specificity and 88.5 % accuracy values. Moreover, the authors conducted single-blind tests with tear samples from 5 individuals, and the results are presented in Figure 7.

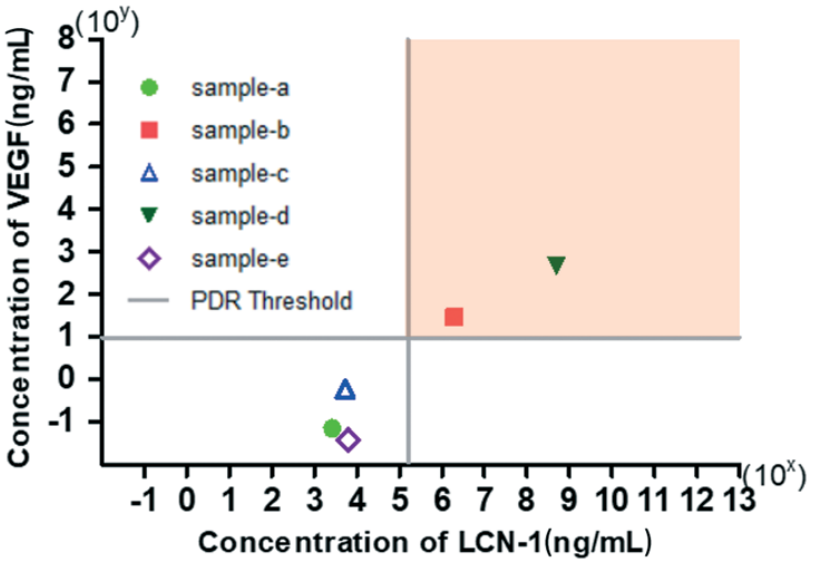

Figure 7. Concentration distribution of the single-blind tests. The solid lines define the thresholds of LCN1 and VEGF for PDR. The 4th quadrant is the suggested PDR domain. The hollow icons represent healthy subjects, whereas the solid icons represent the patients with PDR [129]. Published by The Royal Society of Chemistry (RSC) on behalf of the European Society for Photobiology, the European Photochemistry Association, and RSC.

As can be observed in Figure 7, threshold-based diagnosis was successful for 80 % of cases, with *sample-a* being incorrectly classified as a healthy subject. This sample was obtained from a recovered patient with a history of PDR.

A high sensitivity and reproducible impedimetric biosensor was also reported for the quantification of TNF-α in relevant body fluids, including blood serum and tears [131]. The platform was based on antibody-antigen interactions, and read values between 1 and 25 pg mL^{-1}, with a 0.085 pg mL^{-1} LOD for

tears, and 2 pg mL^{-1} for blood serum, showing great potential as POC platform for inflammatory disease screening and therapeutic monitoring.

A label-free impedimetric biosensor based on a poly(3,4-ethylene diozythiophene)/gold nanoparticles (AuNPs) composite was also reported for the quantification of VEGF, that may be applied to clinical diagnosis of VEGF-mediated diseases [135]. Three different electrode sensor designs were tested (namely free-standing pads, screen printed dots and interdigitated micro-strip electrodes), and the interdigitated design showed better stability and reproducibility. LR and LOD of 1 – 20 pg mL^{-1} and 0.5 pg mL^{-1}, respectively, were achieved.

A diffusometric immunosensing platform was reported for the detection of DR through the quantification of TNF-α in tears [130]. They enhanced the signal by grafting additional AuNPs to capture particles to enhance size changes. Also, a dichotomous method was settled to make the technique suitable for practical use, avoiding calibration. A LOD of 10 pg mL^{-1} was achieved, and also chosen as the threshold value of TNF-α concentration for distinguishing healthy subjects from PDR patients.

Another biosensor with a functionalized multi-layer paper-based platform was developed for the detection of LCF and B2M [128]. This platform was connected to a handheld printed circuit board (PCB) for real-time measurement of LCF and B2M, two biomarkers associated to dry eye syndrome and DR, respectively. A LR between 0.001 and 1 ng mL^{-1} and 1 to 10 mg mL^{-1} was respectively reported.

To achieve precise, low and specific biomarker quantification meant for tear or saliva sample profiling for the diagnosis of DR, the present work used an electrochemical immunosensor. These sensors also bring the advantages of high cost-effectiveness and low response times, and enable the integration in POC devices. Thereafter, electrochemical sensors will be introduced in the following section.

2.5. Electrochemical sensors

Not only in the clinical diagnostics and in medical applications, but also in many other different fields like agriculture, industry and military, the analysis of biological and biochemical data is of extreme importance. However, this translation from biological to measurable electrical data is currently a tedious and time-consuming process. To answer this unmet need, biosensors have been explored widely, with an estimated 60 % annual growth rate, being the healthcare industry its main sponsor [18]. It is widely accepted that a biosensor is “an analytical device which incorporates a biologically active element with an appropriate

physical transducer to generate a measurable signal proportional to the concentration of chemical species in any type of sample" [136]. With advances in device technology, biosensors now sometimes surpass conventional sensing systems in terms of LOD.

Biosensors have two main components: a biorecognition element and a transducer (Figure 8). Biorecognition elements have an immobilized biocomponent meant to detect the specific target analyte. The transducer's role is to make the conversion from the biochemical signal that results from the interaction between the target analyte and the bioreceptor, into an electrical signal. The target analyte's concentration is directly or inversely reflected in this signal.

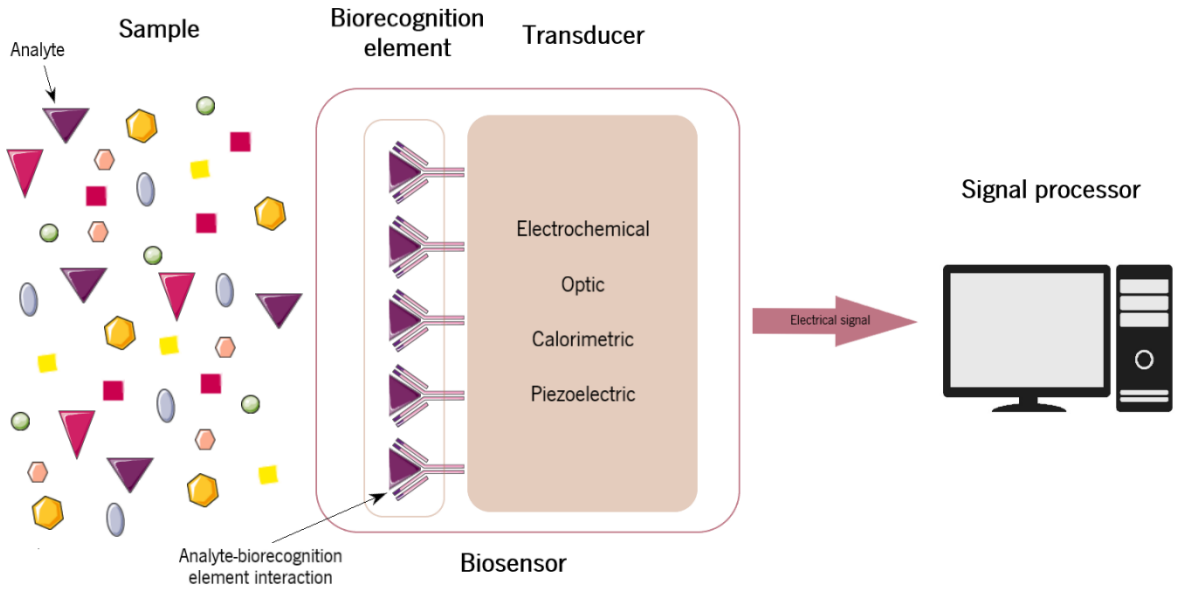

Figure 8. Schematic layout of a biosensor.

When it comes to type of transduction, as pointed out in Figure 8, biosensors are divided into 4 groups: electrochemical, optical, piezoelectric and thermal sensors. This section will focus on electrochemical sensors because of their importance to the present work.

High specificity, sensitivity, and selectivity, in combination with low response time and cost-effectiveness are the reasons why electrochemical biosensors have been highly explored. According to a technical report about the recommended definitions and classification of this type of sensors, "an electrochemical biosensor is a self-contained integrated device, which is capable of providing specific quantitative or semi-

quantitative analytical information using a biological recognition element (biochemical receptor) which is retained in direct spatial contact with an electrochemical transduction element" [137].

2.5.1. Biorecognition elements

The biorecognition element is crucial for the biosensor. Originally, these were extracted from living systems, but advances in material engineering have made recognition element synthesis possible in laboratory [138]. In a solution, molecules collide billions of times per second. The establishment of stable and specific interactions is only possible when the surface properties of one molecule are complementary to the other (*i.e.*, when repulsive forces and entropic costs of bringing them together are surpassed by the attractive forces created by the interaction between the two). Molecular recognition plays a vital part in biosensor systems and is defined as the process of specific binding between molecules (macromolecules or molecular assembly) and respective target molecule/analyte [18]. Biorecognition elements are usually divided into three categories: natural, semi-synthetic and synthetic (Figure 9).

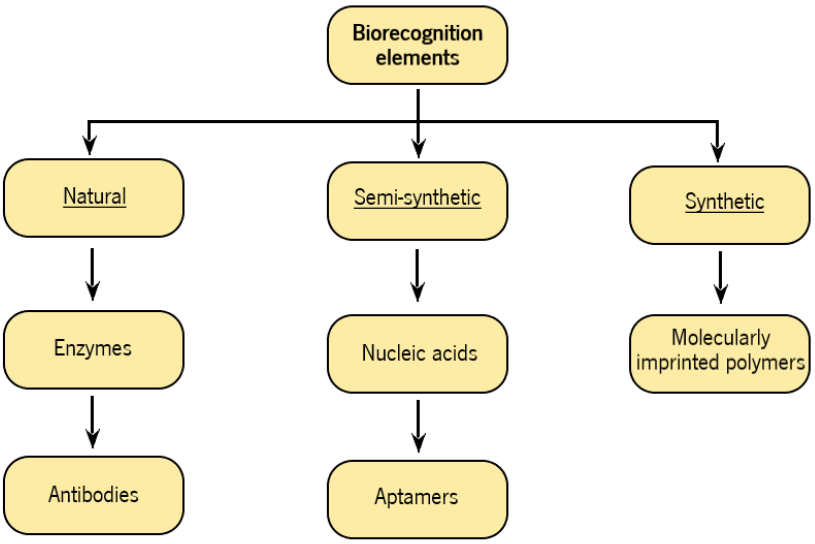

Figure 9. Schematic representation of different biorecognition elements used for biosensing.

In the present work, antibodies were used as biorecognition elements. Antibodies are Y-shaped immunoglobulins formed by two heavy chains and two light chains, which comprise a constant and variable part. The latter binds with the corresponding antigen in a highly specific and selective way [19].

Antibody-based biosensors, or immunosensors, are some of the most preferred types of biosensors due to their high specificity, stability and versatility. Comparable to a lock-and-key model, the interaction between a specific antibody and its unique antigen is highly selective, and a three-dimensional (3D) structure is formed. This unique property of antibodies and their ability to identify molecular structures enables the development of antibodies that bind specifically to chemicals, biomolecules and microorganisms that can be detected at very low concentrations and in complex biological matrices (blood, cerebrospinal fluid - CSF, etc.) [139].

Optical and electrochemical are the most widely used transduction methods for immunosensors. Still, optical-based immunosensors achieve lower sensitivity when compared with electrochemical immunosensors, and the latter provide fast, simple, and economical detection [18]. The use of electrochemical immunosensors will vastly improve public health by providing rapid detection, high sensitivity, and specificity in clinical chemistry, food quality, and environmental monitoring.

2.5.2. Electrodes and interfaces of a biosensor system

In electrochemical systems, charge flows through the interface between an electrochemical conductor (an electrode) and an ionic conductor (an electrolyte). The movement of electrons (and holes) is responsible for the transport of charge in the electrode, while the movement of ions carries charge in the electrolyte phase [20].

A three-electrode cell, schematized in Figure 10, is composed of a working electrode (WE), a reference electrode (RE) and a counter or auxiliary electrode (CE). Since the reactions are only detected in the proximity of the electrodes' surfaces, they have a significant role in the overall performance of the biosensor, and detection ability depends on electrode material, dimensions and surface modifications. The RE is commonly made from Silver/Silver Chloride (Ag/AgCl) and kept distant from the reaction site, so it maintains a known and stable potential. The transduction element of an electrochemical sensor is the WE, where the biochemical reaction takes place. Its potential is monitored relative to the RE. The CE forms a connection with the electrolytic solution, so that a current can be applied to the WE. Platinum, gold, carbon and silicon compounds are commonly chosen materials for the WE and CE, for their conduction and stability [140].

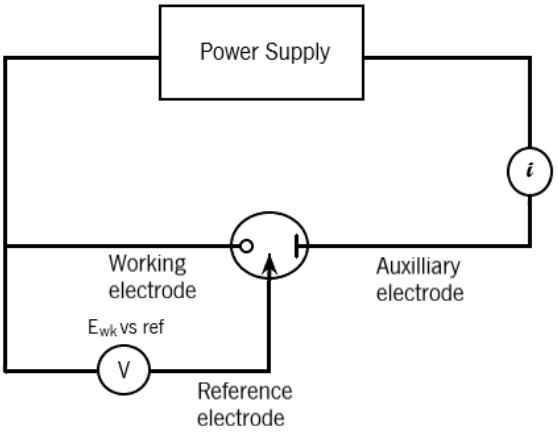

Figure 10. Schematic representation of a three-electrode cell.

Two independent half-reactions describe the chemical changes at the WE and RE. Equations (1) and (2) describe the oxidation and reduction reactions, respectively, where A and B are two hypothetical elements that are being oxidized and reduced.

$$A \rightleftharpoons A^{+} + e^{-} \tag{1}$$

$$B + e^{-} \rightleftharpoons B^{-} \tag{2}$$

Each half-reaction is a function of the interfacial potential difference at the electrode, and the chemical composition of the system near the electrode is consequently altered. Since the WE is the location of interest to study these differences, the RE is made up of phases having essentially constant composition, which results in a fixed potential. Consequently, any changes in the cell are attributed to the WE, and its potential measured with respect to the RE. When more negative potentials are applied to the WE, the energy of the electrons is raised, and they transfer into available electronic states on the electrolyte species. It is said that a reduction current occurs, because a flow of electrons from electrode to solution is happening. On the other hand, more positive potentials applied at the WE lower the electrons' energy and leads to more favorable energy on the electrode, which at some point makes electrons attached to solutes in the electrolyte transfer to the electrode (oxidation current) [20]. The third electrode (CE) functions as a cathode whenever the WE is on anode mode, and *vice versa* [18].

The current resultant from the half-reactions is measured using a potentiostat, that controls the WE's potential. The concentrations of the reduced and oxidized forms of a redox couple are linked to the potential (E) through the Nernst equation (3):

$$E = E^0 + \frac{RT}{nF} \ln\left(\frac{[Oxidized\ form]}{[Reduced\ form]}\right) \quad (3)$$

where E^0 represents the cell's standard potential (V), R is the gas constant (J K^{-1} mol^{-1}), T is the absolute temperature (K), n is the number of electrons transferred, F is the Faraday constant (C mol^{-1}) and $[Oxidized/Reduced\ form]$ is the concentration of the oxidized or reduced species (mol L^{-1}). When different potentials are applied to the WE, the redox species at the electrode's surface adjust their concentration ratios according to the Nernst equation. The resulting electrical signal is related to the recognition process through the target analyte and proportional to the analyte's concentration [18]. Since the extent of chemical reaction is proportional to the amount of charge transferred (which is stated in Faraday's law), these processes are called faradaic.

The occurrence of these redox reactions results on the accumulation of either the oxidized or the reduced species in the electrode's surface. So, the maintenance of the redox reactions relies on the mass transport of the electroactive species from the bulk solution to the WE surface. The concentration gradient between reduced and oxidized species limits these movements, and it is said that diffusion limits mass transport. This will impair the ability of the electrochemical cell to pass current (contributing to the system's impedance), as will be further explained later.

Figure 11 illustrates the electrical double layer formed between the electrode surface and the solution. As can be observed, the solution side of the double layer contains itself several layers. The inner layer, also called compact, Helmholtz or Stern layer, contains solvent molecules and sometimes other species (ions or molecules) that are said to be specifically adsorbed. This area is limited by the inner Helmholtz plane (IHP). Solvated ions oppositely charged to the WE approach the metal, and the position of the centers of the nearest ions is called the outer Helmholtz plane (OHP).

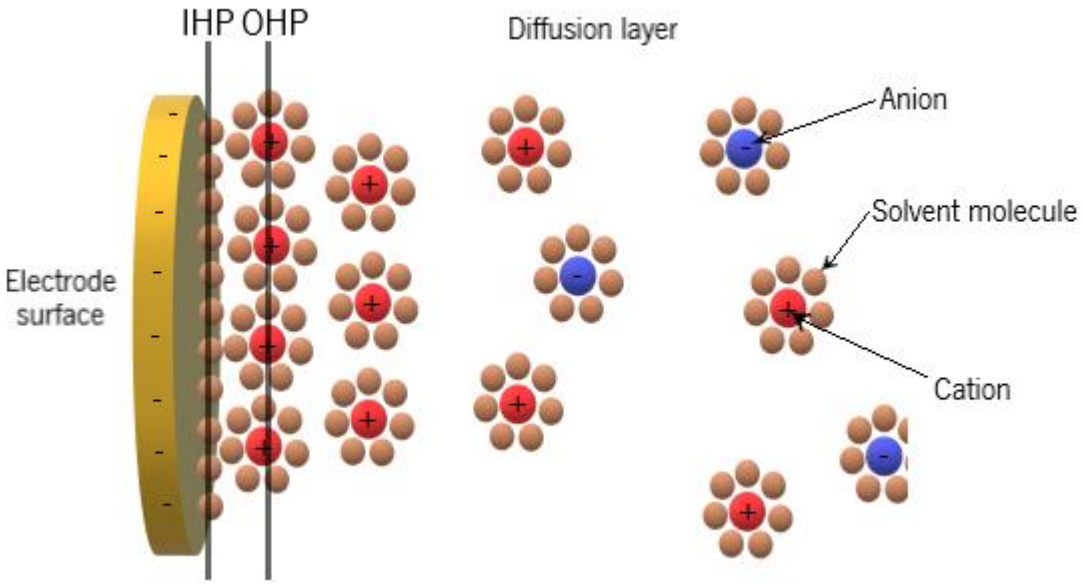

Figure 11. Proposed model for the electrical double layer.

The interaction between the solvated ions and the charged metal of the electrode surface involves only long-range electrostatic forces, essentially independent of the chemical properties of the ions. They are said to be non-specifically adsorbed. Thermal agitation in the solution makes these ions be distributed in a 3D region that is known as the diffusion layer, extending from the OHP into the bulk of the solution [20].

The use of electrochemical sensors relies on very complex phenomena. To simplify the interpretation of results, equivalent circuits are commonly used. These theoretical circuits are simplifications of more complex systems, both behaving similarly. Complex phenomena are replaced by commonly studied circuit elements, enabling much more direct analysis. The present work used a Randles equivalent circuit to mimic the developed system, and an introduction to this type of equivalent circuits follows.

2.5.3. Randles equivalent circuit

Generally speaking, an electrochemical cell can be viewed simply as an impedance to a small sinusoidal excitation. Accordingly, it can be represented by an equivalent circuit of resistors and capacitors. A frequently used circuit called Randles equivalent circuit is schematized in Figure 12. The current passing through the WE is influenced by both the faradaic process (i_f) and double-layer charging (i_c), displayed in parallel so that the resulting current is the sum of both branches. As introduced earlier, a double layer

is formed between the electrode surface and the solution. This acts as a nearly pure capacitor and C_{dl} represents it in the Randles equivalent circuit. Since all current must pass through the solution, its resistance is inserted as a series element (R_s) to account for that effect. On the other hand, simple linear circuit components do not adequately portray faradaic processes because these are not frequency independent. The faradaic process is represented by a general impedance (Z_f), which can be divided into the charge-transfer resistance (R_{ct}), and another general impedance called the Warburg impedance (Z_W) which stands for the above explained resistance to mass transfer, from the bulk solution to the electrode surface and *vice versa* [20].

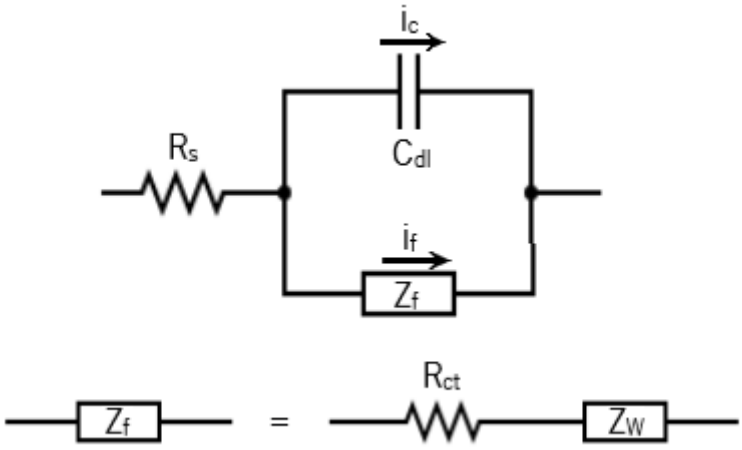

Figure 12. Equivalent circuit of an electrochemical cell and subdivision of Z_f into R_{ct} and Z_W.

As stated before, the capacity of the WE to reduce/oxidize the redox probe is the phenomena of interest when using electrochemical biosensors. Biofunctionalization steps add layers to the electrode surface where the electron transfer process will occur. Applying negative potentials to the WE results in the passage of electrons from the WE surface to the oxidized species, reducing it. This reduced form will then diffuse to the bulk solution [20]. These redox reactions produce a current that can be assessed by the following equation:

$$i = vnFA \tag{4}$$

i representing the current (A), v the electron transfer rate (mol cm^{-2} s^{-1}), n the stoichiometric number of electrons consumed in the electrode reaction, F the Faradaic constant (C mol^{-1}), and finally A the electrode area (cm^2) [20].

The rate of the reduction and oxidation processes is given by equations (5) and (6), respectively.

$$v_c = k_c[O'_{ads}] \tag{5}$$

$$v_a = k_a[R'_{ads}] \tag{6}$$

where v_c and v_a represent the reduction and oxidation reaction rates (mol cm s^{-1}), respectively, k_c and k_a represent the reduction and oxidation reaction rate constants (cm s^{-1}), and last, $[O'_{ads}]$ and $[R'_{ads}]$ represent the concentration of the oxidized or reduced species, respectively, adsorbed on the electrode's surface (mol cm^{-3}) [20]. Substituting v_c or v_a in equations (5) and (6) gives the electrical current flowing from the reduction or oxidation reactions, respectively:

$$i_{reduction} = k_c[O'_{ads}]nFA \tag{7}$$

$$i_{oxidation} = k_a[R'_{ads}]nFA \tag{8}$$

It is therefore possible to conclude that the electrode area, the concentration of redox species on the electrode's surface, the nature of the redox species themselves, and their rate constants determine the current flowing from an electrode. Temperature and electrode potential modulate these variables [20].

Ultimately, the current is governed and limited by the rates of the following processes: a) mass transfer (from the bulk solution to the electrode surface), b) electron transfer (at the electrode surface), c) chemical reactions preceding or following the electron transfer, d) other surface reactions (such as adsorption). In conclusion, modifications that decrease the reaction rate of any of these processes is equivalent to an increase of the resistance of the overall process, reflected on the charge transfer resistance (R_{ct}) [20].

The way a biosensor works and identifies analytes in a solution has already been elucidated. The next section brings light into the methods used to monitor the biofunctionalization process and quantify the target analyte's concentration in solution.

2.5.4. Detection techniques

In an electrochemical biosensor, quantifying the interest analyte may be accomplished by amperometry/voltammetry (where current level is assessed), by electrochemical impedance spectroscopy (EIS, which measures a change in the system's impedance) or by potentiometry (where an alteration in charge accumulation or potential is measured). In the following sections, cyclic voltammetry (CV) and EIS will be presented in detail due to their importance in the present dissertation.

2.5.4.1. Cyclic voltammetry

When potential is kept constant, and current generated by electrochemical reactions is evaluated, the technique is called amperometry. On the other hand, the measurement of current against varying potential, is called voltammetry.

In CV, the potential on the WE is swept at a constant rate (in $V\ s^{-1}$), and the resulting current is recorded *versus* time [140]. The term *cyclic* comes from the fact that, when a specific potential is reached, the sweep is reversed back to the starting potential. Since the sweep rate is constant, and initial and switching potentials are pre-determined, time can be easily converted to potential, resulting in a graphic like the one on Figure 13, where current *versus* applied potential (voltammogram) is shown. The sweep rate must provide enough time for the redox reactions to take place. This technique is one of the most widely used electrochemical techniques to monitor the behavior of electroactive species in solution.

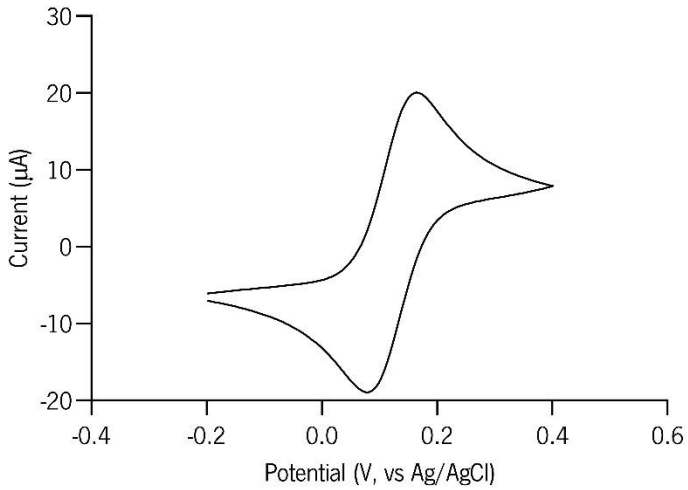

Figure 13. Example of a cyclic voltammogram.

When scanning positively, before reaching the cell's standard potential, only non-faradaic current is produced. Once the standard potential is reached, oxidation of the electrolyte's reduced species starts and faradaic current (in this case, anodic) starts to flow. The current reaches its maximum value at the anodic current peak ($i_{p,a}$). At this point, the concentration of reduced species left to oxidize is nearly depleted in the vicinity of the electrode and delivery of more reduced species to the electrode's surface is dependent on mass transport. Oxidized species accumulate on the electrode's surface, creating a diffusion layer and slowing down the mass transport, which results in the decrease of the anodic current, until further increases in potential no longer reflect on the current value, and a steady-state is reached. When the scan is reversed, the opposite occurs, as the reduction of oxidized species that were concentrated in the vicinity of the electrode starts, and a cathodic current is created [20]. The reversibility of these reactions provides information about electron transfer kinetics between the electrode and the analyte [140]. According to the Nernst equation, the equilibrium should be achieved immediately upon any potential change, when no barrier to electron transfer exists. However, more positive potentials are required to drive the oxidation reaction (or the opposite for reduction) if a barrier to electron transfers is present. This barrier could be built by the increase of a diffusion layer.

Biofunctionalization layers applied in sensors increase the thickness of the diffusion layer, and higher potential variations (ΔE_p) are required to drive the redox reactions. In biosensing, a redox probe is used to mediate the electrochemical reactions at the WE. The peak current's value is proportional to the concentration of the electroactive species.

2.5.4.2. Electrochemical impedance spectroscopy

In the previous section, a large perturbation to the system (potential sweep) was imposed, driving the electrode to a condition far from equilibrium, and its electrode reaction was studied. Another approach is to perturb the cell with alternating current (AC) signals of small magnitude and, at steady state, assess the way the system follows the perturbation. The EIS technique consists on the application of a small sinusoidally varying potential [$E(t)$], and the measurement of the resulting current response [$I(t)$] [140]. The importance of impedance methods comes from the fact that they can sample electron transfer at high frequencies and mass transfer at low frequencies.

As previously mentioned, charge transfer processes have Faradaic and non-Faradaic components. The Faradaic component comes from the electron transfer via a reaction across the electrode-solution interface, when polarization (R_p) and solution (R_s) resistances are surpassed. The non-Faradaic component arises from the charging of the double-layer capacitor (C_{dl}). When a redox reaction happens at the interface, the mass transport of the reactant and product is important for determining the rate of electron transfer. Z_W is the equivalent component that accounts for this mass transport process. The activation barrier at a particular potential is represented by the R_p, but at the standard (or formal) electrode potential, the barrier becomes the R_{ct}. Figure 14 is a schematic representation of the proposed model for the electrical double layer and equivalent circuit.

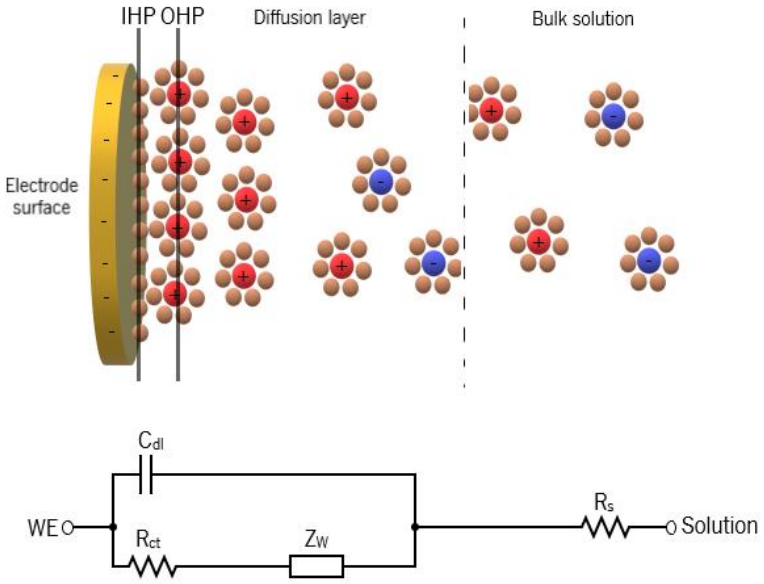

Figure 14. WE - double layer - diffusion layer - bulk solution proposed model and equivalent circuit.

When an AC potential is applied to a system, the current resultant from this perturbation will have an amplitude that is lower than the applied voltage due to resistance, and shifted by an angle θ caused by the reactance (e.g. capacitance or inductance) of that system, as can be seen in Figure 15.

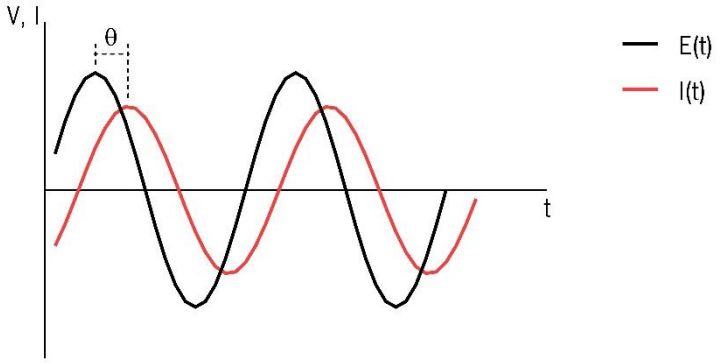

Figure 15. Representation of an applied potential and resultant current.

Therefore, equation (9) characterizes the applied voltage and equation (10) the resultant current.

$$E(t) = E_0 \sin(\omega t);\ \omega = 2\pi f \tag{9}$$

$$I(t) = I_0 \sin(\omega t + \theta) \tag{10}$$

where $E(t)$ represents the potential as a function of time (V), E_0 the initial amplitude (V), ω the angular frequency (rad s^{-1}) and f the frequency (Hz). The impedance of a system (Z), expressed in ohms (**Ω**) is the extension of the concept of the system's resistance, given by Ohm's law:

$$Z(t) = \frac{E(t)}{I(t)} = \frac{E_0 \sin(\omega t)}{I_0 \sin(\omega t + \theta)} = Z_0 \frac{\sin(\omega t)}{\sin(\omega t + \theta)} \tag{11}$$

The impedance can also be expressed in its polar form as such:

$$Z = Z_0 e^{j\theta} \tag{12}$$

where j equals $\sqrt{-1}$, the imaginary number. Using the Euler's formula (Equation 13), it is possible to assess two components of Z (Equation 14).

$$e^{j\theta} = \cos(\theta) + j\sin(\theta) \tag{13}$$

$$Z = Z_0 e^{j\theta} = Z_0(\cos(\theta) + j\sin(\theta)) = Z_0\cos(\theta) + jZ_0\sin(\theta) \tag{14}$$

The first component ($Z_0\cos(\theta)$) is commonly named real impedance (Z'), whereas the second component ($Z_0\sin(\theta)$) is called imaginary impedance (Z''). The sum of the real and imaginary components of impedance is called complex impedance and commonly expressed as:

$$Z = Z' + jZ'' \tag{15}$$

Graphical representations of complex impedances are usually made using Nyquist plots (Figure 16), where the *x* and *y* axes represent the real and imaginary components, respectively, and each point represents the impedance for a specific angular frequency.

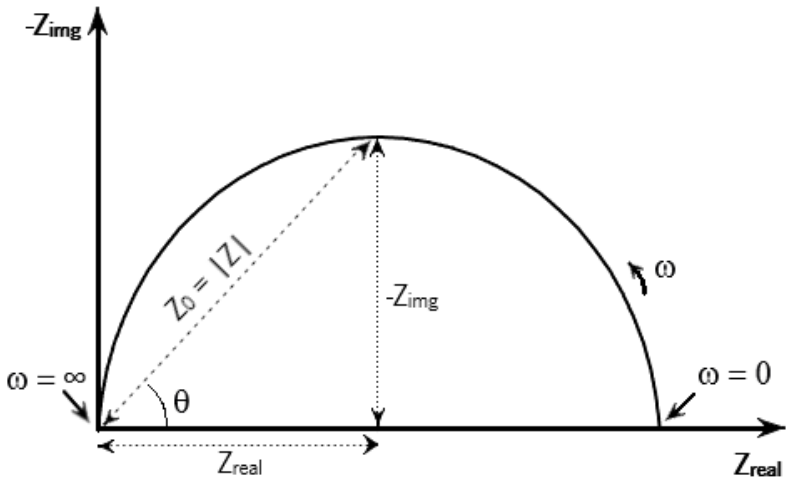

Figure 16. Complex impedance representation through a Nyquist plot.

Another form of analyzing complex impedances is through Bode diagrams (Figure 17), where one can analyze the module ($|Z|$) and phase angle (θ) separately, and as a function of applied frequency.

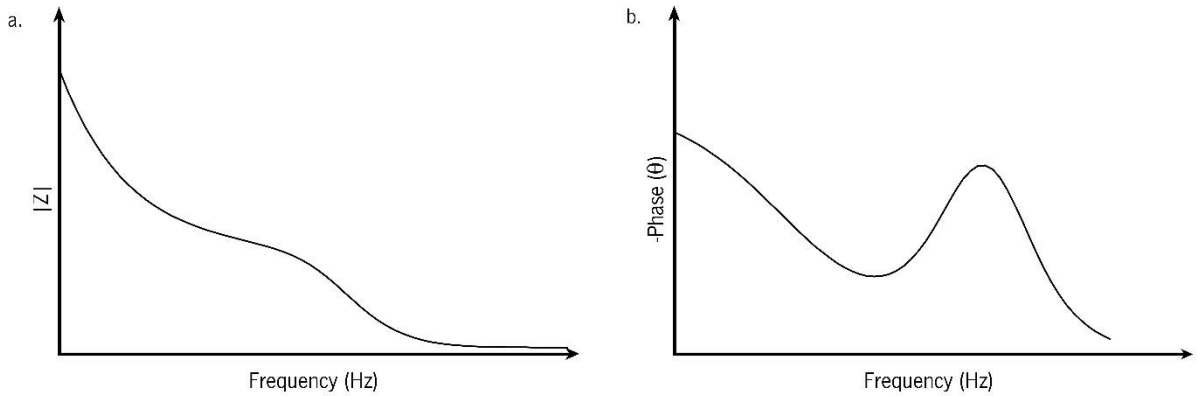

Figure 17. Complex impedance representation through bode diagrams: a. module and b. phase.

As elucidated earlier, in the present dissertation, impedance data was fitted into a Randles equivalent circuit, used to model the physicochemical processes taking place at the WE's surface. The use of equivalent circuits is common when studying biosensors, as they enable one to assess how the different components are contributing to the overall impedance [141]. As exposed earlier, this equivalent circuit's components take into account the diffusion of the redox probe (R_s and Z_W), which are independent from

surface modifications, and also components highly sensitive to interfacial properties of the WE (R_{ct} and C_{dl}).

The resultant Nyquist plot for a representative Randles equivalent circuit can be seen in Figure 18. At high frequencies, a semi-circle region is formed, indicative of kinetically controlled processes, which are influenced by capacitive and resistive effects. At low frequencies, the linear region represents diffusion-limited processes [20].

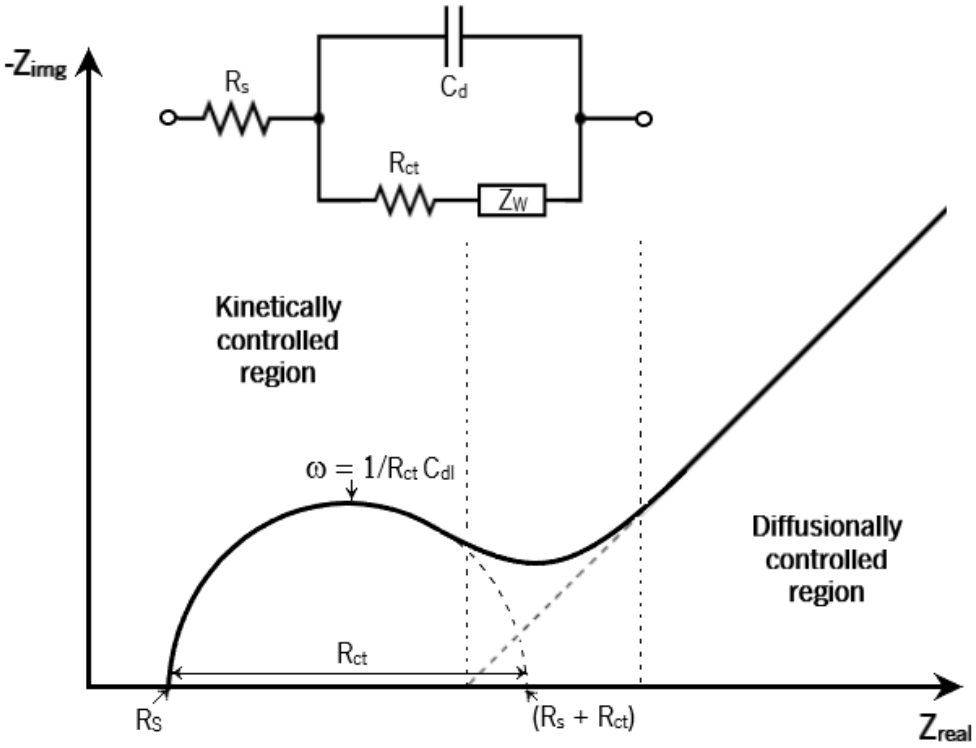

Figure 18. Randles equivalent circuit and respective Nyquist plot.

Equations (16) and (17) describe the real and imaginary components of the equivalent circuit for a given frequency, in the semi-circle region [20]:

$$Z' = R_s + \frac{R_{ct}}{1 + (\omega C_{dl} R_{ct})^2} \tag{16}$$

$$Z'' = \frac{\omega C_{dl} R_{ct}^2}{1 + (\omega C_{dl} R_{ct})^2} \quad (17)$$

The system's R_{ct} is given by the diameter of the semi-circle region of the Nyquist plot. The R_s behaves as a true resistance, independently of applied frequency. The region controlled by diffusion (low frequencies) is characterized by a diagonal line with a slope of 45 °, and Z_W is responsible for this behavior, as diffusion requires long operational times to produce an effect on impedance.

Analyzing Figure 18, it is easily settled that resistive and diffusional effects are easily extracted from Nyquist plots. For capacitance (or inductive) measures, Bode plots (Figure 17) are preferred because phase angle and module are plotted separately against applied frequency.

The phase angle expresses the balance between capacitive and resistive forces of the circuit. At high frequencies, capacitance rules the impedance, while for low frequencies, resistance is dominant. In a purely capacitive circuit, θ = 90 °. In a purely resistive circuit, θ = 0 °. As mentioned earlier, the Warburg impedance is represented in the Nyquist plot as a diagonal line with a slope of 45 °. Therefore, in the bode phase diagram, a pure diffusion limited process is expressed as θ = 45 ° for low frequencies [20]. Since the Randles equivalent circuit is a combination of resistive, capacitive and diffusional processes, the result is a combination of phases (0 ° < θ < 90 °).

When using electrochemical sensors for biomarker detection, potential applied needs to be small when comparing with non-biological applications in order to avoid protein denaturation [142]. Specific biomarker detection is achieved through the modification of the WE, by the consecutive immobilization of layers that alter the WE's conductivity and impedance. Impedance of the system is evaluated, before and after the biorecognition event, using a redox probe such as the ferricyanide couple $[Fe(CN)_6]^{3-/4-}$.

Consecutive layer formation (either chemical or biological) at the surface of the WE results in the increase of the system's impedance, through adsorption, composite layer formation, bio-recognition element immobilization, and target attachment. This process can be monitored evidently through the analysis of the Nyquist plot, where R_{ct} increases with each consecutive layer, or the Bode plot, particularly at low frequencies, where impedance module also increases with additional layers (Figure 19).

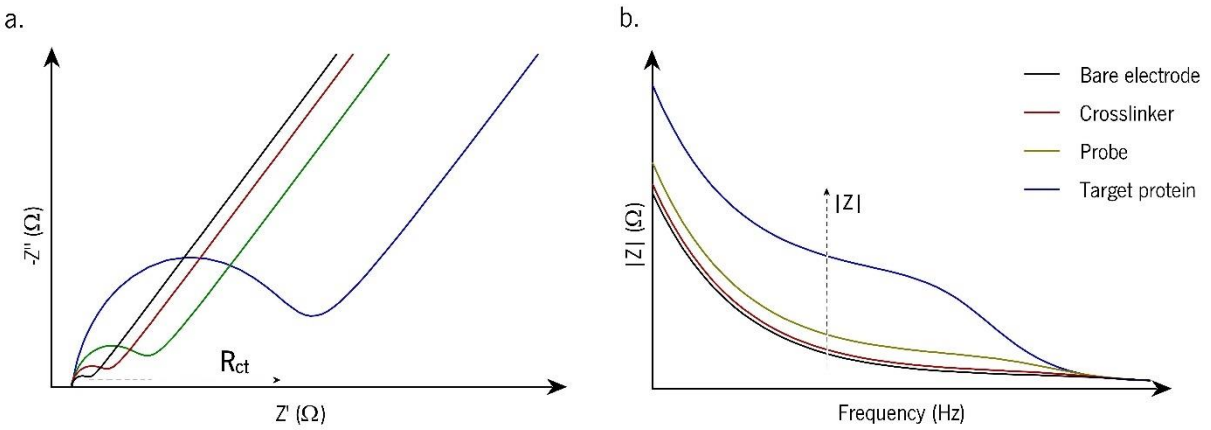

Figure 19. a. Nyquist plot and b. Bode phase plot of a representative optimized biosensor for biomarker detection.

Adding functionalization layers to the surface of the electrode hampers the homogeneity of the electrode's surface, and localized regions with dissimilar reaction rates appear, causing the double layer to behave as an imperfect capacitor. To counteract such phenomena, the constant phase element (CPE) is most frequently used in the place of the capacitor, in equivalent circuit models of biological systems [142].

3. Materials and experimental procedures

The current work presents an electrochemical immunosensor meant to improve DR diagnosing through the quantification of IL-6 and MMP2 in minimally invasive biological fluids. The first step of the experimental procedures consists on the quantification of these two biomarkers in tear samples of DR patients and controls, in order to assess if any difference is found between the two groups and, if so, to determine their concentration ranges. This analysis was performed in the Prof. Dr. Rosa Fernandes' laboratory at the University of Coimbra, using the conventional Luminex method. Then, the protocols followed for the development and optimization of the immunosensing systems are presented. The immunosensor's performance in quantifying IL-6 and MMP2 is then assessed, using standard solutions with biomarker concentrations previously determined in tears, and considered critical for DR diagnosing. Then, a comparative study between conventional methods, namely Luminex and ELISA, and the developed biosensor is made. Finally, as a complementary study, the use of saliva is tested in the IL-6 biosensor, and its performance is compared to the conventional method ELISA. In the present section, the materials needed to achieve, characterize and test such immunosensors are reported.

3.1. Quantification of potential diabetic retinopathy biomarkers IL-6 and MMP2 in tear fluid using conventional Luminex analysis

To prove that IL-6 and MMP2 concentrations are altered in the tears of DR patients, and to determine the concentration ranges and tendencies that distinguish between disease presence or absence, a collaboration was established between INL and the School of Medicine from the University of Coimbra (Prof. Dr. Rosa Fernandes and Prof. Dr. Francisco Ambrósio). They used the conventional biomolecule quantification method Luminex to quantify IL-6 and MMP2 levels in the tears of DR patients and controls.

A total of 14 tear samples were collected from healthy volunteers and DR patients, upon written informed consent (Annex A). Inclusion criteria for the controls were as follows: no history of diabetes or chronic disease, no ocular diseases requiring topical ocular treatments, no abnormal lid anatomy or blinking function in either eye, no dry eye resulting from scarring, no history of any systemic or ocular disorder, and no contact lens wear in the last 8 h. Tear samples were collected by a professional, wearing gloves, by placing a sterile ophthalmology diagnostic strip (Dina strip Schirmer-Plus from *Dina Hitex*) in standardized conditions (strip inserted in the inferior cul-de-sac for 5 min, while subjects closed their eyes

without any anesthetic) of each anonymized subject. Following collection, the wet portion of the strip was soaked in Sodium Chloride 0.9 % (NaCl 0.9 % from *Sigma-Aldrich*) for 1 h to elute tear proteins.

Samples were analyzed using Luminex Multiplex assay (Luminex 100/200 System, *Luminex Corporation*), where the tear concentrations of IL-6 and MMP2 were determined.

3.2. Development and performance of immunosensors for diabetic retinopathy diagnosing based on the quantification of IL-6 and MMP2

3.2.1. Materials and reagents

Phosphate buffer (PB, 10 mM, pH 7.4) and phosphate buffer saline (PBS, 10 mM, pH 7.4) tablets, glycerol, bovine serum albumin (BSA), potassium ferricyanide (III), potassium hexacyanoferrate (II) trihydrate, sodium phosphate bibasic, sodium phosphate monobasic dihydrate and isopropanol (IPA) were obtained from *Sigma Aldrich*. Sulfosuccinimidyl 6-(3'-(2-pyridyldithio)propionamido)hexanoate crosslinker (sulfo-LC-SPDP) was obtained from *Fisher Scientific*.

Anti-IL-6 antibody, recombinant human IL-6, and recombinant human TNF-α were obtained from *Alfagene*. Anti-MMP2 antibody and recombinant human MMP2 were obtained from *BioLegend*.

Sterilized single dose units of NaCl 0.9 % solution were obtained from the local pharmacy.

3.2.2. Experimental setup

A three-electrode cell containing a gold WE (1,6 mm in diameter), a Ag/AgCl RE and a gold CE (C223AT from *DropSens*) with an 8 mm active region is the chosen sensing system (Figure 20.a.). All electrodes are initially cleaned with IPA and deionized milli-Q filtered water, and dried with nitrogen.

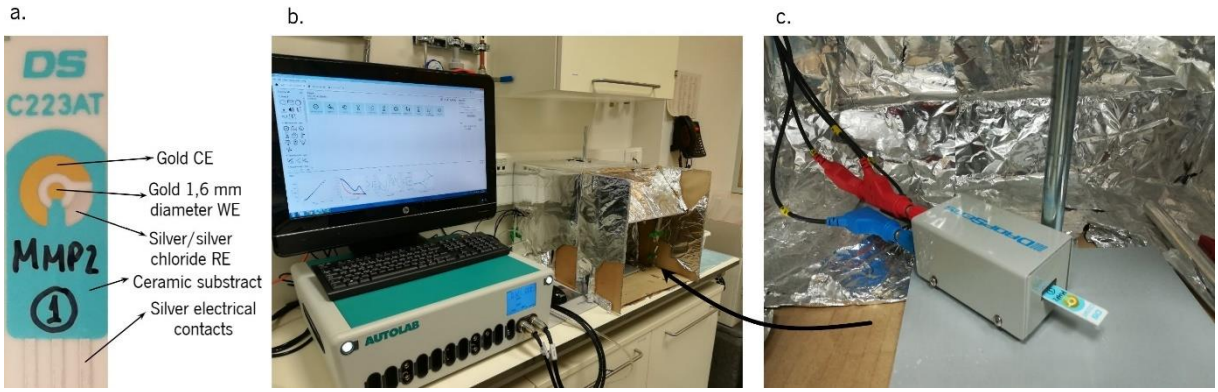

Figure 20. a. Sensor layout, b. electrochemical measurements setup and c. connector.

As noted in Section 2.5.2., charge flow in electrochemical sensors depends on the existence of an electrochemical conductor (an electrode) and an ionic conductor (an electrolyte) [20]. In this work, an electrolyte solution consisting on 5 mM $[Fe(CN)_6]^{3-/4-}$ in 10 mM PBS is produced and used as the ionic conductor. Because this solution is light sensitive, it was stored in an aluminum-wrapped container, and light-proof structures were used throughout the work. Before electrochemical measurements are carried out, 80 µL of the electrolytic solution are positioned on the sensor's active region.

Electrochemical measurements are carried out using a potentiostat/galvanostat, equipped with a frequency response analysis module (PGSTAT302N/FRA32M from *Metrohm Autolab*) controlled by NOVA software (Figure 20.b.). The electrode is connected to the analysis equipment through a connector positioned inside a light-proof box (Figure 20.c.).

In Section 2.5.4, it was explained how CV and EIS can be used for the monitorization of the biofunctionalization process and for biomarker detection and quantification. CV is often used for studying the behavior of electroactive species in solution. The widening of the diffusion layer caused by the consecutive immobilization of biofunctionalization layers can be easily observed in a voltammogram by the increase in ΔE_p values. On the other hand, using EIS enables the study of the frequency influence over the system. The resultant complex impedance plots show the capacitive and resistive forces of the system, and their evolution through the biofunctionalization process or the attachment of the target analyte.

CV is performed to monitor the surface biochemical modifications, using the following conditions: potential scan from -0.4 to +0.4 V, scan rate of 0.05 V s^{-1}. EIS is used to evaluate the functionalization process and further biomarker detection and quantification. A fixed potential of +0.125 V, with a sinusoidal

perturbation of 5 mV (amplitude) at a frequency range from 100000 to 0.1 Hz is used. Impedance data is fitted to a Randles equivalent circuit [R_s(CPE[$R_{ct}Z_w$])] presented in Section 2.5.3 through the NOVA software.

3.2.3. Immunosensors' functionalization process

Specific biomarker detection depends on the modification of the WE. This biofunctionalization process consists on the consecutive immobilization of 1 µL of different-function solutions in the WE, following a protocol described next.

Each immobilization is performed in a dark and humid atmosphere. A petri dish wrapped in aluminum foil and lined with wet paper (Figure 21) achieves such atmosphere. All sensors are dried with nitrogen and rinsed with PB before and after each immobilization, respectively. Moreover, CV and EIS are performed as previously described, before the biofunctionalization process (bare gold WE), and after the immobilization of each layer, in order to monitor and optimize the process, described below.

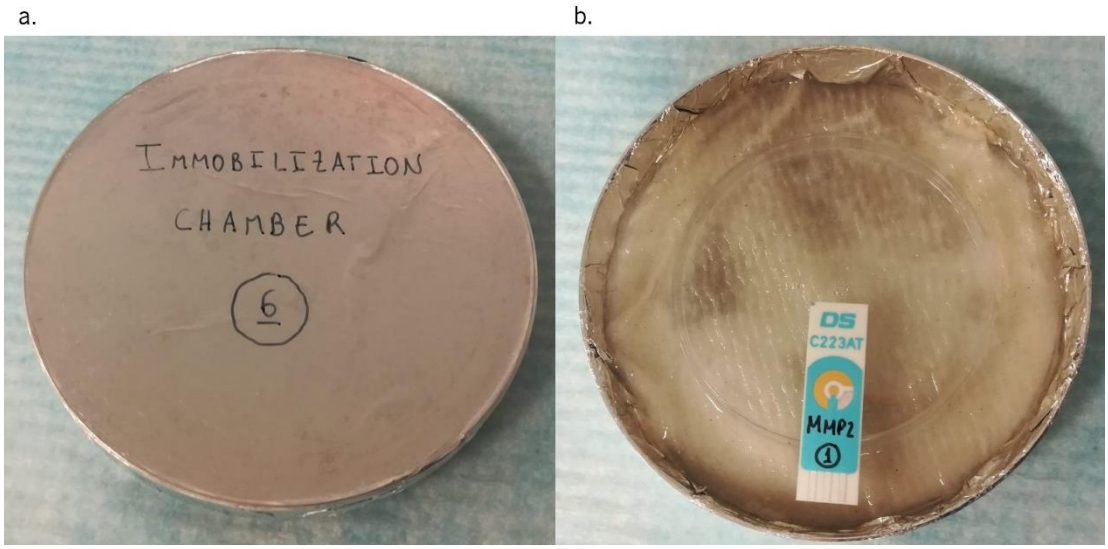

Figure 21. Immobilization chamber a. closed and b. opened.

The first immobilized layer is the crosslinker that forms a self-assembled monolayer (SAM), allowing for the covalent attachment of the biorecognition elements (antibodies) to the electrode's gold surface (Figure 22).

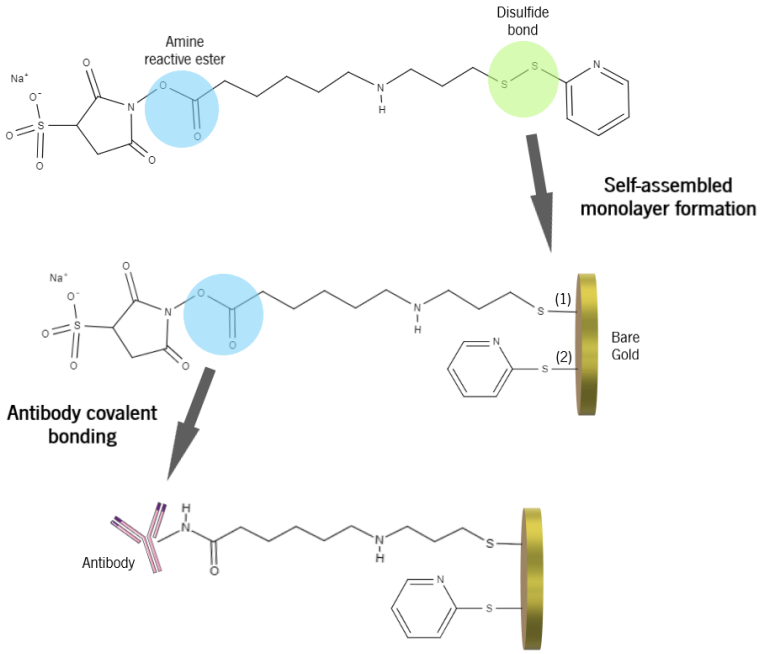

Figure 22. Formation of a SAM between the electrode's surface and Sulfo-LC-SPDP, and consequent covalent bonding of the antibody. (1). sulfosuccinimidyl 6-(3-mercapto propionamido)-hexanoate and (2). 2-mercapto pyridine.

Sulfo-LC-SPDP is the selected crosslinker. As schematized in Figure 22, the disulfide bond breaks and both ends bind to the bare gold surface through chemisorption, forming a SAM of mixed sulfosuccinimidyl 6-(3-mercapto propionamido)-hexanoate [Figure 22.(1)] and 2-mercapto pyridine [Figure 22.(2)]. The first component will afterwards react with the primary amines of the antibody, resulting in a stable covalent bond, while the second acts as a spacer between molecules and provides conductive path for charge flow from solution to electrode surface [143,144].

The formation of a densely packed monolayer is not beneficial for the functionalization of the WE because it dramatically increases the electrode's R_{ct}, and the consequent functionalization and detection steps are measured with scarce sensitivity. In contrast, the formation of a less compact SAM achieved with a crosslinker short immobilization interval allows for the efficient antibody immobilization, without saturating the system. Additionally, as opposed to other SPDP crosslinkers, sulfo-LC—SPDP is water soluble and suffers from hydrolysis of the sulfo-NHS ester (Figure 23), competing with the desirable amine reaction. Therefore, an optimization process is performed to determine the sulfo-LC-SPDP immobilization interval for a successful SAM formation, and prevent significant loss of activity [144].

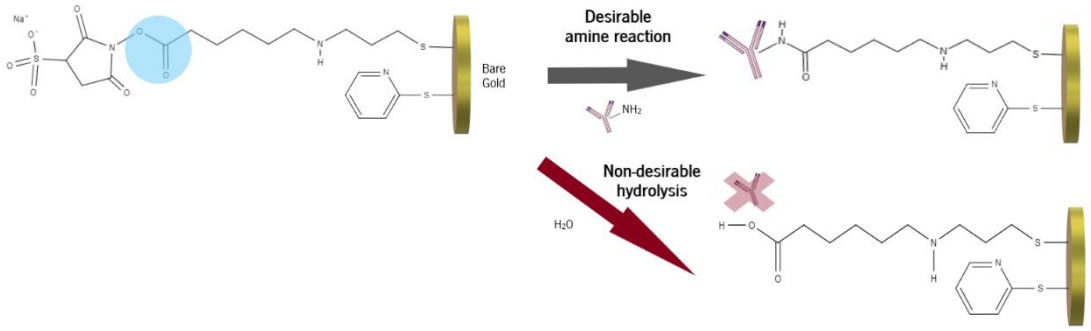

Figure 23. Sulfo-LC-SPDP suffering desirable amine reaction and non-desirable hydrolysis.

The second layer is formed by the biorecognition elements, in this case antibodies, responsible for the nomenclature *immunosensors*. Antibodies are selected for their high specificity, stability and versatility, and for enabling the quantification of very low concentrations in complex biological matrices. The antibodies are specific for each biosensor: for the IL-6 biosensor, the antibody immobilized is anti-IL-6, and for the MMP2 biosensor, the antibody immobilized is anti-MMP2.

The immobilization of bovine serum albumin (BSA) is further applied to prevent unspecific protein binding to the antibodies, as it binds to free NHS ester groups [131].

An optimization process determines the concentrations and immobilization intervals of each biofunctionalization layer. The first layer (sulfo-LC-SPDP) is immobilized at 10 mg mL^{-1} [131], and immobilization intervals from 15 to 30 min are tested. The antibody layer's concentrations and immobilization times are experimented between 0.250 mg mL^{-1} and 0.500 mg mL^{-1}, and 8 to 12 h, respectively. The final biofunctionalization layer (BSA) is tested in concentrations ranging from 0.25 to 1 %, and time intervals from 20 to 30 min. These factors are consecutively altered until the immunosensors can quantify IL-6 and MMP2 in the concentration ranges defined for DR diagnosis in the next section, at which point the concentrations and immobilization intervals of each biofunctionalization layer are considered optimal. These optimized factors are presented in Section 4.2.1.

3.2.4. Immunosensors' analytical performance using standard solutions with IL-6 and MMP2 concentrations based on tears' diabetic retinopathy critical ranges

As stated, the present immunosensors are being developed for the purpose of diagnosing DR through biomarker profiling in minimally invasive biological fluids. As so, the calibration process uses standard solutions containing IL-6 or MMP2 recombinant proteins in concentration ranges relevant for DR diagnosing (previously determined by Luminex), and use NaCl 0.9 % as solvent. NaCl 0.9 % is chosen due to its similarity with tear fluid, and because it is frequently used to recover the protein content of tears, when they are sampled through the absorbent material method, as performed in Section 3.1 [145].

Standard solutions range the following concentrations: 1 pg mL^{-1}, 25 pg mL^{-1}, 50 pg mL^{-1} and 75 pg mL^{-1} of IL-6 or MMP2. The calibration curves are constructed by immobilizing 1 µL of each solution for 30 min at room temperature (RT), from the lower to the higher concentration in the WE of 6 replicate sensors. This way, calibration curves are constructed using the average and standard deviation values. Between each immobilization, the sensors are rinsed with milli-Q water, and electrochemical measurements are performed using the protocol described in Section 3.2.2.

The calibration curves are plotted by means of normalized ΔR_{ct} as a function of the analyte's concentration, in pg mL^{-1}, and fitted to a linear regression. Normalized ΔR_{ct} is obtained as such:

$$Normalized\ \Delta \mathrm{R_{ct}} = \frac{R_{ct}(analyte) - R_{ct}(BSA)}{R_{ct}(BSA)} \tag{18}$$

The LOD is determined as the biomarker concentration in the respective calibration curve at which the normalized ΔR_{ct} corresponds to:

$$Normalized\ R_{ct} = 3 \times SEM_{blank} + normalized\ \Delta R_{ct}(blank) \tag{19}$$

In the previous equation, SEM_{blank} and normalized $\Delta R_{ct}(blank)$ represent the standard error of the mean value and the normalized ΔR_{ct} of pure NaCl 0.9 % [131].

The LRs and LODs achieved with the immunosensors are then compared with the IL-6 and MMP2 concentration values obtained on the tears of healthy controls and DR patients using the Luminex method as described in Section 3.1.

The IL-6 immunosensor is also tested in terms of specificity, by measuring the resultant normalized ΔR_{ct} when 3 different solutions are immobilized: IL-6 (10 pg mL^{-1}, in NaCl 0.9 %), a mixture of IL-6 and TNF-α (10 pg mL^{-1} in NaCl 0.9 %), and TNF-α (10 pg mL^{-1}, in NaCl 0.9 %). Similar to the formation of the calibration curves, 1 µL of each solution is incubated at RT for 30 min before rinsing with milli-Q water. 3 replicate immunosensors are used for testing each solution.

Statistical analysis is performed using GraphPad Prism 8 (*GraphPad Software Inc.*). Differences between experimental conditions are determined using T-Tests, and statistical significance is considered for $P < 0.05$. Results are expressed as mean value ± standard error.

3.3. Comparative study between optimized immunosensors and conventional methods for diagnosing diabetic retinopathy through quantification of IL-6 and MMP2 in tears

The use of minimally invasive biological samples to quantify IL-6 and MMP2 for DR diagnosing and monitoring purposes comes with great challenges. Tear sampling methods deliver minute volumes, and low concentrations are found. In this section, the sample volume requirements, LRs and LODs for IL-6 and MMP2 exhibited on the protocol manuals of two conventional methods used in this dissertation (namely Luminex and ELISA) are compared to the results achieved with the developed immunosensors in standard solutions. All methods are critically analyzed for their ability to quantify IL-6 and MMP2 on the range of concentrations determined on section 3.2 for DR diagnosing in tear fluid.

3.4. IL-6 immunosensor's analytical performance on saliva samples and comparison with the ELISA method

Saliva is a biological fluid collected by non-invasive means. Thus, to complement the previously described studies, saliva samples from a non-DR population are tested to assess the biosensor's viability using this fluid, and its performance is compared with a conventional method, ELISA. For that, saliva samples are

collected from 15 volunteers, using a saliva sampling kit (Salivette, *Sarstedt*), and following product instructions.

An optimized protocol defined by Cruz *et al.* [131] is followed: 50 µL of each sample are used to quantify IL-6 using the ELISA conventional method (Human IL-6 ELISA kit, *Alfagene*). The increased complexity and viscosity of the saliva samples calls for a dilution before quantification using the biosensor, in order to avoid system saturation. An optimization process determined 1:4 as the optimal dilution factor for the quantification of IL-6 in saliva samples using the developed immunosensor. Since the immunosensor is calibrated with NaCl as a diluent (mimicking tear fluid), NaCl is also chosen to dilute the saliva samples. 1 µL of each diluted sample is immobilized for 30 min at RT in the WE of 3 replicate immunosensors, before quantifying IL-6 using the protocol described in Section 3.2.2. The result obtained is then multiplied by 4 to account for the dilution.

4. Results and discussion

In this section, the results achieved from experimental assays are presented and a critical analysis is made. First, tear concentrations of IL-6 and MMP2 from controls and DR patients measured with Luminex, provided by the collaborators from the University of Coimbra, are presented and analyzed. In the next section, the results from the immunosensors' optimized biofunctionalization process are shown, followed by their analytical performance measuring IL-6 and MMP2 in standard solutions prepared according to tears' concentration ranges obtained in the previous study. Subsequently, the performances of Luminex, ELISA and the developed immunosensors are compared for IL-6 and MMP2 quantification. Finally, as a complementary study, the results from the quantification of IL-6 in saliva samples using the immunosensor and the conventional ELISA method are presented and compared.

4.1. Quantification of potential diabetic retinopathy biomarkers IL-6 and MMP2 in tear fluid using conventional Luminex analysis

For both IL-6 and MMP2 biomarkers, the immunosensors were calibrated in ranges determined by a Luminex analysis of tear samples from healthy controls and DR patients, provided by the collaboration between INL and the University of Coimbra. As previously stated, this prior quantification using a conventional biomolecule quantification method ensured that the biofunctionalization process of the biosensor was performed in concentrations that are meaningful and critique for DR diagnosis, given the lack of published literature on the concentration of IL-6 and MMP2 in minimally invasive biological fluids.

In fact, the use of IL-6 and MMP2 as potential DR biomarkers has not been widely explored, justifying the timelessness of the present work. As highlighted in Tables 1 and 2 from section 2.4, some studies have found increased levels of these biomarkers in DR or DM patients, but these results came from invasive biological fluids. As shown in Table 1, only one study by Liu *et al.* quantified IL-6 in tear samples of DR patients and controls [13] and, in this study, no significant difference was found between the groups. Regarding MMP2 quantification in tear samples of DR patients, no studies were found until the date. However, as shown in Table 2, Symeonidis *et al.* found increased levels of MMP2 in tear samples of DM patients [104]. In other biological fluids like the AH, VH and serum, IL-6 and MMP2 were correlated with the presence or severity of DR. As mentioned in section 2.4.2, retinal pathological changes are reflected in tears [111], and tears' proteomic alterations are correlated with other ocular fluids' [134].

The Luminex results for lacrimal IL-6 and MMP2 concentrations, obtained by the University of Coimbra, revealed a positive correlation with DR presence, as DR patients presented significantly superior concentrations of both IL-6 and MMP2, comparing with healthy controls.

The control population showed IL-6 concentrations between 20.6 and 37.7 pg mL^{-1}, with a mean concentration of 25.7 ± 7.0 pg mL^{-1}. On the other hand, DR patients' IL-6 concentrations ranged from 34.1 to 56.7 pg mL^{-1}, with a mean concentration of 42.9 ± 6.6 pg mL^{-1}, which is significantly superior to the control group ($P = 0.001796 < 0.05$).

Regarding MMP2, the control population featured values between 9.3 and 17.7 pg mL^{-1}, with a mean concentration of 10.8 ± 4.1 pg mL^{-1}. The diseased group had concentrations between 11.6 and 23.1 pg mL^{-1}, with a mean value of 18.0 ± 4.6 pg mL^{-1} ($P = 0.0276 < 0.05$), which was also significantly higher than the control population's mean value.

These results are of utmost importance because they showed a tendency for increased concentrations of IL-6 and MMP2 in the tears of DR patients, making them two biomarkers potentially powerful for a biomarker-based molecular diagnosing of DR in a minimally invasive biological fluid. Even though few previously reported studies found altered levels of these two biomarkers in DR and DM, the present analysis has never been done before, to the author's knowledge. The quantification of these biomarkers could be seen as a complementary method, bringing objective and quantitative data to the conventional diagnosing process, which relies on the subjective analysis of imaging techniques performed by specialized technicians [9]. As mentioned in section 2.4.4, the quantification of two biomarkers instead of a single one is preferable, increasing specificity to the disease [11]. Future work may include the development of additional antibody-based biosensors, for other DR-related biomarkers. Moreover, these results highlight the viability of developing a multiplex system for the simultaneous quantification of IL-6, MMP2 and other DR biomarkers in the future.

The concentration ranges found in the present section were the basis for the development, calibration and performance analysis of the immunosensors, described in the next sections.

4.2. Development and performance of immunosensors for diabetic retinopathy diagnosing based on the quantification of IL-6 and MMP2

4.2.1. Immunosensors' functionalization process

In this section, the functionalization process results are discussed. As exposed in section 3.2.3, the biofunctionalization layers were immobilized to the WE according to an optimization process. During this process, the concentrations and immobilization intervals were consecutively altered until the immunosensors were able to quantify IL-6 and MMP2 in the pretended ranges, and thus considered optimal. Figure 24 shows a schematic representation of the optimized biofunctionalization process.

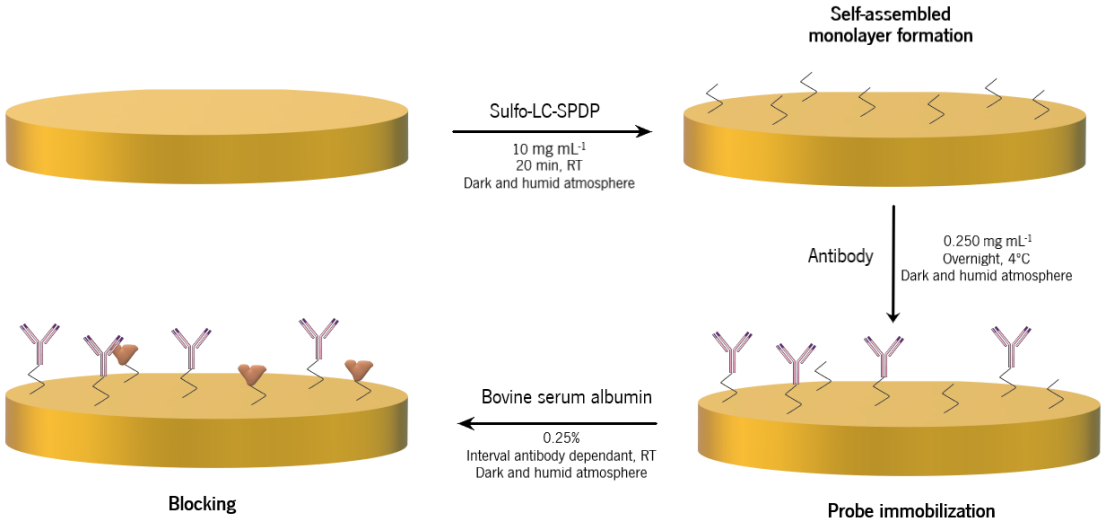

Figure 24. Schematic representation of the immunosensors' optimized functionalization process.

As can be noted in Figure 24, the sulfo-LC-SPDP was the first layer immobilized to the WE to achieve the formation of a SAM, followed by the immobilization of the antibody layer, and finally the BSA to block unspecific bonds. Tables 5 and 6 present the optimized concentrations and immobilization intervals for each functionalization layer for the IL-6 and MMP2 immunosensors, respectively.

Table 5. Optimized characteristics of the IL-6 biosensor functionalization process.

Concentration	Concentration	Immobilization time	Immobilization temperature
Sulfo-LC-SPDP	10 mg mL^{-1}	20 min	RT
Anti-IL-6	0.250 mg mL^{-1}	Overnight	4 °C
BSA	0.25 %	30 min	RT

Table 6. Optimized characteristics of the MMP2 biosensor functionalization process.

Concentration	Concentration	Immobilization time	Immobilization temperature
Sulfo-LC-SPDP	10 mg mL^{-1}	20 min	RT
Anti-MMP2	0.250 mg mL^{-1}	Overnight	4 °C
BSA	0.25 %	20 min	RT

As can be observed, the three layers of the biofunctionalization process, for both the IL-6 and MMP2 biosensors, varied subtly. For their resemblance, and for simplification purposes, these functionalization steps will be presented and discussed together.

As exposed on Section 3.2.3, CV and EIS were the techniques used to evaluate and monitor the chemical modifications performed on the gold WE, regarding electron transfer kinetics and redox processes.

The correct formation of a sulfo-LC-SPDP SAM, and subsequent layers were monitored and confirmed by the analysis of the CV voltammograms and EIS. The analysis of the wave peak-to-peak potential difference (ΔE_p), given by the difference between the anodic ($E_{p,a}$) and cathodic ($E_{p,c}$) peaks of CV, was used to study the functionalization process. Figure 25 illustrates a voltammogram from the biofunctionalization process.

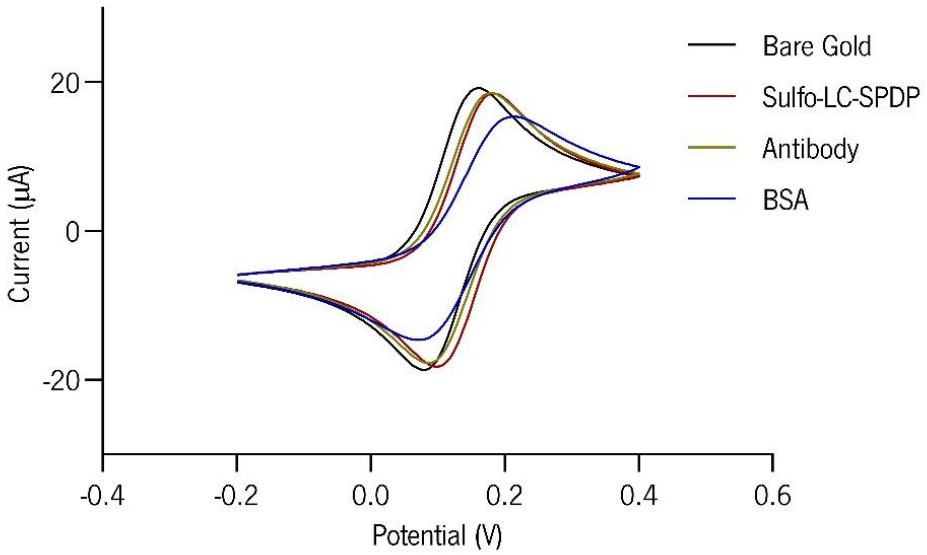

Figure 25. CV of the different immobilization steps of a representative optimized immunosensor.

The scan starts and the potential sweeps forward into more positive, oxidative potentials. In an initial stage, the $[Fe(CN)_6]^{4-}$ remains in the reduced form, as the potential is not sufficient to oxidize it into $[Fe(CN)_6]^{3-}$. When the onset of oxidation is reached, the current increases exponentially as oxidation occurs in the vicinity of the electrode surface. A linear increase is then observed as there is still abundant concentrations of the reduced form near the electron surface, within the diffusion layer. As the reduced form gets depleted and the diffuse layer extends, the current response decreases from linearity and reaches a maximum peak (anodic peak current, $i_{p,a}$) at the anodic peak potential ($E_{p,a}$). At this point, the current increase caused by more positive potentials is counterbalanced by a decreasing flux of analyte caused by the distance to the electrode surface. Hereafter, the current is limited by the mass transport of the $[Fe(CN)_6]^{4-}$ species from the bulk solution to the diffusion layer, resulting in a decrease in current until a steady-state is reached, where further increases in potential no longer reflect on the current value.

As the potential is reversed towards more negative values, a re-reduction process of $[Fe(CN)_6]^{3-}$ species that were accumulated at the electrode surface starts. This process mirrors that for the oxidation, but with an opposite scan direction and a cathodic peak current ($i_{p,c}$) correspondent to a cathodic peak potential ($E_{p,c}$). The reversible nature of this process reflects in equal magnitudes of the peak currents (with opposite signs). The difference between the peak potentials (ΔE_p) is caused by the diffusion limitation.

The modification and biofunctionalization of the WE results in a wider diffusion layer, making it harder for the $[Fe(CN)_6]^{3-/4-}$ species to reach the electrode surface. As a result, the ΔE_p value increases with each immobilization step, as can be observed in Table 7. Moreover, the absolute values for the anodic and cathodic current peaks decrease as a result of an increased resistance to charge-transfer, indicating suitable surface modification. According with published literature, this increase in ΔE_p and decrease in peak current is typical, and characterizes a successful biofunctionalization process [146].

Table 7. Anodic and cathodic peak potential variations of a representative optimized immunosensor.

	Bare Gold	Sulfo-LC-SPDP	Antibody	BSA
ΔE_p (mV)	80,6	85,6	100,7	141,0

Figure 26 shows the Nyquist plots of the functionalization steps. The circular symbols correspond to experimental data. As enounced before, this data was fitted to a modified Randles circuit, $R_s(CPE[R_{CT}Z_W])$, to model the physicochemical process occurring at the surface of the WE, using the NOVA software. The results for the equivalent circuit are also represented in Figure 26 by solid lines.

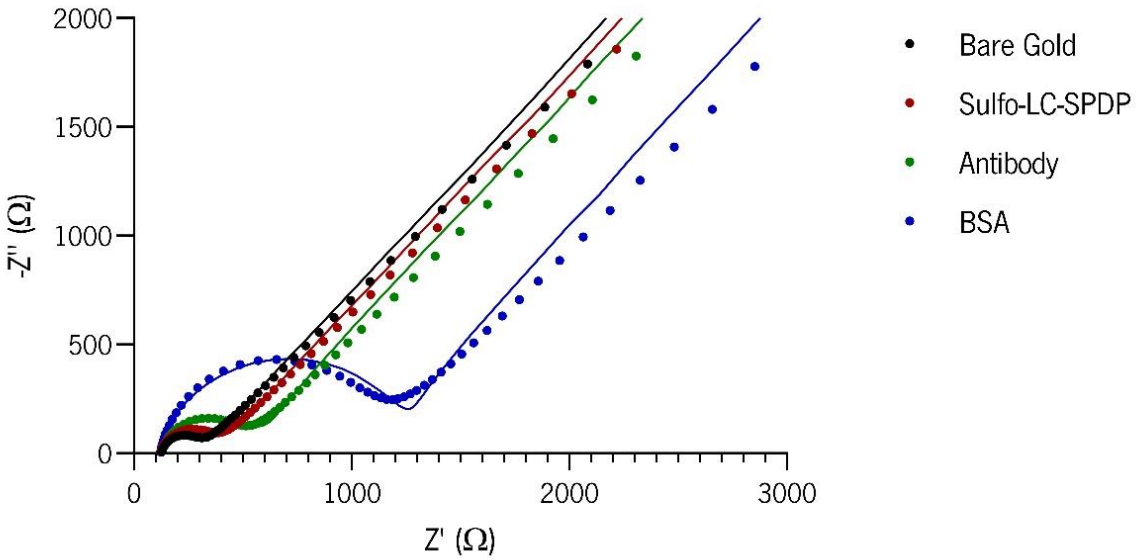

Figure 26. Nyquist plots of the different immobilization steps of a representative optimized immunosensor. Symbols represent experimental results, and lines represent respective equivalent circuit results.

The use of the Randles equivalent circuit is validated by the agreement between the experimental and fitted data observed in Figure 26, which allows for the extrapolation of the different electrical components' values, through simulation using the NOVA software. As explained in section 2.5.3, R_{ct} represents the resistance to charge-transfer, which means that its increase correlates with electron transfer blockage. Consequently, R_{ct} is the most commonly used parameter to evaluate the concentration of a molecule of interest, and in the present work was used for biomarker detection and quantification [20].

For the small semicircle component of the bare gold's Nyquist plot and large diffusion-controlled region, a fast electron-transfer process occurs on the un-functionalized WE. By the immobilization of Sulfo-LC-SPDP, the SAM formation widens the diffusion layer between the bulk electrolyte solution and the electrode surface, resulting in a slightly increased R_{ct}. The biofunctionalization with the antibody and BSA further insulate the WE, resulting in further increases of the R_{ct} value [20,146,147].

The impedance module and phase angle can also be displayed separately in bode plots, as a function of the frequency applied. Figure 27 shows bode plots of the biofunctionalization process.

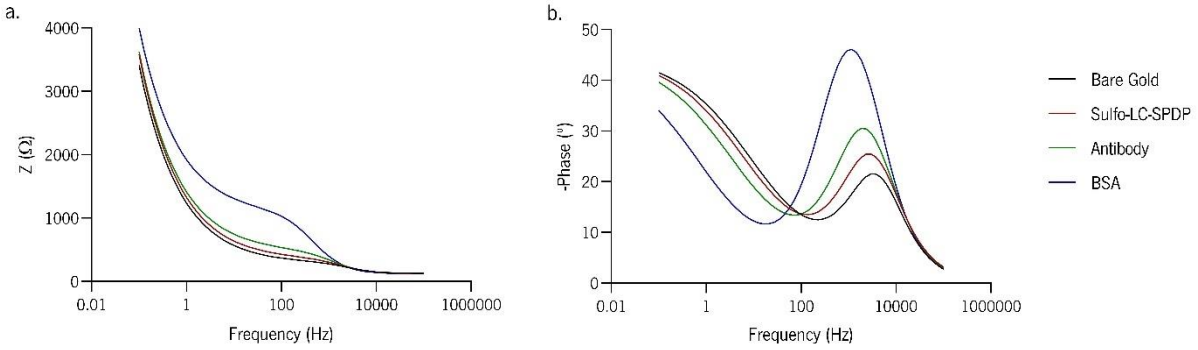

Figure 27. Bode plots of the biofunctionalization process of a representative optimized immunosensor, a. representing the module and b. the phase angle.

The impedance was used for observing the interfacial mechanisms of the electrode. For frequencies below 100 Hz, the system's impedance value is determined by the capacitive behavior of the electrode, which acts as an open circuit for very low frequencies, and decreases its impedance value with increasing frequencies. As so, its magnitude increases with each functionalization step in this section of the x axis, because the double layer's resistive property was increased by a denser and thicker isolation layer [148].

At higher frequencies, the solution's resistance to diffusion starts to influence the magnitude of impedance and the conduction of ions in the bulk solution dominates the signal. These results are confirmed by the phase angle, which tends to zero (characterizing purely resistive processes), for frequencies above 10 kHz. When lower frequencies are applied, the phase angle shifts to more negative values, manifesting the capacitive behavior of the immunosensor functionalization. For each consecutive immobilization step, lower phase angles are reached. Since the -90 ° hallmark is never registered, it can be concluded that the formed system between the electrode surface and the assembled layers behaves as an imperfect capacitor. Upon the initial frequencies applied below 10 Hz, the phase angle tends to -45 °, characteristic of diffusion limited processes [20].

Although capacitance increases with charge accumulation on the electrical double layer, the current obtained from this process is non-Faradaic as it results from charge-discharge processes. Since a redox probe is used in these measurements, the Faradaic current resultant from the redox reactions will prevail and impose the impedance value. As so, the formation of biofunctionalization layers that increasingly block the access of the redox probe to the electrode surface therefore increasing the resistance to charge transfer can be assumed as dominant and responsible for the impedance value.

Overall, the presented electrochemical data confirm the successful immunosensor modification and biofunctionalization with the SAM, antibody and BSA layers. Hereon, the IL-6 and MMP2 biosensors will be addressed separately, for the immunosensors' analytical performance analysis.

4.2.2. Immunosensors' analytical performance using standard solutions with IL-6 and MMP2 concentrations based on tears' diabetic retinopathy critical ranges

As explained in section 3.1, the tear samples used for the Luminex analysis were collected using an absorbent material, that was subsequently eluted in NaCl 0.9 % to recover tear protein content. It is also known that NaCl 0.9 % is a solution comparable to the tear matrix, frequently used as lubricant or cleaning agent [145]. Thereat, NaCl 0.9 % was used as a medium to perform all analytical performance analysis.

Increasing concentrations of IL-6 and MMP2 were diluted in NaCl 0.9 % (according to IL-6 and MMP2 range values found in healthy individuals and DR patients in Section 4.1) to construct calibration curves as the increase of the normalized ΔR_{ct} value relative to BSA. Since literature lacks IL-6 and MMP2 expected concentrations in minimally invasive biological fluids of DR patients, the range of concentrations

selected for the developed immunosensors included values above and below those obtained by Luminex in Section 4.1, from 1 to 75 pg mL^{-1}.

Nyquist plots for the IL-6 and MMP2 immunosensors and correspondent calibration curves obtained by plotting the normalized ΔR_{ct} as a function of the analyte's concentration in pg mL^{-1}, are represented in Figure 28.

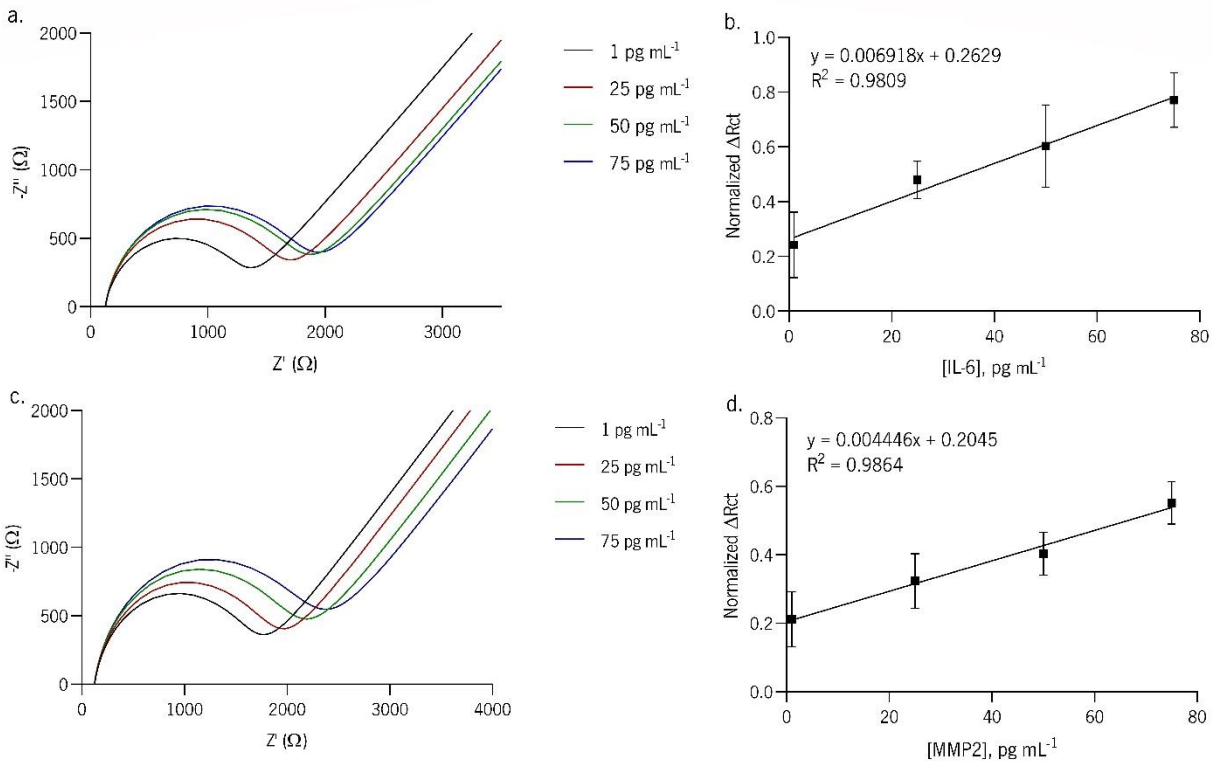

Figure 28. Representative Nyquist plots and respective calibration curves: a. and b. IL-6 immunosensor, c. and d. MMP2 immunosensor.

Linear responses were achieved for normalized ΔR_{ct} values correspondent to IL-6 and MMP2 concentrations between 1 and 75 pg mL^{-1}. The IL-6 immunosensor's equation for normalized ΔR_{ct} as a function of IL-6 concentration was:

$$Normalized\ \Delta R_{ct} = 0.006918 \times [IL-6] + 0.2629 \quad (20)$$

achieved with a coefficient of determination (R^2) of 0.98, revealing appropriate fitting of the calibration curve to linear regression.

For the MMP2 biosensor, R^2 was also appropriate (0.99), and the equation for normalized ΔR_{ct} as a function of MMP2 concentration was:

$$Normalized\ \Delta R_{ct} = 0.004446 \times [MMP2] + 0.2045 \quad (21)$$

The abovementioned results show that the developed immunosensors are able to quantify IL-6 and MMP2 concentrations in standard solutions based on NaCl 0.9 %, between values that were determined for DR diagnosing and monitoring in minimally invasive biological fluids, using only 1 µL of solution.

As stated, the goal of the developed immunosensors is to enable IL-6 and MMP2 quantification in minimally invasive biological fluids of healthy controls and DR patients, for diagnosing purposes. In section 4.1, the range of IL-6 and MMP2 concentrations found in the tears of healthy controls and DR patients was presented, resultant from Luminex analysis. Table 8 compares the concentrations previously obtained in the tears of healthy controls and DR patients, with the immunosensors' LRs and LODs, to assess if they are suitable for quantifying IL-6 and MMP2 in DR critique ranges.

Table 8. Comparison between tear concentrations of IL-6 and MMP2 in healthy controls and DR patients determined by Luminex analysis, and the biosensors' LRs and LODs.

	IL-6 (pg mL^{-1})	MMP2 (pg mL^{-1})
Concentration range in healthy controls (Luminex analysis)	20.6 – 37.7	9.3 – 17.7
Concentration range in DR patients (Luminex analysis)	34.1 – 56.7	11.6 – 23.1
Biosensor's LR	1 – 75	1 – 75
Biosensor's LOD	0.8	0.6

Tears' IL-6 and MMP2 concentrations previously found in both healthy controls and DR patients are within the immunosensors' analytical profiles. Moreover, the immunosensors' LODs are much lower than the minimum concentrations found in healthy controls, which is important because of the lack of guidelines for IL-6 and MMP2 values in DR patients' minimally invasive biological fluids. These immunosensors' analytical profiles are, therefore, suitable for the quantification of IL-6 and MMP2 concentrations in ranges found critical for DR diagnosing.

Moreover, to assess the biosensors' specificity in respective biomarker detection, the IL-6 immunosensor was tested with three standard solutions, using NaCl 0.9 % as solvent. The first solution contained only the target analyte IL-6 (10 pg mL^{-1}), the second solution contained a mixture of IL-6 (10 pg mL^{-1}) and TNF-α (10 pg mL^{-1}), and the third solution contained only TNF-α (10 pg mL^{-1}). The results for this experiment are illustrated in Figure 29.

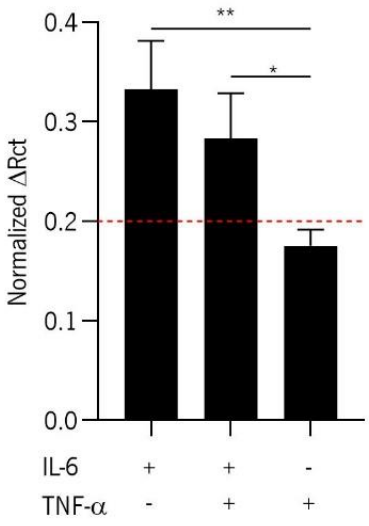

Figure 29. IL-6-immunosensor specificity test. The plus and minus signs represent the presence and absence, respectively, of the respective biomarker in solution. The red dashed line represents the sensor's LOD, previously determined.

Statistically significant differences were observed when comparing solutions where the target analyte IL-6 was present (first and second columns from Figure 29) with the solution where IL-6 was absent (third column from Figure 29), confirming that the developed immunosensor is able to distinguish between presence and absence of the target analyte. On the other hand, no statistically significant difference was

found between the two solutions containing IL-6 (first two columns from Figure 29), which showed that the immunosensor was able to identify the target analyte, despite the presence of TNF-α in solution. Moreover, no statistically significant difference distinguished the TNF-α solution (third column from Figure 29) and the immunosensor's LOD determined previously, and marked as a red dashed line in Figure 29. Thereafter, the absence of the target analyte produced a response that was statistically equivalent to the LOD. These results showed that the IL-6 immunosensor was able to detect IL-6 in solutions, in a specific way, regarding TNF-α and the concentration tested [131]. In the future, testing the sensor's specificity for other biomarkers (including MMP2), and different concentrations is envisioned.

4.3. Comparative study between optimized immunosensors and conventional methods for diagnosing diabetic retinopathy through quantification of IL-6 and MMP2 in tears

DR diagnosing and monitoring through the molecular profiling of minimally invasive biological fluids is a very challenging matter. Not only do tears bring a scarceness of sample volume, they also have very low protein content, and biomarkers are usually at much lower concentrations than in other body fluids [127]. Accordingly, techniques adequate for tear profiling need to require very low sample volumes, and to be able to achieve very low concentrations.

Table 9 compares the sample volume requirements, LR and LOD achieved using conventional biomolecule quantification techniques, namely Luminex and ELISA, for the quantification of IL-6 and MMP2 biomarkers in biological samples (obtained from the protocol manuals), and with the immunosensors developed in the present dissertation using standard solutions, according to the concentration ranges obtained by the Luminex analysis of healthy controls' and DR patients' tears.

Table 9. Luminex *vs* ELISA *vs* Biosensor for the quantification of IL-6 and MMP2, regarding sample volume requirements, LR and LOD.

Biomarker	Parameter	ELISA	Luminex	Biosensor
IL-6	Sample volume required (µL)	50 - 100	50	1
	LR (pg mL^{-1})	2 – 200	7 – 5000	1 – 75
	LOD (pg mL^{-1})	2	0.36	0.8
MMP2	Sample volume required (µL)	50 - 100	50	1
	LR (pg mL^{-1})	156 – 10000	100 – 100000	1 - 75
	LOD (pg mL^{-1})	43.8	3.8	0.6

As mentioned in section 2.4.2, tear samples can be collected by a capillary tube or through the insertion of an absorbent material in the subject's eye, and subsequent elution for the recovery of tear content. Both methods depend on the subject's tear production rate. The capillary method delivers a volume between 2 and 10 µL per eye, while the second achieves between 20 and 60 µL of sample [149]. Tear production is considered normal when at least 40 µL are extracted by the second method, and abnormal for smaller volumes [150]. It has already been noted that the first method delivers the purest result, free of mucous layer cells.

ELISA assays can be optimized to enable the biomarker quantification in a 50 µL sample, but commonly require 100 µL to do so [118]. The protocol used in this dissertation was optimized by Cruz *et al.* [131], and only required 50 µL of tear sample, enabling the use of the Schirmer's strip for biomarker quantification, when the subject's tear production is high enough to achieve that amount of fluid. However, ELISA assays can only quantify one biomarker at a time, meaning that a 50 µL tear sample volume resultant from a single collection would result in the quantification of a single biomarker. Duplicate (or further) analysis is, therefore, disabled for this method. When the capillary method is used for sampling, the volume obtained is not enough to fulfill the optimized requirement of 50 µL, disabling the use of the ELISA method to analyze the samples collected by these means. For the mentioned arguments, ELISA is not a truly adequate method for tear sample profiling, in terms of volume requirements.

On the other hand, Luminex is a multiplex technique, which means that a single sample of 50 µL can quantify a large number of biomarkers [119]. 50 µL of tear fluid can be collected through the absorbent

material method, as performed by the University of Coimbra. As with ELISA, however, not all subjects deliver this amount of fluid. The sample volumes resultant from capillary collection are also not adequate for Luminex analysis.

Similar to the ELISA method, at this stage, the biosensor can only quantify one biomarker at a time. However, minute sample volume requirements of a single µL per test enable the use of both collection techniques, repeated analysis and multiple biomarker assessment. Additionally, the presented systems can, in the future, be incorporated into a multiplex system, using microfluidic strategies to quantify IL-6, MMP2 and possibly other biomarkers in a minute volume of tear fluid. It is important to note that, as mentioned earlier in Section 2.4.2, DR often coexists with dry eye syndrome and other conditions that affect the patient's tear production. As so, the need for minute sample volumes is a great advantage for the use of the proposed biosensors.

When it comes to LRs and LODs, the ELISA method quantifies concentrations between 2 and 200 pg mL^{-1} and has a LOD of 2 pg mL^{-1} for IL-6, which, as noted in Section 4.1, is adequate for DR diagnosing. However, ELISA MMP2 assay has an optimum detection range between 156 and 10000 pg mL^{-1}, and the lowest value detectable at 43.8 pg mL^{-1}. These values make the ELISA method unsuitable for the quantification of tears' MMP2 concentrations for DR diagnosing, since the minimum value detected by ELISA is higher than the maximum value found in the tears of DR patients, reported previously in Section 4.1 as 23.1 pg mL^{-1}.

Regarding Luminex, the LR for IL-6 quantification stands between 7 and 5000 pg mL^{-1}, with a LOD of 0.36 pg mL^{-1}. These values are accordant with healthy subjects' and DR patients' tear IL-6 concentrations. However, for MMP2 quantification, even though the LOD is 3.8 pg mL^{-1}, the optimal detection LR goes from 100 to 100000 pg mL^{-1}, which means that, even though it is able to detect small concentrations found in DR's patients and controls, Luminex does not deliver its best accuracy for MMP2 concentrations below 100 pg mL^{-1}, and consequently, for DR critique ranges in minimally invasive biological fluids.

With LRs between 1 and 75 pg mL^{-1}, and LODs of 0.8 and 0.6 pg mL^{-1} for IL-6 and MMP2, respectively, the developed immunosensors have LRs and LODs that include all concentrations found in the tears of healthy subjects and DR patients. Minimum values found in tears are within the optimal LR for both immunosensors, and comparing with either ELISA or Luminex, the upper limits of the LRs are closer to the maximum values detected in tears.

Taking into account all the abovementioned arguments, the immunosensors show high potential for DR diagnosing through IL-6 and MMP2 biomarker quantification in tear fluid. They are the only method where samples collected through both sampling methods are viable, and their LRs and LODs are more suited for the quantification of DR critical concentrations in tears, than the ELISA and Luminex assays. Additionally, their high performance in very low concentrations allows for sample dilution, with less risk of the lower concentrations falling below the minimum optimal reading values. This brings an enormous advantage, as tear's collection rates are one of tear analysis' downfalls, allowing repeated multiplex analysis. Additionally, the use of the immunosensors enables their integration in an affordable multiplex portable device, for a fast *in situ* POC measurement.

4.4. IL-6 immunosensor's analytical performance on saliva samples and comparison with the ELISA method

As a complementary study using minimally invasive fluids, the IL-6 immunosensor's performance was tested in 15 saliva samples from a non-DR population, and compared with the results obtained with the ELISA method. Saliva sampling is even less discomfortable for the patients than tear sampling, and it has been used for biomarker analysis purposes [14]. When comparing with tears, saliva's anatomical position in the body is further away from the retina, which makes local ocular alterations less likely to be detected in saliva than in tear fluid. Moreover, as previously stated in Section 3.4, saliva is a complex and viscous fluid, and therefore, an optimization process resulted in a 1:4 dilution factor in NaCl 0.9 % of the saliva samples, to avoid system saturation, before following the protocol presented in Section 3.2. Table 10 compares the results for IL-6 concentration in saliva samples obtained with the ELISA method and the IL-6 immunosensor.

Table 10. ELISA *vs* IL-6 immunosensor results for the quantification of IL-6 in 15 saliva samples. n.d. stands for not detected.

Sample	ELISA (pg mL^{-1})	Biosensor (pg mL^{-1})
1	n.d.	n.d.
2	n.d.	n.d.
3	n.d.	n.d.
4	2.2 ± 0.1	2.1 ± 0.1
5	2.4 ± 0.1	2.5 ± 0.4
6	3.6 ± 0.5	3.6 ± 0.5
7	2.3 ± 0.7	2.1 ± 0.2
8	3.5 ± 0.4	3.3 ± 0.5
9	2.3 ± 0.2	2.8 ± 0.5
10	n.d.	2.2 ± 0.1
11	n.d.	1.5 ± 0.1
12	n.d.	1.3 ± 0.1
13	n.d.	2.0 ±0.1
14	n.d.	1.4 ± 0.2
15	n.d.	1.6 ± 0.1

In samples 1 – 3, no IL-6 was detected in both measuring instruments. For that reason, it can be concluded that these samples had a null IL-6 concentration, or it was lower than the lowest LOD achieved for both techniques: 0.8 pg mL^{-1}, which belonged to the immunosensor.

When testing samples 4 – 9, both ELISA and the immunosensor were able to detect IL-6 in low concentrations, and similar results were obtained. One can conclude that the immunosensor's performance matches ELISA's performance, within this range.

Samples 10 – 15 unveiled the immunosensor's superiority to ELISA. In this range of concentrations, the conventional method failed to detect IL-6 in the samples, as they were very close or inferior to its LOD for IL-6 (2 pg mL^{-1}). On the contrary, the biosensor was able to quantify these very low concentrations.

This test validates the use of this biosensor for quantifying IL-6 in clinical saliva samples with IL-6 concentrations between 0.8 and approximately 4.0 pg mL^{-1}. The biosensor matched the conventional

ELISA method's performance for detecting low concentrations of IL-6 that were within the reading range of the conventional method, and even surpassed it in terms of LOD, accomplishing the quantification of very low concentrations of IL-6 in saliva samples, undetected by ELISA. As exposed in Section 2.4, the quantification of IL-6 in minimally invasive body fluids obtained from DR patients is almost unexplored, and therefore there are no guidelines for the concentrations to expect. Moreover, the present section shows that IL-6 is present in saliva samples at very low concentrations. The presence of DR could result in increased IL-6 concentrations. However, as stated, the distance of this fluid to the retina would probably result in very subtle alterations. Accordingly, the high sensitivity of the immunosensor in very low IL-6 concentrations could be a major factor for the potential use of saliva for the diagnosis and monitoring of DR.

5. Concluding remarks and future work

In this final section, the concluding remarks regarding DR's problematic factors and all experimental procedures applied in the present dissertation for the development and optimization of IL-6 and MMP2 immunosensors for the diagnosis of DR through minimally invasive biological fluids are stated. Finally, some suggestions are made as future work to continue the development of the presented high potential technology.

5.1. Concluding remarks

DR, classically regarded as a microvascular disorder of the retina, is the most common complication arising from DM and the leading worldwide cause of acquired vision loss in working-aged adults. It progresses silently for a long period of time, with a significant percentage of its patients left undiagnosed.

Most of the treatments are applied at later stages of the disease when vision is already affected, and none of them are fully capable of attenuating clinical progression or reversing damage to the retina. Moreover, they are ineffective in a large proportion of DR patients. Early detection of subclinical DR represents an urgent and unmet need in providing timely recognition and management for patients.

Technologies used to assess and monitor DR progression have been improving over the past years, and many novel biomarker-based technologies have been explored to answer the difficulties of conventional diagnosing methods, that are rather complex expensive technologies solely based on the qualitative evaluation of ophthalmic images, that require specialized professionals, do not take into account the complete spectrum of DR-caused alterations, and deliver a subjective evaluation. Affordable POC diagnosing and monitoring technologies would vastly improve diagnostic performances and relieve health services from avoidable costs associated to this complication. Moreover, the use of minimally invasive biological fluids to identify DR risk patients could significantly improve the visual outcome of patients with DM.

Tears are a minimally-invasively acquired sample that reflect pathological ophthalmic alterations. The use of this fluid enables continuous monitoring and comparison with a control population. Scantiness of fluid and low protein concentrations are, however, the downfalls of tear molecular profiling. Saliva is another biological fluid that can be collected causing even less discomfort to the patient than tear sampling. Even though it has been more explored as a biomarker source fluid for oral conditions, and it is not an ocular fluid, some studies have found altered biomarker concentrations in DR patients' saliva.

IL-6 and MMP2 are two proteins that have been linked with DR, and can potentially be used for diagnosing, monitoring and stratification. However, very few studies have quantified IL-6 and MMP2 in minimally invasive biological fluids, making the present study very relevant and timely for the DR research field. A collaboration with the University of Coimbra revealed a positive correlation between IL-6 and MMP2 concentration in tears, and DR presence, using a conventional method for biomolecule quantification, namely Luminex. A total of 14 tear samples were analyzed. Tears' IL-6 concentration ranged from 20.6 to 37.7 pg mL^{-1} in the control population, and from 34.1 to 56.7 pg mL^{-1} in DR patients. The mean concentration value was 25.7 ± 7.0 pg mL^{-1} and 42.9 ± 6.6 pg mL^{-1} for controls and DR patients, respectively, which corresponded to a statistically significant difference ($P = 0.001796 < 0.05$). Regarding MMP2, the control population featured IL-6 tear concentrations between 9.3 and 17.7 pg mL^{-1}, with a mean value of 10.8 ± 4.1 pg mL^{-1}, while the DR population featured concentrations between 11.6 and 23.1 pg mL^{-1} and a mean value of 18.0 ± 4.6 pg mL^{-1}, with another statistically significant difference distinguishing the two groups ($P = 0.0276 < 0.05$). These results showed great potential for the use of IL-6 and MMP2 quantification in tear samples as a quantitative factor for the diagnosing and monitoring of DR.

The biofunctionalization of IL-6 and MMP2 immunosensors was achieved and monitored using CV and EIS, and the experimental data was fitted to a Randles equivalent circuit where system components and interactions were simplified. The biofunctionalization layers consecutively immobilized to the surface of the WE were a cross-linker (sulfo-LC-SPDP), meant to create a SAM and react with the second biofunctionalization layer comprising antibodies as biorecognition elements, to achieve specific biomarker detection. The third and final biofunctionalization layer immobilized was the BSA, that prevented unspecific protein binding to the antibodies. Calibration curves for the IL-6 and MMP2 immunosensors were constructed using standard solutions of either IL-6 or MMP2, respectively, with concentrations ranging from 1 to 75 pg mL^{-1} in NaCl, considering the concentration ranges obtained with Luminex, and achieved LODs of 0.8 pg mL^{-1} for IL-6 and 0.6 pg mL^{-1} for MMP2, using only 1 µL of solution. NaCl 0.9 % was the solvent used for the standard solutions since it was also used for eluting and recovering tear components upon sampling, and because it is a solution that is similar to tear matrix, frequently used to lubricate and clean the eye. These curves were fitted to a linear regression with R^2 0.9809 and 0.9864 for IL-6 and MMP2, respectively.

The developed immunosensors' LRs and LODs were compared to the IL-6 and MMP2 concentrations found in the tears of heathy controls and DR patients, and considered suitable for DR diagnosing

purposes. The IL-6 immunosensor was further tested to assess its specificity, which was confirmed with the presence of IL-6 being detected despite the presence of TNF-α, and no significant signal resultant from IL-6 absence in solution. As exposed previously, tear profiling comes with demanding challenges in terms of LOD and very low sample volumes. The proposed immunosensors were, therefore, compared in terms of sample volume requirements, LR and LOD with the characteristics presented on the manuals of two conventional biomolecule quantifying methods, namely Luminex and ELISA, to assess which technique is best suitable for IL-6 and MMP2 quantification in tear fluid for DR diagnosing and monitoring. For IL-6, both ELISA and Luminex had adequate LRs and LODs for DR critique values in tears. For MMP2, ELISA's LR and LOD revealed to be unsuitable for DR diagnosing in tear samples. On the other hand, Luminex has an adequate LOD, but the LR for which it delivers optimal results comprises values above the maximum MMP2 concentration quantified in DR patients' tears. Analyzing sample volume requirements, both the ELISA (50 – 100 µL) and Luminex (50 µL) methods are only suitable for analyzing samples collected with the absorbent material method. However, it is important to note that DR is commonly accompanied by dry eye syndrome, and not all subjects reach the 50 µL sample volume hallmark needed for the use of either of these conventional methods. In contrast, the biosensor requires a minute sample volume of 1 µL per test, making it suitable for all tear sample collection methods. Also, repeated analysis of multiple biomarkers is enabled, and low LODs allow for sample dilution. This proves the proposed biosensing systems to have high potential for IL-6 and MMP2 quantification in tear samples for DR diagnosing purposes, when compared with the analyzed conventional techniques.

As a complementary study, the IL-6 biosensor was tested in 15 saliva samples, and the results were compared with the conventional biomolecule quantification ELISA method. The outcomes were very promising for the immunosensor, since it was able to match ELISA's performance in concentrations detected with this method, and surpassed it for very low concentrations, managing to quantify the concentration of 6 saliva samples that were undetected with the conventional method. This ability to reach very low concentrations is especially important because there is no information regarding salivary IL-6 concentrations in DR. Since saliva is also a non-invasive biological fluid, the present work shows great potential for the use of this fluid, not only for DR, but for biomarker analysis in other diseases. The analysis of saliva could complement tear profiling for the management of DR.

In conclusion, two biosensing systems were presented. They proved to be capable of measuring IL-6 and MMP2 concentrations found to be critical for DR diagnosis, using minute sample volumes. It is also important to note that these immunosensors can be integrated into a portable multiplex system, for an

in situ simultaneous analysis of multiple biomarkers, that is much cheaper and simpler than the conventionally used techniques, and does not require a trained professional to perform. This opens the doors for a simple, fast and quantitative analysis technology to emerge, improve and personalize DR diagnosis.

During this project, a Progress Report paper entitled "Minimally invasive molecular sensing for improved diagnosis of diabetic retinopathy" was written by Maria Vieira, Vanessa F. Cardoso, Mariana Carvalho, António F. Ambrósio, Rosa Fernandes and Inês M. Pinto and submitted to a high impact Journal: Advanced Biosystems (Annex B). Also, a research paper entitled "IL-6 and TNF-α salivary levels in children with mental health problems: a lab-on-a-chip for immune quantification" by Andrea Cruz, Maria Vieira *et al.* is in preparation. The market value for this project was confirmed by its selection for the 2020 edition of the University of Porto's Business Ignition Programme, where a business model has been designed for a DR-chip. The agenda, participating groups and aims of this programme can be consulted in bip.up.pt/bip-2020.

5.2. Future work

The present work shows promising results on the potential use of a biosensing device for DR diagnosis, stratification and monitoring, through minimally invasive biological fluids' biomarker profiling. However, further investigation is still required, namely:

- The functionalization and optimization of a variety of different biomarkers for DR diagnosis;
- Specificity analysis for a larger variety of biomarkers;
- Clinical validation in minimally invasive biological fluids;
- Profiling of a larger population of healthy controls and DR patients, in different disease stages, in order to define standard values;
- Construction of a multiplex system, using microfluidic approaches for simultaneous multiple biomarker analysis;
- Design of an artificial intelligence system to conjugate the conventional (structural) and molecular (quantifiable) data for a multi-factor personalized diagnosis of DR;
- Translation of this technology to other diseases and strategic fluids.

6. References

[1] I.D. Federation, IDF Diabetes Atlas - 2019, 2019. https://doi.org/10.1289/image.ehp.v119.i03.

[2] R.L. Thomas, S. Halim, S. Gurudas, S. Sivaprasad, D.R. Owens, IDF Diabetes Atlas: A review of studies utilising retinal photography on the global prevalence of diabetes related retinopathy between 2015 and 2018, Diabetes Res. Clin. Pract. 157 (2019) 107840. https://doi.org/10.1016/j.diabres.2019.107840.

[3] N. Cheung, P. Mitchell, T.Y. Wong, Diabetic retinopathy., Lancet (London, England). 376 (2010) 124–136. https://doi.org/10.1016/S0140-6736(09)62124-3.

[4] D.S.W. Ting, G.C.M. Cheung, T.Y. Wong, Diabetic retinopathy: global prevalence, major risk factors, screening practices and public health challenges: a review., Clin. Experiment. Ophthalmol. 44 (2016) 260–277. https://doi.org/10.1111/ceo.12696.

[5] W. Yang, T.M. Dall, P. Halder, P. Gallo, S.L. Kowal, P.F. Hogan, M. Petersen, Economic costs of diabetes in the U.S. in 2012, Diabetes Care. 36 (2013) 1033–1046. https://doi.org/10.2337/dc12-2625.

[6] M. Villarroel, A. Ciudin, C. Hernandez, R. Simo, Neurodegeneration: An early event of diabetic retinopathy., World J. Diabetes. 1 (2010) 57–64. https://doi.org/10.4239/wjd.v1.i2.57.

[7] T.A.S. Group, A.E.S. Group, Effects of Medical Therapies on Retinopathy Progression in Type 2 Diabetes, N. Engl. J. Med. 363 (2010) 233–244. https://doi.org/10.1056/NEJMoa1001288.

[8] Early Treatment Diabetic Retinopathy Study Research Group, Grading Diabetic Retinopa thy from Stereoscopic Color Fundus Photographs- An Extension of the Modified Airlie House Classification, Ophthalmology. 98 (1991) 786–806. https://doi.org/10.1016/S0161-6420(13)38012-9.

[9] M.D. Abramoff, P.E. Fort, I.C. Han, K.T. Jayasundera, E.H. Sohn, T.W. Gardner, Approach for a Clinically Useful Comprehensive Classification of Vascular and Neural Aspects of Diabetic Retinal Disease., Invest. Ophthalmol. Vis. Sci. 59 (2018) 519–527. https://doi.org/10.1167/iovs.17-21873.

[10] A.A. Khan, A.H. Rahmani, Y.H. Aldebasi, Diabetic Retinopathy: Recent Updates on Different Biomarkers and Some Therapeutic Agents., Curr. Diabetes Rev. 14 (2018) 523–533. https://doi.org/10.2174/1573399813666170915133253.

[11] C.-J. Jeng, Y.-T. Hsieh, C.-M. Yang, C.-H. Yang, C.-L. Lin, I.-J. Wang, Diabetic Retinopathy in Patients with Diabetic Nephropathy: Development and Progression., PLoS One. 11 (2016) e0161897. https://doi.org/10.1371/journal.pone.0161897.

[12] G. Velez, P.H. Tang, T. Cabral, G.Y. Cho, D.A. Machlab, S.H. Tsang, A.G. Bassuk, V.B. Mahajan, Personalized proteomics for precision health: Identifying biomarkers of vitreoretinal disease, Transl. Vis. Sci. Technol. 7 (2018). https://doi.org/10.1167/tvst.7.5.12.

[13] J. Liu, B. Shi, S. He, X. Yao, M.D.P. Willcox, Z. Zhao, Changes to tear cytokines of type 2 diabetic patients with or without retinopathy, Mol. Vis. 16 (2010) 2931–2938.

[14] C.S. Chee, K.M. Chang, M.F. Loke, V.P. Angela Loo, V. Subrayan, Association of potential salivary biomarkers with diabetic retinopathy and its severity in type-2 diabetes mellitus: a proteomic analysis by mass spectrometry., PeerJ. 4 (2016) e2022. https://doi.org/10.7717/peerj.2022.

[15] L. Najafi, M. Malek, A.E. Valojerdi, R. Aghili, M.E. Khamseh, A.E. Fallah, M.R.F. Tokhmehchi, M.J. Behrouz, Dry eye and its correlation to diabetes microvascular complications in people with type 2 diabetes mellitus., J. Diabetes Complications. 27 (2013) 459–462. https://doi.org/10.1016/j.jdiacomp.2013.04.006.

[16] M. Mysliwiec, A. Balcerska, K. Zorena, J. Mysliwska, P. Lipowski, K. Raczynska, The role of vascular endothelial growth factor, tumor necrosis factor alpha and interleukin-6 in pathogenesis of diabetic retinopathy., Diabetes Res. Clin. Pract. 79 (2008) 141–146. https://doi.org/10.1016/j.diabres.2007.07.011.

[17] K. Noda, S. Ishida, M. Inoue, K. Obata, Y. Oguchi, Y. Okada, E. Ikeda, Production and activation of matrix metalloproteinase-2 in proliferative diabetic retinopathy., Invest. Ophthalmol. Vis. Sci. 44 (2003) 2163–2170. https://doi.org/10.1167/iovs.02-0662.

[18] C.M. Pandey, B.D. Malhotra, Biosensors - Fundamentals and applications, 2nd ed., Walter de Gruyter, Berlin/Boston, 2019. https://doi.org/https://doi.org/10.1515/9783110641080-201.

[19] B. Byrne, E. Stack, N. Gilmartin, R.O. Kennedy, Antibody-Based Sensors: Principles, Problems and Potential for Detection of Pathogens and Associated Toxins, (2009) 4407–4445. https://doi.org/10.3390/s90604407.

[20] A.J. Bard, L.R. Faulkner, Electrochemical methods - Fundamentals and applications, 2nd ed., John Wiley & Sons, Inc., New York, 2001. https://doi.org/10.1038/s41929-019-0277-8.

[21] G. Dahlquist, Can we slow the rising incidence of childhood-onset autoimmune diabetes? The overload hypothesis, Diabetologia. 49 (2006) 20–24. https://doi.org/10.1007/s00125-005-0076-4.

[22] D. Pascolini, S.P. Mariotti, Global estimates of visual impairment: 2010, Br. J. Ophthalmol. 96 (2012) 614–618. https://doi.org/10.1136/bjophthalmol-2011-300539.

[23] J.W.Y. Yau, S.L. Rogers, R. Kawasaki, E.L. Lamoureux, J.W. Kowalski, T. Bek, S.-J. Chen, J.M. Dekker, A. Fletcher, J. Grauslund, S. Haffner, R.F. Hamman, M.K. Ikram, T. Kayama, B.E.K. Klein, R. Klein, S. Krishnaiah, K. Mayurasakorn, J.P. O'Hare, T.J. Orchard, M. Porta, M. Rema, M.S. Roy, T. Sharma, J. Shaw, H. Taylor, J.M. Tielsch, R. Varma, J.J. Wang, N. Wang, S. West, L. Xu, M. Yasuda, X. Zhang, P. Mitchell, T.Y. Wong, Global prevalence and major risk factors of diabetic retinopathy., Diabetes Care. 35 (2012) 556–564. https://doi.org/10.2337/dc11-1909.

[24] D.S. Fong, L. Aiello, T.W. Gardner, G.L. King, G. Blankenship, J.D. Cavallerano, F.L. Ferris, R. Klein, Retinopathy in Diabetes, Diabetes Care. 27 (2004). https://doi.org/10.2337/diacare.27.2007.s84.

[25] J.C. Javitt, L.P. Aiello, Y. Chiang, F.L. Ferris III, J.K. Canner, S. Greenfield, Preventive Eye Care in People with Diabetes Is Cost-Saving to the Federal Government. Implications for health-care reform, 17 (1994) 909–917.

[26] E. Heintz, A.-B. Wirehn, B.B. Peebo, U. Rosenqvist, L.-A. Levin, Prevalence and healthcare costs of diabetic retinopathy: a population-based register study in Sweden., Diabetologia. 53 (2010) 2147–2154. https://doi.org/10.1007/s00125-010-1836-3.

[27] J. Lechner, O.E. O'Leary, A.W. Stitt, The pathology associated with diabetic retinopathy., Vision Res. 139 (2017) 7–14. https://doi.org/10.1016/j.visres.2017.04.003.

[28] J. Kur, E.A. Newman, T. Chan-Ling, Cellular and physiological mechanisms underlying blood flow

regulation in the retina and choroid in health and disease., Prog. Retin. Eye Res. 31 (2012) 377–406. https://doi.org/10.1016/j.preteyeres.2012.04.004.

[29] J. Cunha-Vaz, R. Bernardes, C. Lobo, Blood-retinal barrier., Eur. J. Ophthalmol. 21 Suppl 6 (2011) S3-9. https://doi.org/10.5301/EJO.2010.6049.

[30] I. Klaassen, C.J.F. Van Noorden, R.O. Schlingemann, Molecular basis of the inner blood-retinal barrier and its breakdown in diabetic macular edema and other pathological conditions., Prog. Retin. Eye Res. 34 (2013) 19–48. https://doi.org/10.1016/j.preteyeres.2013.02.001.

[31] A. Bringmann, T. Pannicke, J. Grosche, M. Francke, P. Wiedemann, S.N. Skatchkov, N.N. Osborne, A. Reichenbach, Müller cells in the healthy and diseased retina, Prog. Retin. Eye Res. 25 (2006) 397–424. https://doi.org/10.1016/j.preteyeres.2006.05.003.

[32] F. Ginhoux, M. Greter, M. Leboeuf, S. Nandi, P. See, S. Gokhan, M.F. Mehler, S.J. Conway, L.G. Ng, E.R. Stanley, I.M. Samokhvalov, M. Merad, Fate mapping analysis reveals that adult microglia derive from primitive macrophages, Science (80-.). 330 (2010) 841–845. https://doi.org/10.1126/science.1194637.

[33] T. Langmann, Microglia activation in retinal degeneration, J. Leukoc. Biol. 81 (2007) 1345–1351. https://doi.org/10.1189/jlb.0207114.

[34] T. Bek, Diameter Changes of Retinal Vessels in Diabetic Retinopathy., Curr. Diab. Rep. 17 (2017) 82. https://doi.org/10.1007/s11892-017-0909-9.

[35] M. Brownlee, The pathobiology of diabetic complications: A unifying mechanism, Diabetes. 54 (2005) 1615–1625. https://doi.org/10.2337/diabetes.54.6.1615.

[36] S. Roy, T.S. Kern, B. Song, C. Stuebe, Mechanistic Insights into Pathological Changes in the Diabetic Retina: Implications for Targeting Diabetic Retinopathy., Am. J. Pathol. 187 (2017) 9–19. https://doi.org/10.1016/j.ajpath.2016.08.022.

[37] E. Csosz, E. Deak, G. Kallo, A. Csutak, J. Tozser, Diabetic retinopathy: Proteomic approaches to help the differential diagnosis and to understand the underlying molecular mechanisms., J. Proteomics. 150 (2017) 351–358. https://doi.org/10.1016/j.jprot.2016.06.034.

[38] T. Nishikawa, D. Edelstein, X.L. Du, S.I. Yamagishi, T. Matsumura, Y. Kaneda, M.A. Yorek, D. Beebe, P.J. Oates, H.P. Hammes, I. Glardino, M. Brownlee, Normalizing mitochondrial superoxide production blocks three pathways of hyperglycaemic damage, Nature. 404 (2000) 787–790. https://doi.org/10.1038/35008121.

[39] T. Yuuki, T. Kanda, Y. Kimura, N. Kotajima, J. Tamura, I. Kobayashi, S. Kishi, Inflammatory cytokines in vitreous fluid and serum of patients with diabetic vitreoretinopathy., J. Diabetes Complications. 15 (2001) 257–259.

[40] H.-P. Hammes, Pericytes and the pathogenesis of diabetic retinopathy., Horm. Metab. Res. = Horm. Und Stoffwechselforsch. = Horm. Metab. 37 Suppl 1 (2005) 39–43. https://doi.org/10.1055/s-2005-861361.

[41] M. Mizutani, T.S. Kern, M. Lorenzi, Accelerated death of retinal microvascular cells in human and experimental diabetic retinopathy, J. Clin. Invest. 97 (1996) 2883–2890. https://doi.org/10.1172/JCI118746.

[42] A.B. El-Remessy, M. Al-Shabrawey, Y. Khalifa, N.-T. Tsai, R.B. Caldwell, G.I. Liou, Neuroprotective

and blood-retinal barrier-preserving effects of cannabidiol in experimental diabetes., Am. J. Pathol. 168 (2006) 235–244. https://doi.org/10.2353/ajpath.2006.050500.

[43] J.D. Boss, P.K. Singh, H.K. Pandya, J. Tosi, C. Kim, A. Tewari, M.S. Juzych, G.W. Abrams, A. Kumar, Assessment of Neurotrophins and Inflammatory Mediators in Vitreous of Patients With Diabetic Retinopathy, Invest. Ophthalmol. Vis. Sci. 58 (2017) 5594–5603. https://doi.org/10.1167/iovs.17-21973.

[44] Y. Suzuki, M. Nakazawa, K. Suzuki, H. Yamazaki, Y. Miyagawa, Expression profiles of cytokines and chemokines in vitreous fluid in diabetic retinopathy and central retinal vein occlusion., Jpn. J. Ophthalmol. 55 (2011) 256–263. https://doi.org/10.1007/s10384-011-0004-8.

[45] J. Tang, T.S. Kern, Inflammation in Diabetic Retinopathy, Prog. Retin. Eye Res. 30 (2011) 343–358. https://doi.org/10.1038/jid.2014.371.

[46] S.F. Abcouwer, Müller cell-microglia cross talk drives neuroinflammation in diabetic retinopathy, Diabetes. 66 (2017) 261–263. https://doi.org/10.2337/dbi16-0047.

[47] F.S. Sorrentino, M. Allkabes, G. Salsini, C. Bonifazzi, P. Perri, The importance of glial cells in the homeostasis of the retinal microenvironment and their pivotal role in the course of diabetic retinopathy., Life Sci. 162 (2016) 54–59. https://doi.org/10.1016/j.lfs.2016.08.001.

[48] M. Stem, T. Gardner, Neurodegeneration in the Pathogenesis of Diabetic Retinopathy: Molecular Mechanisms and Therapeutic Implications, Curr. Med. Chem. 20 (2013) 3241–3250. https://doi.org/10.2174/09298673113209990027.

[49] S. Karadeniz, P. Zimmet, Diabetes eye health, 2013.

[50] T.Y. Wong, C.M.G. Cheung, M. Larsen, S. Sharma, R. Simo, Diabetic retinopathy., Nat. Rev. Dis. Prim. 2 (2016) 16012. https://doi.org/10.1038/nrdp.2016.12.

[51] J. Chu, Y. Ali, Diabetic retinopathy: A review, Drug Dev. Res. 69 (2008) 1–14. https://doi.org/10.1002/ddr.20222.

[52] A.J. Barber, E. Lieth, S.A. Khin, D.A. Antonetti, A.G. Buchanan, T.W. Gardner, Neural apoptosis in the retina during experimental and human diabetes. Early onset and effect of insulin., J. Clin. Invest. 102 (1998) 783–791. https://doi.org/10.1172/JCI2425.

[53] T.E. Fox, X. Han, S. Kelly, A.H. 2nd Merrill, R.E. Martin, R.E. Anderson, T.W. Gardner, M. Kester, Diabetes alters sphingolipid metabolism in the retina: a potential mechanism of cell death in diabetic retinopathy., Diabetes. 55 (2006) 3573–3580. https://doi.org/10.2337/db06-0539.

[54] T.W. Gardner, J.M. Sundstrom, A proposal for early and personalized treatment of diabetic retinopathy based on clinical pathophysiology and molecular phenotyping., Vision Res. 139 (2017) 153–160. https://doi.org/10.1016/j.visres.2017.03.006.

[55] N. Maniadakis, E. Konstantakopoulou, Cost Effectiveness of Treatments for Diabetic Retinopathy: A Systematic Literature Review., Pharmacoeconomics. 37 (2019) 995–1010. https://doi.org/10.1007/s40273-019-00800-w.

[56] A.R. Santiago, R. Boia, I.D. Aires, A.F. Ambrosio, R. Fernandes, Sweet Stress: Coping With Vascular Dysfunction in Diabetic Retinopathy., Front. Physiol. 9 (2018) 820. https://doi.org/10.3389/fphys.2018.00820.

[57] K. Selvaraj, K. Gowthamarajan, V.V.S.R. Karri, U.K. Barauah, V. Ravisankar, G.M. Jojo, Current

treatment strategies and nanocarrier based approaches for the treatment and management of diabetic retinopathy., J. Drug Target. 25 (2017) 386–405. https://doi.org/10.1080/1061186X.2017.1280809.

[58] M. Shani, T. Eviatar, D. Komaneshter, S. Vinker, Diabetic Retinopathy -Incidence And Risk Factors In A Community Setting- A Longitudinal Study., Scand. J. Prim. Health Care. 36 (2018) 237–241. https://doi.org/10.1080/02813432.2018.1487524.

[59] M. Whitehead, S. Wickremasinghe, A. Osborne, P. Van Wijngaarden, K.R. Martin, Diabetic retinopathy: a complex pathophysiology requiring novel therapeutic strategies., Expert Opin. Biol. Ther. 18 (2018) 1257–1270. https://doi.org/10.1080/14712598.2018.1545836.

[60] A.M. Abu-El-Asrar, L. Dralands, L. Missotten, I.A. Al-Jadaan, K. Geboes, Expression of apoptosis markers in the retinas of human subjects with diabetes., Invest. Ophthalmol. Vis. Sci. 45 (2004) 2760–2766. https://doi.org/10.1167/iovs.03-1392.

[61] E.J. Barrett, Z. Liu, M. Khamaisi, G.L. King, R. Klein, B.E.K. Klein, T.M. Hughes, S. Craft, B.I. Freedman, D.W. Bowden, A.I. Vinik, C.M. Casellini, Diabetic microvascular disease: An endocrine society scientific statement, J. Clin. Endocrinol. Metab. 102 (2017) 4343–4410. https://doi.org/10.1210/jc.2017-01922.

[62] W. Wang, A.C.Y. Lo, Diabetic Retinopathy: Pathophysiology and Treatments., Int. J. Mol. Sci. 19 (2018). https://doi.org/10.3390/ijms19061816.

[63] R. Klein, B.E. Klein, S.E. Moss, M.D. Davis, D.L. DeMets, The Wisconsin epidemiologic study of diabetic retinopathy. II. Prevalence and risk of diabetic retinopathy when age at diagnosis is less than 30 years., Arch. Ophthalmol. (Chicago, Ill. 1960). 102 (1984) 520–526. https://doi.org/10.1001/archopht.1984.01040030398010.

[64] J.A. Wells, A.R. Glassman, A.R. Ayala, L.M. Jampol, L.P. Aiello, A.N. Antoszyk, B. Arnold-Bush, C.W. Baker, N.M. Bressler, D.J. Browning, M.J. Elman, F.L. Ferris, S.M. Friedman, M. Melia, D.J. Pieramici, J.K. Sun, R.W. Beck, Aflibercept, Bevacizumab, or Ranibizumab for Diabetic Macular Edema, 372 (2015) 1193–1203. https://doi.org/10.1056/NEJMoa1414264.Aflibercept.

[65] G.D. Calderon, O.H. Juarez, G.E. Hernandez, S.M. Punzo, Z.D. De La Cruz, Oxidative stress and diabetic retinopathy: Development and treatment, Eye. 31 (2017) 1122–1130. https://doi.org/10.1038/eye.2017.64.

[66] J. Luan, F. Ando, H. Hirose, O. Yasui, Vitrectomy results in proliferative diabetic retinopathy, Int. J. Ophthalmol. 5 (2005) 852–854.

[67] J.G. Gross, A.R. Glassman, L.M. Jampol, S. Inusah, L.P. Aiello, A.N. Antoszyk, C.W. Baker, B.B. Berger, N.M. Bressler, D. Browning, M.J. Elman, F.L. 3rd Ferris, S.M. Friedman, D.M. Marcus, M. Melia, C.R. Stockdale, J.K. Sun, R.W. Beck, Panretinal Photocoagulation vs Intravitreous Ranibizumab for Proliferative Diabetic Retinopathy: A Randomized Clinical Trial., JAMA. 314 (2015) 2137–2146. https://doi.org/10.1001/jama.2015.15217.

[68] X. Zhang, S. Bao, D. Lai, R.W. Rapkins, M.C. Gillies, Intravitreal triamcinolone acetonide inhibits breakdown of the blood-retinal barrier through differential regulation of VEGF-A and its receptors in early diabetic rat retinas, Diabetes. 57 (2008) 1026–1033. https://doi.org/10.2337/db07-0982.

[69] S. Matsuda, F. Gomi, Y. Oshima, M. Tohyama, Y. Tano, Vascular endothelial growth factor reduced

and connective tissue growth factor induced by triamcinolone in ARFE19 cells under oxidative stress, Investig. Ophthalmol. Vis. Sci. 46 (2005) 1062–1068. https://doi.org/10.1167/iovs.04-0761.

[70] S.F. Abcouwer, Angiogenic Factors and Cytokines in Diabetic Retinopathy, J. Clin. Cell. Immunol. (2011) 1–12. https://doi.org/10.4172/2155-9899.s1-011.

[71] R. Turner, R. Holman, I. Stratton, C. Cull, V. Frighi, S. Manley, D. Matthews, A. Neil, H. McElroy, E. Kohner, C. Fox, D. Hadden, D. Wright, Tight blood pressure control and risk of macrovascular and microvascular complications in type 2 diabetes, Br. Med. J. 317 (1998) 703–713. https://doi.org/10.1136/bmj.317.7160.703.

[72] X.D. Chen, T.W. Gardner, Psychophysical assessments of diabetic retinopathy, Surv. Ophthalmol. (2020) 1–18. https://doi.org/10.1016/j.survophthal.2020.08.003.

[73] F.L. Ferris, How Effective Are Treatments for Diabetic Retinopathy?, JAMA J. Am. Med. Assoc. 269 (1993) 1290–1291. https://doi.org/10.1001/jama.1993.03500100088034.

[74] M.D. Abramoff, M.K. Garvin, M. Sonka, Retinal imaging and image analysis, IEEE Rev. Biomed. Eng. 3 (2010) 169–208. https://doi.org/10.1109/RBME.2010.2084567.

[75] E.T.D.R.S.R. Group, Classification of diabetic retinopathy from fluorescein angiograms, Ophthalmology. 98 (1991) 807–822. https://doi.org/10.1016/S0161-6420(13)38013-0.

[76] Early Treatment Diabetic Retinopathy Study Research Group, Fundus Photographic Risk Factors for Progression of Diabetic Retinopathy: ETDRS Report Number 12, Ophthalmology. 98 (1991) 823–833. https://doi.org/10.1016/S0161-6420(13)38014-2.

[77] M.F.. Goldberg, L.M. Jampol, Knowledge of diabetic retinopathy before and 18 years after the Airlie House Symposium on Treatment of Diabetic Retinopathy., Ophthalmology. 94 (1987) 741–746. https://doi.org/10.1016/s0161-6420(87)33524-9.

[78] H. Khalid, R. Schwartz, L. Nicholson, J. Huemer, M.H. El-Bradey, D.A. Sim, P.J. Patel, K. Balaskas, R.D. Hamilton, P.A. Keane, R. Rajendram, Widefield optical coherence tomography angiography for early detection and objective evaluation of proliferative diabetic retinopathy, Br. J. Ophthalmol. (2020) 1–6. https://doi.org/10.1136/bjophthalmol-2019-315365.

[79] J. Chua, R. Sim, B. Tan, D. Wong, X. Yao, X. Liu, D.S.W. Ting, D. Schmidl, M. Ang, G. Garhöfer, L. Schmetterer, Optical Coherence Tomography Angiography in Diabetes and Diabetic Retinopathy, J. Clin. Med. 9 (2020) 1723. https://doi.org/10.3390/jcm9061723.

[80] P. Massin, A. Girach, A. Erginay, A. Gaudric, Optical coherence tomography: a key to the future management of patients with diabetic macular oedema., Acta Ophthalmol. Scand. 84 (2006) 466–474. https://doi.org/10.1111/j.1600-0420.2006.00694.x.

[81] R.F. Spaide, J.M. Klancnik, M.J. Cooney, Retinal vascular layers imaged by fluorescein angiography and optical coherence tomography angiography, JAMA Ophthalmol. 133 (2015) 45–50. https://doi.org/10.1001/jamaophthalmol.2014.3616.

[82] R.F. Spaide, J.G. Fujimoto, N.K. Waheed, Image artifacts in optical coherence tomography angiography, 2016. https://doi.org/10.1111/ceo.12781.

[83] A.A. Fawzi, Consensus on Optical Coherence Tomographic Angiography Nomenclature: Do We Need to Develop and Learn a New Language?, JAMA Ophthalmol. 176 (2017) 139–148.

https://doi.org/10.1001/jamaophthalmol.2017.0149.Consensus.

[84] R.P.C. Lira, C.L. de A. Oliveira, M.V.R.B. Marques, A.R. Silva, C. de C. Pessoa, Adverse reactions of fluorescein angiography: A prospective study, Arq. Bras. Oftalmol. 70 (2007) 615–618. https://doi.org/10.1590/S0004-27492007000400011.

[85] L.A. Yannuzzi, K.T. Rohrer, L.J. Tindel, R.S. Sobel, M.A. Costanza, W. Shields, E. Zang, Fluorescein Angiography Complication Survey, Ophthalmology. 93 (1986) 611–617. https://doi.org/10.1016/S0161-6420(86)33697-2.

[86] I.E. Mohamed, M.A. Mohamed, M. Yousef, M.Z. Mahmoud, B. Alonazi, Use of ophthalmic B-scan ultrasonography in determining the causes of low vision in patients with diabetic retinopathy., Eur. J. Radiol. Open. 5 (2018) 79–86. https://doi.org/10.1016/j.ejro.2018.05.002.

[87] P. Pusparajah, L.-H. Lee, K. Abdul Kadir, Molecular Markers of Diabetic Retinopathy: Potential Screening Tool of the Future?, Front. Physiol. 7 (2016) 200. https://doi.org/10.3389/fphys.2016.00200.

[88] A.D. Association, Diagnosis and classification of diabetes mellitus, Diabetes Care. 33 (2010). https://doi.org/10.2337/dc10-S062.

[89] R.A. Kowluru, Q. Zhong, J.M. Santos, Matrix metalloproteinases in diabetic retinopathy: potential role of MMP-9., Expert Opin. Investig. Drugs. 21 (2012) 797–805. https://doi.org/10.1517/13543784.2012.681043.

[90] M. Maggio, J.M. Guralnik, D.L. Longo, L. Ferrucci, Interleukin-6 in Aging and Chronic Disease: a Magnificent Pathway, JJournals Gerontol. - Ser. A Biol. Sci. Med. Sci. 61 (2006) 319–335. https://www.ncbi.nlm.nih.gov/pmc/articles/PMC2645627/pdf/nihms45646.pdf.

[91] P.A. Klimiuk, S. Sierakowski, R. Latosiewicz, J.P. Cylwik, B. Cylwik, J. Skowronski, J. Chwiecko, Interleukin-6, soluble interleukin-2 receptor and soluble interleukin-6 receptor in the sera of patients with different histological patterns of rheumatoid synovitis, Clin. Exp. Rheumatol. 21 (2003) 63–69.

[92] R. Atreya, J. Mudter, S. Finotto, J. Müllberg, T. Jostock, S. Wirtz, M. Schütz, B. Bartsch, M. Holtmann, C. Becker, D. Strand, J. Czaja, J.F. Schlaak, H.A. Lehr, F. Autschbach, G. Schürmann, N. Nishimoto, K. Yoshizaki, H. Ito, T. Kishimoto, P.R. Galle, S. Rose-John, M.F. Neurath, Blockade of interleukin 6 trans signaling suppresses T-cell resistance against apoptosis in chronic intestinal inflammation: Evidence in Crohn disease and experimental colitis in vivo, Nat. Med. 6 (2000) 583–588. https://doi.org/10.1038/75068.

[93] H. Funatsu, H. Yamashita, T. Mimura, H. Noma, S. Nakamura, S. Hori, Risk evaluation of outcome of vitreous surgery based on vitreous levels of cytokines., Eye (Lond). 21 (2007) 377–382. https://doi.org/10.1038/sj.eye.6702213.

[94] U.E. Koskela, S.M. Kuusisto, A.E. Nissinen, M.J. Savolainen, M.J. Liinamaa, High vitreous concentration of IL-6 and IL-8, but not of adhesion molecules in relation to plasma concentrations in proliferative diabetic retinopathy., Ophthalmic Res. 49 (2013) 108–114. https://doi.org/10.1159/000342977.

[95] C. Gustavsson, C.-D. Agardh, E. Agardh, Profile of intraocular tumour necrosis factor-alpha and interleukin-6 in diabetic subjects with different degrees of diabetic retinopathy., Acta Ophthalmol. 91 (2013) 445–452. https://doi.org/10.1111/j.1755-3768.2012.02430.x.

[96] V. V Chernykh, E. V Varvarinsky, E. V Smirnov, D. V Chernykh, A.N. Trunov, Proliferative and inflammatory factors in the vitreous of patients with proliferative diabetic retinopathy., Indian J. Ophthalmol. 63 (2015) 33–36. https://doi.org/10.4103/0301-4738.151464.

[97] H. Chen, X. Zhang, N. Liao, F. Wen, Assessment of biomarkers using multiplex assays in aqueous humor of patients with diabetic retinopathy., BMC Ophthalmol. 17 (2017) 176. https://doi.org/10.1186/s12886-017-0572-6.

[98] X. Yi, J. Sun, L. Li, Q. Wei, Y. Qian, X. Chen, L. Ma, 1,25-Dihydroxyvitamin D3 Deficiency is Involved in the Pathogenesis of Diabetic Retinopathy in the Uygur Population of China., IUBMB Life. 68 (2016) 445–451. https://doi.org/10.1002/iub.1501.

[99] C.J. Malemud, Matrix metalloproteinases (MMPs) in health and disease: An overview, Front. Biosci. 11 (2006) 1696–1701. https://doi.org/10.2741/1915.

[100] G. Mohammad, R.A. Kowluru, Matrix metalloproteinase-2 in the development of diabetic retinopathy and mitochondrial dysfunction., Lab. Invest. 90 (2010) 1365–1372. https://doi.org/10.1038/labinvest.2010.89.

[101] A. Das, P.G. McGuire, C. Eriqat, R.R. Ober, E.J. DeJuan, G.A. Williams, A. McLamore, J. Biswas, D.W. Johnson, Human diabetic neovascular membranes contain high levels of urokinase and metalloproteinase enzymes., Invest. Ophthalmol. Vis. Sci. 40 (1999) 809–813.

[102] K.M. Thrailkill, R.C. Bunn, C.S. Moreau, G.E. Cockrell, P.M. Simpson, H.N. Coleman, J.P. Frindik, S.F. Kemp, J.L. Fowlkes, Matrix metalloproteinase-2 dysregulation in type 1 diabetes., Diabetes Care. 30 (2007) 2321–2326. https://doi.org/10.2337/dc07-0162.

[103] S.A. Peeters, L. Engelen, J. Buijs, N. Chaturvedi, J.H. Fuller, C.G. Schalkwijk, C.D. Stehouwer, Plasma levels of matrix metalloproteinase-2, -3, -10, and tissue inhibitor of metalloproteinase-1 are associated with vascular complications in patients with type 1 diabetes: the EURODIAB Prospective Complications Study., Cardiovasc. Diabetol. 14 (2015) 31. https://doi.org/10.1186/s12933-015-0195-2.

[104] C. Symeonidis, E. Papakonstantinou, A. Galli, I. Tsinopoulos, A. Mataftsi, S. Batzios, S.A. Dimitrakos, Matrix metalloproteinase (MMP-2, -9) and tissue inhibitor (TIMP-1, -2) activity in tear samples of pediatric type 1 diabetic patients: MMPs in tear samples from type 1 diabetes, Graefe's Arch. Clin. Exp. Ophthalmol. 251 (2013) 741–749. https://doi.org/10.1007/s00417-012-2221-3.

[105] É. Csősz, E. Deák, G. Kalló, A. Csutak, J. Tőzsér, Diabetic retinopathy: Proteomic approaches to help the differential diagnosis and to understand the underlying molecular mechanisms, J. Proteomics. 150 (2017) 351–358. https://doi.org/10.1016/j.jprot.2016.06.034.

[106] B.-B. Gao, X. Chen, N. Timothy, L.P. Aiello, E.P. Feener, Characterization of the vitreous proteome in diabetes without diabetic retinopathy and diabetes with proliferative diabetic retinopathy., J. Proteome Res. 7 (2008) 2516–2525. https://doi.org/10.1021/pr800112g.

[107] J.M. Skeie, V.B. Mahajan, Proteomic interactions in the mouse vitreous-retina complex, PLoS One. 8 (2013) 1–14. https://doi.org/10.1371/journal.pone.0082140.

[108] T. Yoshimura, K. Sonoda, M. Sugahara, Y. Mochizuki, H. Enaida, Y. Oshima, A. Ueno, Y. Hata, H. Yoshida, T. Ishibashi, Comprehensive analysis of inflammatory immune mediators in vitreoretinal diseases., PLoS One. 4 (2009) e8158. https://doi.org/10.1371/journal.pone.0008158.

[109] U.R. Chowdhury, B.J. Madden, M.C. Charlesworth, M.P. Fautsch, Proteome analysis of human aqueous humor, Investig. Ophthalmol. Vis. Sci. 51 (2010) 4921–4931. https://doi.org/10.1167/iovs.10-5531.

[110] S.-Y. Chiang, M.-L. Tsai, C.-Y. Wang, A. Chen, Y.-C. Chou, C.-W. Hsia, Y.-F. Wu, H.-M. Chen, T.-H. Huang, P.-H. Chen, H.-T. Liu, H.-A. Shui, Proteomic analysis and identification of aqueous humor proteins with a pathophysiological role in diabetic retinopathy., J. Proteomics. 75 (2012) 2950–2959. https://doi.org/10.1016/j.jprot.2011.12.006.

[111] N.J. Van Haeringen, Clinical biochemistry of tears, Surv. Ophthalmol. 26 (1981) 84–96. https://doi.org/10.1016/0039-6257(81)90145-4.

[112] A. Berta, Collection of tear samples with or without stimulation, Am. J. Ophthalmol. 96 (1983) 115–116. https://doi.org/10.1016/0002-9394(83)90473-7.

[113] H. Razooki Hasan, N.N.A. Aburahma, A.K.A. Al-Kazaz, Oxidative stress status in sera and saliva of type 2 diabetic Iraqi patients with and without proliferative diabetic retinopathy, Asian J. Chem. 31 (2019) 719–722. https://doi.org/10.14233/ajchem.2019.21789.

[114] H.C. Gerstein, J.F.E. Mann, Q. Yi, B. Zinman, S.F. Dinneen, B. Hoogwerf, J.P. Hallé, J. Young, A. Rashkow, C. Joyce, S. Nawaz, S. Yusuf, Albuminuria and risk of cardiovascular events, death, and heart failure in diabetic and nondiabetic individuals, J. Am. Med. Assoc. 286 (2001) 421–426. https://doi.org/10.1001/jama.286.4.421.

[115] N.U. Khan, J. Lin, X. Liu, H. Li, W. Lu, Z. Zhong, H. Zhang, M. Waqas, L. Shen, Insights into predicting diabetic nephropathy using urinary biomarkers, Biochim. Biophys. Acta - Proteins Proteomics. 1868 (2020) 140475. https://doi.org/10.1016/j.bbapap.2020.140475.

[116] D.P. Hainsworth, A. Gangula, S. Ghoshdastidar, R. Kannan, A. Upendran, Diabetic Retinopathy Screening Using a Gold Nanoparticle–Based Paper Strip Assay for the At-Home Detection of the Urinary Biomarker 8-Hydroxy-2′-Deoxyguanosine, Am. J. Ophthalmol. 213 (2020) 306–319. https://doi.org/10.1016/j.ajo.2020.01.032.

[117] M. Roda, C. Ciavarella, G. Giannaccare, P. Versura, Biomarkers in Tears and Ocular Surface: A Window for Neurodegenerative Diseases., Eye Contact Lens. 0 (2019) 1–6. https://doi.org/10.1097/ICL.0000000000000663.

[118] S. Aydin, A short history, principles, and types of ELISA, and our laboratory experience with peptide/protein analyses using ELISA, Peptides. 72 (2015) 4–15. https://doi.org/10.1016/j.peptides.2015.04.012.

[119] H. Zhao, Q. Li, M. Ye, J. Yu, Tear luminex analysis in dry eye patients, Med. Sci. Monit. 24 (2018) 7595–7602. https://doi.org/10.12659/MSM.912010.

[120] J.D. Boss, P.K. Singh, H.K. Pandya, J. Tosi, C. Kim, A. Tewari, M.S. Juzych, G.W. Abrams, A. Kumar, Assessment of neurotrophins and inflammatory mediators in vitreous of patients with diabetic retinopathy, Investig. Ophthalmol. Vis. Sci. 58 (2017) 5594–5603. https://doi.org/10.1167/iovs.17-21973.

[121] K.S. Park, S.S. Kim, J.C. Kim, H.C. Kim, Y.S. Im, C.W. Ahn, H.K. Lee, Serum and tear levels of nerve growth factor in diabetic retinopathy patients., Am. J. Ophthalmol. 145 (2008) 432–437. https://doi.org/10.1016/j.ajo.2007.11.011.

[122] P. Khaloo, R. Qahremani, S. Rabizadeh, M. Omidi, A. Rajab, F. Heidari, G. Farahmand, M. Bitaraf,

H. Mirmiranpour, A. Esteghamati, M. Nakhjavani, Nitric oxide and TNF-α are correlates of diabetic retinopathy independent of hs-CRP and HbA1c, Endocrine. (2020) 536–541. https://doi.org/10.1007/s12020-020-02353-x.

[123] M. Nalini, B. V. Raghavulu, A. Annapurna, P. Avinash, V. Chandi, N. Swathi, Wasim, M. Nalini., B. V. Raghavulu, A. Annapurna, P. Avinash, V. Chandi, N. Swathi, Wasim, Correlation of various serum biomarkers with the severity of diabetic retinopathy, Diabetes Metab. Syndr. Clin. Res. Rev. 11 (2017) S451–S454. https://doi.org/10.1016/j.dsx.2017.03.034.

[124] C. Costagliola, V. Romano, M. De Tollis, F. Aceto, R. Dell'Omo, M.R. Romano, C. Pedicino, F. Semeraro, TNF-alpha levels in tears: A novel biomarker to assess the degree of diabetic retinopathy, Mediators Inflamm. 2013 (2013). https://doi.org/10.1155/2013/629529.

[125] K. Kovacs, K. V Marra, G. Yu, S. Wagley, J. Ma, G.C. Teague, N. Nandakumar, K. Lashkari, J.G. Arroyo, Angiogenic and Inflammatory Vitreous Biomarkers Associated With Increasing Levels of Retinal Ischemia., Invest. Ophthalmol. Vis. Sci. 56 (2015) 6523–6530. https://doi.org/10.1167/iovs.15-16793.

[126] N.E. Abu-Yaghi, N.M. Abu Tarboush, A.M. Abojaradeh, A.S. Al-Akily, E.M. Abdo, L.O. Emoush, Relationship between Serum Vascular Endothelial Growth Factor Levels and Stages of Diabetic Retinopathy and Other Biomarkers, J. Ophthalmol. 2020 (2020). https://doi.org/10.1155/2020/8480193.

[127] S. Hagan, E. Martin, A. Enriquez-de-Salamanca, Tear fluid biomarkers in ocular and systemic disease: potential use for predictive, preventive and personalised medicine., EPMA J. 7 (2016) 15. https://doi.org/10.1186/s13167-016-0065-3.

[128] M.S. Khan, K. Dighe, Z. Wang, E. Daza, A.S. Schwartz-Duval, C.P. Rowley, I.A. Calvillo, S.K. Misra, L.T. Labriola, D. Pan, Label-free detection of lactoferrin and beta-2-microglobuin in contrived tear film using a low-cost electrical biosensor chip, 2017 IEEE Healthc. Innov. Point Care Technol. HI-POCT 2017. 2017-Decem (2017) 72–75. https://doi.org/10.1109/HIC.2017.8227587.

[129] J.-Y. Wang, J.-S. Kwon, S.-M. Hsu, H.-S. Chuang, Sensitive tear screening of diabetic retinopathy with dual biomarkers enabled using a rapid electrokinetic patterning platform, Lab Chip. 20 (2020) 356–362. https://doi.org/10.1039/c9lc00975b.

[130] H.-S. Chuang, Y. Chen, H.-P. Cheng, Enhanced diffusometric immunosensing with grafted gold nanoparticles for detection of diabetic retinopathy biomarker tumor necrosis factor-alpha., Biosens. Bioelectron. 101 (2018) 75–83. https://doi.org/10.1016/j.bios.2017.10.002.

[131] A. Cruz, R. Queirós, C.M. Abreu, C. Barata, R. Fernandes, R. Silva, A.F. Ambrósio, R. Soares-Dos-Reis, J. Guimarães, M.J. Sá, J.B. Relvas, P.P. Freitas, I. Mendes Pinto, Electrochemical Immunosensor for TNFα-Mediated Inflammatory Disease Screening, ACS Chem. Neurosci. 10 (2019) 2676–2682. https://doi.org/10.1021/acschemneuro.9b00036.

[132] J.-C. Wang, H.-Y. Ku, T. Chen, H.-S. Chuang, Detection of low-abundance biomarker lipocalin 1 for diabetic retinopathy using optoelectrokinetic bead-based immunosensing., Biosens. Bioelectron. 89 (2017) 701–709. https://doi.org/10.1016/j.bios.2016.11.014.

[133] Y. Zhao, M. Cao, J.F. McClelland, Z. Shao, M. Lu, A photoacoustic immunoassay for biomarker detection, Biosens. Bioelectron. 85 (2016) 261–266. https://doi.org/10.1016/j.bios.2016.05.028.

[134] É. Csősz, E. Deák, G. Kalló, A. Csutak, J. Tőzsér, Diabetic retinopathy: Proteomic approaches to help the differential diagnosis and to understand the underlying molecular mechanisms, J. Proteomics. 150 (2017) 351–358. https://doi.org/10.1016/j.jprot.2016.06.034.

[135] M. Kim, R.J. Iezzi, B.S. Shim, D.C. Martin, Impedimetric Biosensors for Detecting Vascular Endothelial Growth Factor (VEGF) Based on Poly(3,4-ethylene dioxythiophene) (PEDOT)/Gold Nanoparticle (Au NP) Composites., Front. Chem. 7 (2019) 234. https://doi.org/10.3389/fchem.2019.00234.

[136] A. Touhami, Biosensors and nanobiosensors: design and applications, in: A. Seifalian, A. de Mel, D.M. Kalaskar (Eds.), Nanomedicine, One Central Press Ltd, Mancheste, United Kingdom, 2014.

[137] D.R. Thévenot, K. Toth, R.A. Durst, G.S. Wilson, Electrochemical biosensors: Recommended definitions and classification, Biosens. Bioelectron. 16 (2001) 121–131. https://doi.org/10.1016/S0956-5663(01)00115-4.

[138] M.L.Y. Sin, K.E. Mach, P.K. Wong, J.C. Liao, Advances and challenges in biosensor-based diagnosis of infectious diseases, Expert Rev. Mol. Diagn. 14 (2014) 225–244. https://doi.org/10.1586/14737159.2014.888313.Advances.

[139] S.C.B. Gopinath, T.H. Tang, Y. Chen, M. Citartan, J. Tominaga, T. Lakshmipriya, Sensing strategies for influenza surveillance, Biosens. Bioelectron. 61 (2014) 357–369. https://doi.org/10.1016/j.bios.2014.05.024.

[140] D. Grieshaber, R. MacKenzie, J. Vörös, E. Reimhult, Electrochemical biosensors - Sensor principles and architectures, Sensors. 8 (2008) 1400–1458. https://doi.org/10.3390/s8031400.

[141] J.E.B. Randles, Kinetics of rapid electrode reactions, (1947).

[142] E.P. Randviir, C.E. Banks, Electrochemical impedance spectroscopy: An overview of bioanalytical applications, Anal. Methods. 5 (2013) 1098–1115. https://doi.org/10.1039/c3ay26476a.

[143] S.K. Arya, K.Y. Wang, C.C. Wong, A.R.A. Rahman, Anti-EpCAM modified LC-SPDP monolayer on gold microelectrode based electrochemical biosensor for MCF-7 cells detection, Biosens. Bioelectron. 41 (2013) 446–451. https://doi.org/10.1016/j.bios.2012.09.006.

[144] G.T. Hermanson, Bioconjugate techniques, 2013.

[145] G. Carracedo, C. Villa-Collar, A. Martin-Gil, M. Serramito, L. Santamaría, Comparison Between Viscous Teardrops and Saline Solution to Fill Orthokeratology Contact Lenses Before Overnight Wear, Eye Contact Lens. 44 (2018) S307–S311. https://doi.org/10.1097/ICL.0000000000000416.

[146] M. Roushani, A. Valipour, M. Valipour, Layer-by-layer assembly of gold nanoparticles and cysteamine on gold electrode for immunosensing of human chorionic gonadotropin at picogram levels, Mater. Sci. Eng. C. 61 (2016) 344–350. https://doi.org/10.1016/j.msec.2015.12.088.

[147] S. Rana, A. Bharti, S. Singh, A. Bhatnagar, N. Prabhakar, Gold-silver core-shell nanoparticle–based impedimetric immunosensor for detection of iron homeostasis biomarker hepcidin, Microchim. Acta. 187 (2020). https://doi.org/10.1007/s00604-020-04599-8.

[148] J.K. Lee, S.R. Shin, A. Desalvo, G. Lee, J.Y. Lee, A. Polini, S. Chae, H. Jeong, J. Kim, H. Choi, H.Y. Lee, Nonmediated, Label-Free Based Detection of Cardiovascular Biomarker in a Biological Sample, Adv. Healthc. Mater. 6 (2017) 1–7. https://doi.org/10.1002/adhm.201700231.

[149] S.M. Lam, L. Tong, X. Duan, A. Petznick, M.R. Wenk, G. Shui, Extensive characterization of human tear fl uid collected using different techniques unravels the presence of novel lipid amphiphiles, J. Lipid Res. 55 (2014) 289–298. https://doi.org/10.1194/jlr.M044826.

[150] J. Tiffany, The normal tear film, Dev. Ophthalmol. 41 (2008) 1–20. https://doi.org/10.1159/000131066.

A. Ethics statement

The use of human samples was approved by the Ethics Committee of the Centro Hospitalar e Universitário de Coimbra and has the reference CHUC-059-18.

B. Proof of paper submission

Advanced Biosystems

Minimally invasive molecular sensing for advanced diagnosis of diabetic retinopathy

--Manuscript Draft--

Manuscript Number:	adbi.202000462
Article Type:	Progress Report
Corresponding Author:	Ines Mendes Pinto International Iberian Nanotechnology Laboratory Braga, (Select) PORTUGAL
Corresponding Author E-Mail:	ines.m.pinto@inl.int
Order of Authors:	Maria Vieira
	Vanessa F. Cardoso
	Mariana Carvalho
	António F. Ambrósio
	Rosa Fernandes
	Ines Mendes Pinto
Keywords:	Biosensors, Point-of-care, Molecular Biomarkers, Diabetic Retinopathy
Section/Category:	
Abstract:	Diabetic retinopathy (DR) is the most common diabetic eye disease and the leading cause of vision loss and impairment in working-age adults. It progresses from mild to severe non-proliferative or proliferative DR based on several pathological features including the magnitude of blood-retinal barrier breakdown, and neovascularization. Available treatments, including anti-vascular and anti-inflammatory pharmacological interventions, and retinal laser photocoagulation, are inefficient on halting disease progression in a significantly high percentage of patients and have many associated risks. Such treatments are applied mostly in the advanced stages of DR. Nevertheless, recent studies have shown that anti-vascular endothelial growth factor (anti-VEGF) based therapy could potentially limit DR progression if applied at early stages, highlighting the importance of early disease diagnostics.
Suggested Reviewers:	
Opposed Reviewers:	
Author Comments:	
Additional Information:	
Question	**Response**
Please submit a plain text version of your cover letter here.	Dear Dr. Kerstin Brachhold, Following our email exchange and your positive feedback about the potential interest of Advanced Biosystems on our study, we are submitting our manuscript entitled “Minimally invasive molecular sensing for advanced diagnosis of diabetic retinopathy” for publication as a Progress Report. Diabetic retinopathy (DR) is the most common diabetic eye disease and the leading cause of vision loss and impairment in working-aged adults. It progresses from mild to severe non-proliferative or proliferative diabetic retinopathy based on several factors including the magnitude of blood-retinal barrier breakdown, and neovascularization. In the past few decades, optical coherence tomography angiography has proved its utility for quantifying retinal and optic nerve changes in patients with retinal diseases, which has vastly improved DR diagnostics. Dilated indirect ophthalmoscopy coupled with biomicroscopy and seven-standard field stereoscopic 30º fundus photography are also

	accepted methods for examining DR. However, all these methodologies are solely based on morphological examination of the retinal vascularization, and are not suitable for point-of-care and recurrent evaluation. This raises the need for new technologies to enable early and quantitative diagnosis of diabetic retinopathy. In this progress report, we critically discuss the possibility to infer an earlier diagnosis of DR from direct and minimally to non-invasive molecular profiling of the eye. We will provide an overview on recently developed molecular based-technologies for quantitative label-free assessment of DR biomarkers in tears (and also in urine and blood), such as diffusometric, optoelectronic and electrochemical immunosensors and immunosorbent assays and discuss their potential clinical application for point-of-care DR diagnostics and monitoring. Thank you for your consideration. With kind regards, Inês Mendes Pinto, PharmD, PhD
Do you or any of your co-authors have a conflict of interest to declare?	No. The authors declare no conflict of interest.